

SWZDI

Smart Work Zone Deployment Initiative

Report Title		Report Date: 2006
Design of Portable Rumble Strips		
Principle Investigator Name Meyer, Eric Affiliation Meyer ITS Address Lawrence, KS 66047 Phone (785) 843-2718 Fax (785) 843-2647 Email emeyer@MeyerITS.com		Vendor Name and Address «Vendor»
Author(s) and Affiliation(s) Rick Hale, The University of Kansas Ray Taghavi, The University of Kansas Jeff Olafsen, The University of Kansas Gaurav Mathur, The University of Kansas		
Supplemental Funding Agency Name and Address (if applicable)		
Supplemental Notes		
Abstract <p>In 2003, the states involved in the Midwest Smart Work Zone Deployment Initiative identified portable rumble strips (i.e., rumble strips that require no adhesive or fasteners, making them applicable for very short term work zones) as a high priority and solicited vendors for products to be evaluated by the study. Recognizing that no existing product strictly met the requirements cited in the solicitation, this research was proposed to develop a design for such a device based on aerodynamic and static exploration. The work began with wind tunnel and computational fluid dynamics (CDF) analyses to identify and estimate the critical forces acting on the roadway in the wake of a tractor-trailer. Vehicle simulation packages were used to examine the horizontal (i.e., sliding) force applied to the device by vehicle tires. Prototypes were developed and tested using a sound meter to monitor the sound levels inside the vehicle and both accelerometers mounted to a prototype strip and a high-speed video camera to monitor the interaction between the tires and the strips and to record the strip's response to the impact during traversal.</p> <p>Based on the analyses conducted in this work, a strip can be constructed that will resist the lifting forces in a truck wake, will not slide down the pavement, and will resist tipping even during heavy braking. Some bounce is inevitable. A segmented design was adopted to help minimize the effects of bounce, and a prototype was fabricated and tested to examine the performance.</p> <p>In order for the strip to resist the lifting forces and the tipping forces, it must be fabricated from solid steel (or something with an equal or greater specific gravity), and needs to be at least 1" high in order to avoid requiring excessive widths. A 1.25" height is recommended, yielding a recommended breadth of 4 to 6 inches. A 4"</p>		

breadth prototype and a 6" breadth prototype were fabricated and tested with a loaded tractor trailer at 60 mph. Significant bounce was observed, but only in those elements struck by the tires. The adjacent elements did not move, resulting in no net translation of the strip as a whole. No tipping, sliding, or lifting due to negative pressures in the truck wake were observed.

Based on these results, the design developed in this study is a feasible solution for the need for portable rumble strips.

Smart Work Zone Deployment Initiative

2004 Program Year

DESIGN OF PORTABLE RUMBLE STRIPS

Final Report

December 2006

Submitted by:

Eric Meyer, PhD, PE (Primary Contact)
Meyer ITS
Lawrence, KS 66047
(785) 843-2718 (voice)
(785) 843-2647 (fax)
emeyer@MeyerITS.com

Rick Hale, PhD
Associate Professor, Aerospace Engineering
The University of Kansas

Ray Taghavi, PhD
Professor, Aerospace Engineering
The University of Kansas

Jeff Olafsen, PhD
Assistant Professor, Physics and Astronomy
The University of Kansas

Gaurav Mathur
Research Assistant, Dept of Aerospace Engineering
The University of Kansas

Abstract

In 2003, the states involved in the Midwest Smart Work Zone Deployment Initiative identified portable rumble strips (i.e., rumble strips that require no adhesive or fasteners, making them applicable for very short term work zones) as a high priority and solicited vendors for products to be evaluated by the study. Recognizing that no existing product strictly met the requirements cited in the solicitation, this research was proposed to develop a design for such a device based on aerodynamic and static exploration. The work began with wind tunnel and computational fluid dynamics (CFD) analyses to identify and estimate the critical forces acting on the roadway in the wake of a tractor-trailer. Vehicle simulation packages were used to examine the horizontal (i.e., sliding) force applied to the device by vehicle tires. Prototypes were developed and tested using a sound meter to monitor the sound levels inside the vehicle and both accelerometers mounted to a prototype strip and a high-speed video camera to monitor the interaction between the tires and the strips and to record the strip's response to the impact during traversal.

Based on the analyses conducted in this work, a strip can be constructed that will resist the lifting forces in a truck wake, will not slide down the pavement, and will resist tipping even during heavy braking. Some bounce is inevitable. A segmented design was adopted to help minimize the effects of bounce, and a prototype was fabricated and tested to examine the performance.

In order for the strip to resist the lifting forces and the tipping forces, it must be fabricated from solid steel (or something with an equal or greater specific gravity), and needs to be at least 1" high in order to avoid requiring excessive widths. A 1.25" height is recommended, yielding a recommended breadth of 4 to 6 inches. A 4" breadth prototype and a 6" breadth prototype were fabricated and tested with a loaded tractor trailer at 60 mph. Significant bounce was observed, but only in those elements struck by the tires. The adjacent elements did not move, resulting in no net translation of the strip as a whole. No tipping, sliding, or lifting due to negative pressures in the truck wake were observed.

Based on these results, the design developed in this study is a feasible solution for the need for portable rumble strips.

Table of Contents

ABSTRACT	2
TABLE OF CONTENTS	3
LIST OF FIGURES.....	5
LIST OF TABLES.....	6
INTRODUCTION	7
APPROACH	8
AERODYNAMIC STUDY	9
COMPUTATIONAL FLUID DYNAMICS (CFD) ANALYSIS	13
<i>Model Development</i>	14
<i>Geometry clean up in Aero CAD</i>	15
<i>Boundary Surface Definition</i>	16
<i>Meshing the volume</i>	18
<i>Defining boundary conditions and continuum</i>	18
<i>CFD Analysis Results</i>	20
<i>CFD Results for Influence of Bypassing Trucks</i>	25
VEHICLE MODELING ANALYSIS.....	32
<i>Speed-Force Relationship</i>	33
<i>Sliding Forces</i>	33
<i>Estimating Frictional Resistance to Sliding</i>	34
<i>Temporal Relationship of Forces</i>	34
PRELIMINARY DESIGN.....	35
PROFILE	37
FLANGE DESIGN	38
<i>Flexible Flanges</i>	38
<i>Rigid Flanges</i>	38
COMPOSITION	42
PRELIMINARY PROTOTYPES	44
FIELD TEST 1	44
FIELD TEST 2	45
ESTABLISHING DESIGN VALUES	50
FIELD TEST 3	51
REVISED DESIGN	56
FINAL PROTOTYPES.....	61
FINAL DESIGN	64
FIELD TEST 4.....	65
FIELD TEST 5	68
RESULTS.....	73
EFFECTS OF SPEED.....	73
TRANSLATION	76
BRAKING	77
CONCLUSIONS AND FINAL DESIGN.....	80

BOUNCE REDUCTION	80
INSTALLATION AND REMOVAL	81
AREAS FOR FUTURE DEVELOPMENT	81
ACKNOWLEDGMENTS.....	82
REFERENCES	83
APPENDIX A: DISCUSSION OF TRUCKSIM RESULTS.....	85

List of Figures

FIGURE 1. PROBLEM STATEMENT.	8
FIGURE 2. ACTUAL KENWORTH T600 (LEFT) AND 1/16 SCALE MODEL (RIGHT).	9
FIGURE 3. VIEW INSIDE WIND TUNNEL SHOWING MODEL, FALSE FLOOR, RAMPS, AND SEAL TAPE.	10
FIGURE 4. LOCATION OF PRESSURE TRANSDUCERS RELATIVE TO MODEL.	11
FIGURE 5. CLOSER VIEW OF TRANSDUCER LOCATIONS BEHIND TRAILER	11
FIGURE 6. CENTERLINE TRANSDUCER LOCATIONS UNDER MODEL SHOWN WITHOUT TRACTOR	12
FIGURE 7. MARKING CAB FEATURES ON PHOTOGRAPH	14
FIGURE 8. WIRE FRAME MODEL CONSISTING OF MARKED AND REFERENCED FEATURES	15
FIGURE 9. UNSTRUCTURED TRIANGULAR SURFACE MESHES	17
FIGURE 10. LONGITUDINAL SECTION DISPLAYING TETRAHEDRAL ELEMENTS	18
FIGURE 11. COMPUTATIONAL MODELS WITH AND WITHOUT DIFFUSER.	19
FIGURE 12. GENERAL CHARACTERISTICS OF FLOW AROUND A TRACTOR-TRAILER SHOWN BY STREAM TUBES.	20
FIGURE 13. PATH LINES OF DOWNSTREAM TRAILER WAKE.	21
FIGURE 14. VELOCITY VECTORS ON A LONGITUDINAL PLANE ON RIGHT SIDE OF VEHICLE.	21
FIGURE 15. STATIC PRESSURE DISTRIBUTION ON THE TUNNEL FLOOR.	22
FIGURE 16. TOTAL PRESSURE ALONG A LONGITUDINAL PLANE ON RIGHT SIDE OF MODEL.	23
FIGURE 17. COMPARISON OF EXPERIMENTAL AND CFD CENTERLINE FLOOR PRESSURES UNDER MODEL AT AN INLET SPEED OF 80 MPH AND ZERO YAW	24
FIGURE 18. OUTLINE OF THE TRUCK GRID FOR FREE AIR CASE.	25
FIGURE 19. GENERATED TRUCK MESH.	26
FIGURE 20. FLOW CHARACTERISTICS OF THE TRUCK (FREE AIR & SPEED: 70 MPH).	26
FIGURE 21. RESIDUALS OF THE TRUCK IN FREE AIR CASE (70 MPH).	27
FIGURE 22. DYNAMIC PRESSURE DISTRIBUTIONS (70 MPH).	28
FIGURE 23. PRESSURE DISTRIBUTIONS OF THE BOTTOM SURFACE OF THE TRUCK.	28
FIGURE 24. FORCE INCREMENT OF THE OUTSIDE BOTTOM SURFACE OF THE TRUCK AT 70 MPH.	29
FIGURE 25. FORCE OF THE OUTSIDE BOTTOM SURFACE OF THE TRUCK AT THE 1/2 TRUCK WIDTH.	31
FIGURE 26. HORIZONTAL LOAD FOR PASSENGER CARS.	32
FIGURE 27. HORIZONTAL LOADS ON CAB AXLES OF A TRACTOR TRAILER.	33
FIGURE 28. CONCEPTUAL DESIGN DESCRIBED IN THE ORIGINAL WORK PLAN.	36
FIGURE 29. SKETCH OF INITIAL TIRE-STRIP IMPACT.	37
FIGURE 30. ILLUSTRATION OF A TRIMMED BAR DESIGN.	38
FIGURE 31. CONCEPTUAL DESIGN USING SEGMENTED STRIP AND RIGID TRUSS FLANGES.	40
FIGURE 32. INITIAL FULLY SPECIFIED DESIGN.	41
FIGURE 33. FLANGED DESIGN WITH SINGLE CROSS MEMBER.	42
FIGURE 34. PLOT OF CRITICAL PRESSURES FROM WIND TUNNEL DATA.	43
FIGURE 35. CROSS-SECTION OF A 1.50'-RADIUS PROTOTYPE.	44
FIGURE 36. SECTION VIEW OF FOUR SIZES OF PROTOTYPE RUMBLE STRIPS, 1.50" TO 0.75" (L TO R).	45
FIGURE 37. WOODEN PROTOTYPE RUMBLE STRIP IN PLACE FOR TESTING.	47
FIGURE 38. NYLON RESTRAINING STRAP.	48
FIGURE 39. KEY FRAMES FROM VIDEO OF TRUCK TIRE ON STRIP.	49
FIGURE 40. ANGLE OF CONTACT (IN DEGREES) AT TIME OF EACH IMAGE.	50
FIGURE 41. SPECTROGRAM FOR PASSENGER CAR AT 19 MPH.	51
FIGURE 42. SPECTROGRAM FOR PASSENGER CAR AT 39 MPH.	52
FIGURE 43. SPECTROGRAM FOR DUMP TRUCK AT 20 MPH.	53
FIGURE 44. SPECTROGRAM FOR DUMP TRUCK AT 37 MPH.	54
FIGURE 45. WAVE FORMS FOR PASSENGER CAR AND DUMP TRUCK AT 20, 30, AND 40 MPH.	55
FIGURE 46. WAVE FORMS FOR TRUCK (TOP) AND CAR (BOTTOM) AT 20 MPH.	55
FIGURE 47. CONCEPTUAL DESIGN—TOP VIEW.	56
FIGURE 48. RENDERINGS OF CAD MODEL WITH CENTERBOX AND FLANGES.	58
FIGURE 49. RENDERINGS OF THE CONNECTOR MODELS.	59
FIGURE 50. RELATIONSHIP BETWEEN THE BAR HEIGHT AND THE BREADTH NEEDED TO RESIST LIFT.	61
FIGURE 51. PROPOSED ASSEMBLY.	62

FIGURE 52. CORNER TREATMENT SPECIFICATIONS.	63
FIGURE 53. MAXIMUM SPACINGS FOR EXTERIOR DIMENSIONS	64
FIGURE 54. END TREATMENT OF 4" STRIP (ACTUAL SIZE).	65
FIGURE 55. STRIP STATE AS RESET AND FOLLOWING ONE PASS AT 20 MPH, 30 MPH, AND 40 MPH.....	66
FIGURE 56. MOVEMENT ON FOUR SUCCESSIVE PASSES (I.E., WITHOUT RESETTING).	66
FIGURE 57. MOVEMENT OF 4-IN STRIP DURING SUCCESSIVE TRAVERSALS.....	67
FIGURE 58. BOUNCE OF 4-IN STRIP DURING TRAVERSAL WHILE BRAKING	68
FIGURE 59. PASSENGER CAR TRAVERSING STRIP.	70
FIGURE 60. TRACTOR TRAILER USED FOR TESTING.	71
FIGURE 61. BEFORE AND AFTER IMAGES OF TEST RUN 35.	72
FIGURE 62. STRIP MOVEMENT BY VEHICLE AND STRIP WIDTH	73
FIGURE 63. STRIP MOVEMENT BY SPEED.....	74
FIGURE 64. MAXIMUM VERTICAL DISPLACEMENT FOLLOWING AXLE 1 (RUNID=36).	75
FIGURE 65. MAXIMUM VERTICAL DISPLACEMENT FOLLOWING AXLE 3 (RUNID=36).	75
FIGURE 66. MAXIMUM VERTICAL DISPLACEMENT FOLLOWING AXLE 5 (RUNID=36).	75
FIGURE 67. STRIP MOVEMENT OVER MULTIPLE PASSES	76
FIGURE 68. STRIP MOVEMENT WHILE BRAKING	77
FIGURE 69. SOUND PRESSURE LEVELS (SPL) VERSUS SPEED BY VEHICLE AND STRIP TYPE.	85
FIGURE 70. SOUND PRESSURE LEVELS (SPL) VERSUS SPEED FOR VARIOUS STRIP TYPES AND CONFIGURATIONS.	86
FIGURE 71. VIBRATION AND SPEED FOR VARIOUS STRIP TYPES AND CONFIGURATIONS.	87
FIGURE 72. CHANGES IN VIBRATION WITH SPEED FOR VARIOUS STRIP TYPES AND CONFIGURATIONS.	88
FIGURE 73. CHANGES IN VIBRATION PARAMETERS WITH SPEED FOR ASSORTED STRIPS AND VEHICLES.	90
FIGURE 74. CHANGES IN SOUND PARAMETERS WITH SPEED FOR ASSORTED STRIPS AND VEHICLES.....	91

List of Tables

TABLE 1. TIME AVERAGED EXPERIMENTAL DATA	13
TABLE 2. FORCE INCREMENT OF THE OUTSIDE BOTTOM SURFACE OF THE TRUCK AT 70 MPH.....	29
TABLE 3. FORCE INCREMENT ON THE OUTSIDE BOTTOM SURFACE OF THE TRUCK AT 1/2 DISTANCE.....	30
TABLE 4. GENERATED SUCTION FORCE AT THE 1/2 DISTANCE.....	30
TABLE 5. VALUES FOR THE COEFFICIENT OF FRICTION FOR RUBBER.....	34
TABLE 6. TEST CASES EXECUTED.....	69
TABLE 7. EFFECTS OF BRAKING ON 4-IN AND 6-IN STRIPS (AXLE 3).	78
TABLE 8. EFFECTS OF BRAKING ON 4-IN AND 6-IN STRIPS (AXLE 5).	79

Introduction

Transportation agencies are continually considering how to make highways safer and more efficient. In particular, safety in work zones garners special attention because of the necessity of disrupting normal highway conditions and the frequent need for personnel to work in close proximity to moving traffic. The most effective tool in preventing vehicle-worker collisions is positive separation, such as a Jersey barrier between the work area and the traffic flow. In situations where positive separation is not possible because of geometric issues or is infeasible because of the scope of the work being done, numerous devices are utilized to make sure the driving public clearly understands how they are to navigate the work zone.

Rumble strips are devices widely used in advance of work zones to enhance the effectiveness of other devices such as flaggers, static signing, or temporary traffic signals. Drivers who are not expecting a work zone will respond more slowly than those who have been alerted in advance. Rumble strips act as a generic warning that road conditions merit special attention. The intention is that the sound and vibration will capture the attention of drivers—particularly those who may be inattentive for whatever reason—and increase the likelihood that they will see and observe the warning signs and other traffic control devices associated with the work zone.

Studies provide strong evidence that continuous rumble strips along the shoulder reduce roadway departures. (e.g., FHWA, 1998; Carlson and Miles, 2003) Rumble strips in the traveled lane in advance of work zones, however, are more difficult to conclusively prove effective. Accident studies are not feasible because the nature of work zones is that they are temporary, and durations are rarely long enough to observe statistically significant patterns with respect to crashes. Although there are many studies suggesting that rumble strips in the traveled lane are effective, (e.g., Noel et al, 1989; Harwood, 1993; FHWA, 2000; Zaidel et al, 1986; Owens, 1967) there are also studies that find rumble strips to be ineffective. Studies of rumble strips used in work zones are commonly found in both categories. (e.g., Noel et al, 1989; Harwood, 1993; Richards et al, 1985; Benekohal et al, 1992; Fontaine et al, 2000) Nonetheless, the intuitive perception of the value of this type of device has led to very widespread use.

However, there are many work zones for which rumble strips might enhance safety, but for which the duration is so brief that the installation and removal time required to use conventional rumble strips is prohibitive. Recognizing that rumble strips are only an incremental improvement, the safety benefits gained for very short duration work zones is likely offset by the extra worker exposure incurred during installation. To address the need for a rumble strip that can be installed and removed quickly enough to merit use in very short term work zones, the Federal Highway Administration (FHWA), through the Strategic Highway Research Program (SHRP), funded research to develop a portable device to provide audible and tactile warning to drivers. (Stout et al, 1993)

The SHRP-funded research resulted in the development of a rumble mat, a heavy rubber mat with ridges on the upper side that could be set in the roadway to provide rumble and vibration for passing vehicles. Regretfully, the device was only applicable at low speeds (e.g., 40 mph or less). At higher speeds, the wake of tractor trailers is strong enough to lift the mat from the pavement, creating an unsafe condition. These mats are used for low-speed situations by many

transportation agencies, but those who have tried them in situations where highway speeds are prevalent have all found that they do not reliably stay on the pavement. Stout et al affirmed the value of the concept and the need for additional research.

In 2003, the Midwest Smart Work Zone Deployment Initiative (now called Smart Work Zone Deployment Initiative, or SWZDI) issued a solicitation asking vendors to provide products for testing that might fill the role of *portable* rumble strip. Since 1999, the study has funded several studies of products billed as *temporary* rumble strips, or strips that can be applied and removed more easily than conventional asphalt strips. The intent was to reduce risk to workers by reducing exposure during rumble strip installation and to provide contractors with a convenient alternative to asphalt strips. Applicable work zones include those expected to be in place for several days to several months. In the 2003 solicitation, *portable* rumble strips were distinguished from *temporary* strips by several characteristics. They must be reusable, preferably use no adhesives or fasteners, and must be appropriate for work zones of duration of a day or less. Figure 1 shows an excerpt from the solicitation.

PROBLEM STATEMENT:

The Midwest Smart Work Zone Deployment Initiative seeks proposals for products to be evaluated as portable rumble strips for use in work zones with durations of less than a day. These products must be reusable, and it is anticipated that they will install without adhesives. Products to be evaluated will be selected on the following criteria.

1. Ease of installation and removal
2. Ability to remain in place under traffic, including heavy trucks at highway speeds
3. Ability to generate perceptible noise and vibration (though not egregiously severe so as to alarm drivers)

Figure 1. Problem Statement.

Approach

In the absence of any commercial products that strictly meet the criteria outlined in the solicitation, this study was proposed to design such a device. While the originally proposed approach was modified slightly in response to early analysis results, the fundamental components have remained the same. First, wind tunnel analysis and computer modeling were used to identify and quantify the critical pressures existing in the wake of a tractor trailer. Vehicle modeling software was then employed to examine the forces involved in the interaction between the tire and the strip. Finally, a full scale prototype was tested. A second project has

now been funded by the SWZDI to revise the design based on the results of the testing and fabricate and test a second generation prototype.

Aerodynamic Study

The primary issue prompting the SWZDI's search for a portable rumble strip was the SHRP Rumble Mat's tendency to lift off the pavement in the wake of trucks traveling at highway speeds. Such a condition results when the force exerted by the negative air pressure above the mat is greater than the weight of the mat. Once leaving the pavement, the "flight" of the device is much more complicated to predict, but conditions associated with the initial departure from the pavement are fairly simple. With that in mind, if the negative pressures associated with a truck wake are known, then a device can be designed to possess sufficient mass per unit area to prevent its lifting off the pavement. If a height for the device can be established, then the necessary density of the material can be calculated and a fabrication material selected accordingly.

To determine the negative pressures associated with a truck wake, a 1/16 scale model of a Kenworth T600 Tractor-Trailer was secured inside a wind tunnel. Figure 2 shows the model on the right and an actual version of the truck on the left.



Figure 2. Actual Kenworth T600 (left) and 1/16 scale model (right).

A false floor was fabricated from a thin metal sheet and secured to the wind tunnel at a height of 0.8 inches above the original floor with the aid of transverse wooden stiffeners. Four-degree ramps were attached to the false floor at the forward and aft section. Aluminum tape was used to seal all sides and gaps to prevent air from entering under the false floor. The model itself was bolted rigidly to this false floor. Figure 3 shows the model mounted on the false floor within the test-section of the tunnel.

The false floor was designed to also accommodate the mounting of pressure transducers on the floor, under and in the vicinity of the model. A total of 14 pressure transducers were flush

mounted to the false floor. The relative locations of the pressure transducers on the tunnel floor and bolts used to secure the model are shown in Figure 4. Figure 5 and Figure 6 show the photographs of the setup with the transducer locations indicated.



Figure 3. View inside wind tunnel showing model, false floor, ramps, and seal tape.

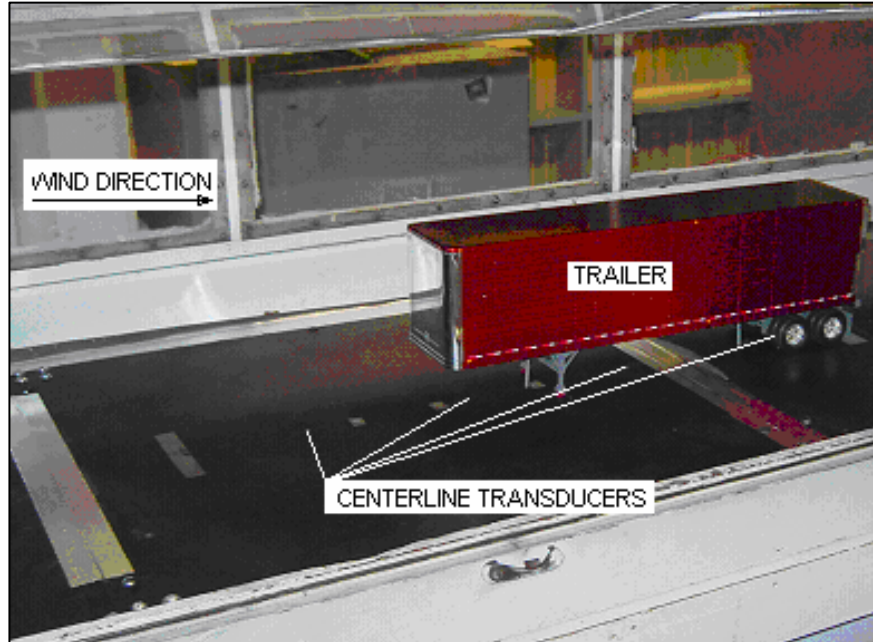


Figure 6. Centerline transducer locations under model shown without tractor

The orientation of the false floor and the truck represented the basic case of zero yaw and level surface. All of the measurements taken and the subsequent modeling analyses pertained to the basic case.

Voltages associated with the various transducers were recorded, and calibration of the transducers provided for the conversion from voltages to an associated pressure. The time-averaged (30 sec) values are shown in Table 1. Shaded cells contain the lowest values for each speed condition.

Table 1. Time averaged experimental data

V_{wind} (V_{inlet}) ¹	Static pressure (psig)		
	63.0 mph (50 mph)	74.2 mph (60 mph)	84.8 mph (70 mph)
Kulite no			
14	-0.079	-0.1061	-0.1332
13	-0.0954	-0.1618	-0.2356
12	-0.0783	-0.1349	-0.1595
11	-0.1008	-0.1303	-0.1451
10	-0.1011	-0.138	-0.165
1	-0.1224	-0.1912	-0.2439
2	x	x	x
3	-0.1076	-0.157	-0.2153
4	-0.1531	-0.2224	-0.2817
5	-0.058	-0.095	-0.1019
6	-0.0922	-0.1806	-0.2109
7	-0.1381	-0.2018	-0.2549
8	-0.1168	-0.1699	-0.2337
9	-0.1009	-0.1115	-0.1328

¹ V_{wind} refers to the ambient free flow wind speed in the test section; V_{inlet} refers to the nominal wind speed upstream of the diffuser.

Computational Fluid Dynamics (CFD) Analysis

Because of the inherent constraints in physical testing, a computational model was developed to provide additional detail into the characteristics of the airflow surrounding a tractor trailer. The data in Table 1 were used to validate the model, and the model provided insights that could not be drawn from the physical measurements taken.

A three-dimensional computer model of the truck was created using close-range photogrammetry. The model was cleaned up in Aero CAD and geometry simplified a little. The model excluded the vertical exhaust pipes on the cab and much of the underbody detail (e.g., transmission components, gas tanks, etc.) to reduce the time required to conduct analyses, which increases with increases in the complexity of the shape being studied. This was deemed an acceptable generalization given that the primary focus was the dominating flow characteristics of tractor-trailer, which would not likely be affected significantly by the simplifications.

The model was imported as a wireframe into the preprocessor, GAMBIT 2.0, for generating a volume grid. A course mesh of roughly 0.6 million tetrahedral elements was generated and then refined twice to give an intermediate mesh consisting of 0.9 million elements and a fine mesh of 1.7 million elements.

The grid was then read into the computational fluid dynamics (CFD) solver, FLUENT 5.6, and various cases were run at a constant zero yaw angle with a stationary ground and non-rotating wheels. The simulations were designed to model the experimental tests with boundary conditions being defined from experimental data. FLUENT was also used for post-processing and analyzing the results. A parametric study was conducted to study grid convergence.

The following sections provide additional detail about each of the steps mentioned above.

Model Development

Stereo images of the cab and trailer were taken and used to generate the initial wireframe model of each component. The images were imported into PhotoModeler, and object features like points, lines, curves, edges and cylinders were appropriately marked so that they could be referenced between photos and their calculated 3-D location. Figure 7 shows the feature marking in progress within PhotoModeler. Marked features were then referenced between images so that their three-dimensional spatial relationships could be determined. Figure 8 shows a view of the resulting wireframe model.



Figure 7. Marking cab features on photograph

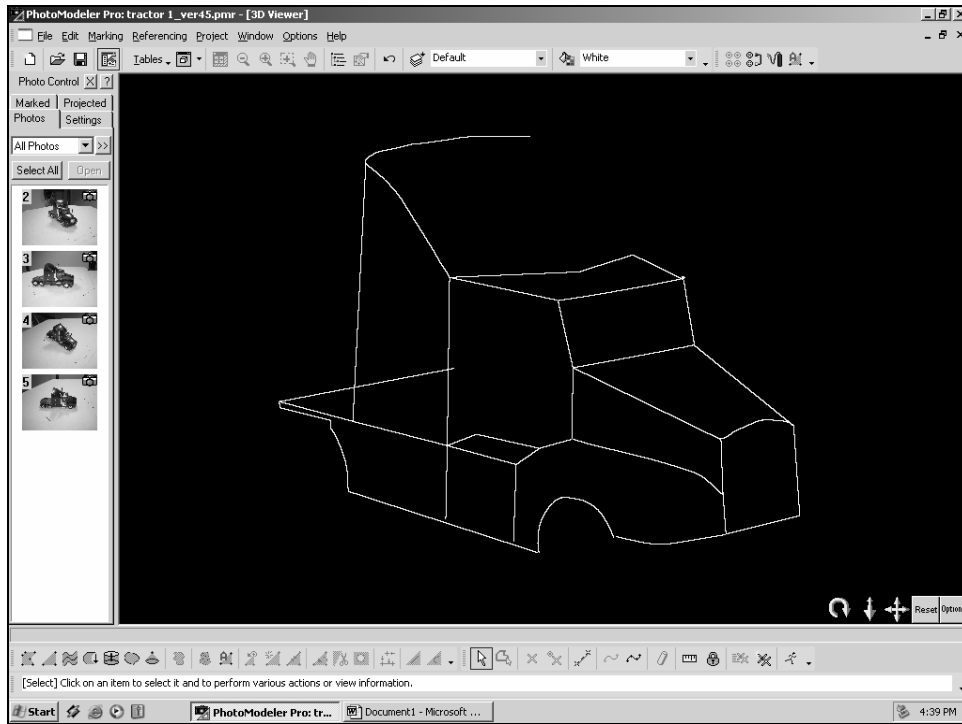


Figure 8. Wire frame model consisting of marked and referenced features

Geometry clean up in Aero CAD

As with any CAD model being used for computational purposes, the accuracy of the tractor-trailer wire-frame model must be checked and geometry cleaned up to resolve connectivity issues that may surface during grid generation (i.e., corners where the ends of wireframe elements do not coincide precisely). To do this, the completed wire frame model was exported from PhotoModeler into Aero CAD in IGES format.

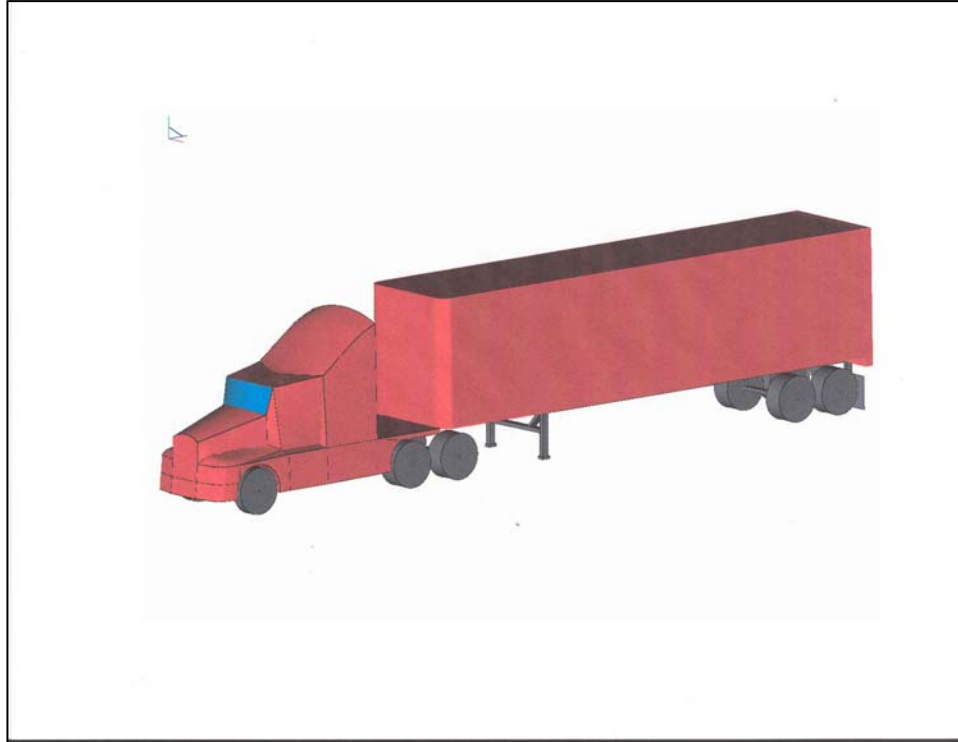


Figure 9a 3-D CAD model after geometry clean up in Aero CAD

The tractor and trailer were imported separately into different layers for ease in handling. Since only one half of the tractor was modeled in PhotoModeler, the geometry was mirrored about the plane of symmetry to complete the tractor. Both the tractor and trailer geometry were cleaned up and any discontinuities corrected. Tractor-trailer alignment was checked and gap distance fixed. Finally a rectangular box was created around the vehicle with dimensions of the wind-tunnel test section. The exact test section cross-section and floor ramps were modeled later on in GAMBIT. The height of the vehicle chassis from the tunnel floor was adjusted based on the experimental setup. Also, the bottom of each tire was cut off so that they sat flat on the floor. The cut-off height was decided based on an estimated contact surface area.

Boundary Surface Definition

Grid or mesh generation is probably the most critical aspect of a CFD problem and consumes up to 80% of human resources. Grid generation involves discretizing boundary surfaces of the flow domain and creating a volumetric grid before a code is used to solve the governing equations. Generally, a 'good' mesh is defined as one that is computationally efficient and possesses excellent resolution in the regions of interest to capture the pertinent flow characteristics.

The tractor-trailer wireframe was converted into a volumetric model by first creating faces from the existing edges and then stitching the faces to form two independent volumes, the trailer being one volume and the tractor or cab portion being the second. The third volume created was the wind tunnel test-section which represents the flow domain.

For GAMBIT to mesh the flow domain, i.e. the volume between the tractor-trailer and the modeled test-section, the tractor and trailer volumes must be subtracted from the test-section volume. This was done using the boolean functions for volumes. The resulting volume represents the fluid zone and is ready to be meshed.

All surfaces were meshed with triangular elements using the *pave scheme* and by specifying the node spacing based on an interval size. The *pave scheme* is the only scheme available for triangular elements and results in a mesh consisting of irregular triangular elements. The node spacing can be assigned by either specifying an interval size, interval count, or as percentage of the shortest edge. Based on the input parameters for the element type, scheme, and spacing, GAMBIT assigns nodes on the face and creates elements. Finer meshes were created for all the faces on the under-side of the tractor-trailer including the test-section floor immediately below the model. The skewness of face mesh elements needs to be kept under check, because highly skewed elements can prevent meshing of the volume. All faces were checked for highly skewed and inverted (negative area) elements. The maximum skewness was less than 0.77. Figure 9b shows the cab-trailer face meshes for the coarse grid.

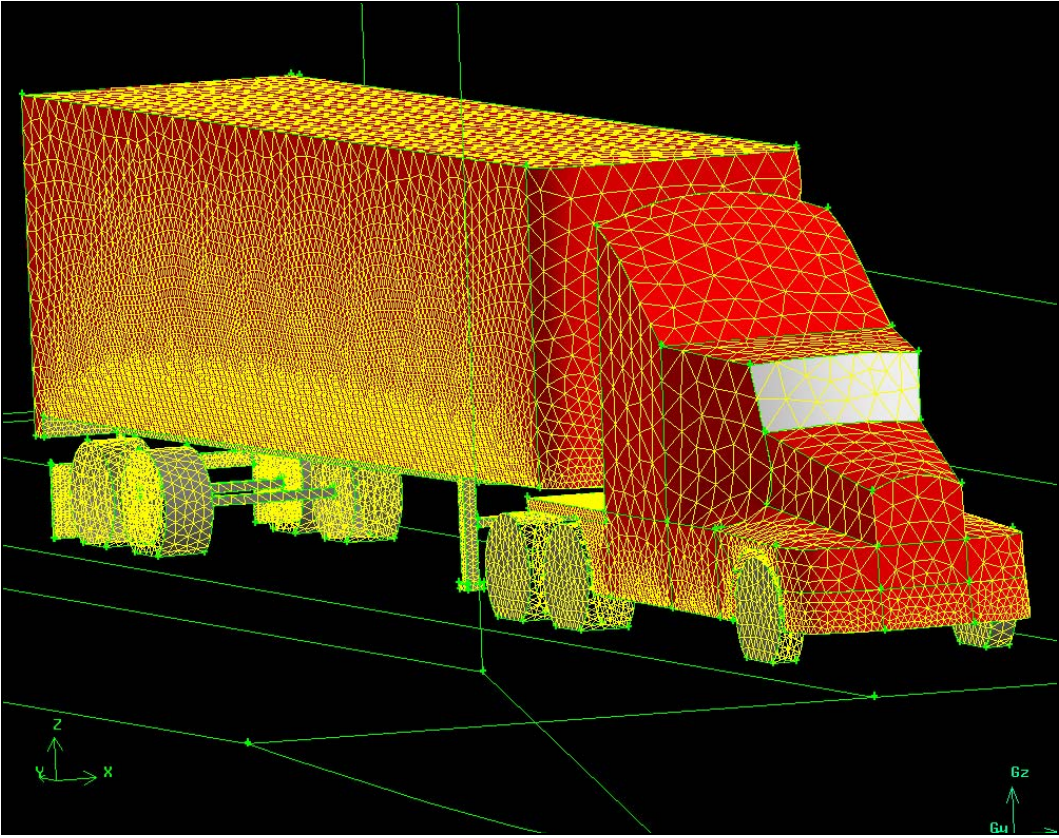


Figure 9b. Unstructured triangular surface meshes

Meshing the volume

The volume was meshed using tetrahedral elements and the TGrid scheme. Since all faces were previously meshed, no node spacing was specified for the volume. Based on the fine face meshes on the model and the relatively sparse face meshes on the test-section walls, GAMBIT creates an optimal unstructured grid with higher grid density in the vicinity of the tractor-trailer. The grid is most concentrated on the under-side and behind the trailer. The total number of elements for the coarse mesh was 0.57 million. The volume grid was checked for skewed and inverted (negative volumes) elements. The maximum skewness was found to be below 0.8. In order to conduct a parametric study and establish grid independence, this coarse mesh was refined twice to an intermediate mesh with 0.97 million elements and a fine mesh with 1.77 million elements. Figure 10 displays the tetrahedral elements in the vicinity of the model on a longitudinal plane.

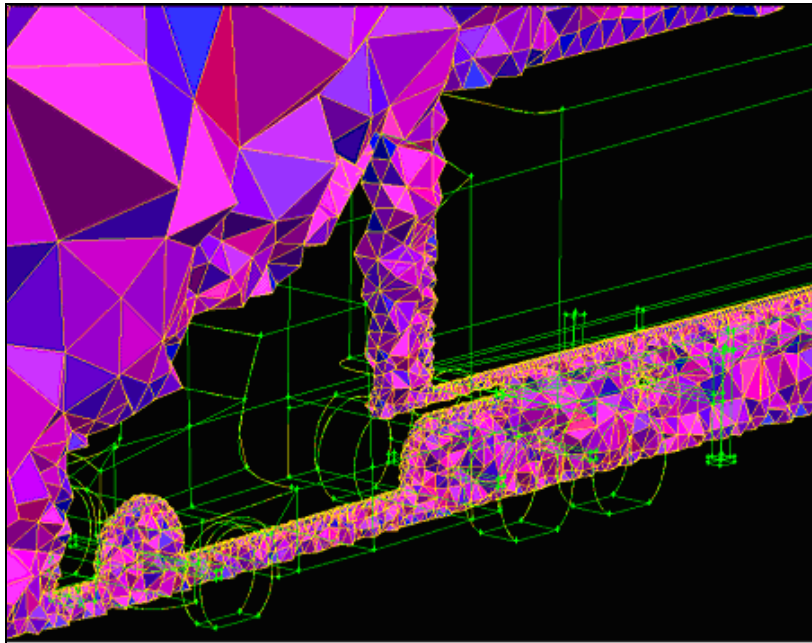


Figure 10. Longitudinal section displaying tetrahedral elements

Defining boundary conditions and continuum

When computational fluid dynamics is used to simulate a real physical system, the boundaries of the domain in the computational model need to be correctly defined in order to accurately represent the physical system. The allowable boundary types are decided by the kind of solver selected in GAMBIT, which is FLUENT 5 for the present case. The physical system being modeled is the test section of an open wind tunnel, and the associated boundaries are the test section inlet, outlet, and walls including the tunnel floor. This case is identified as Case 1. Subsequently, a diffuser was also added, and the same procedure was followed, as previously described. This case is identified as Case 2. Figure 11 illustrates the difference between the two cases.

The test section and diffuser sides, roof and floor were defined as *walls*. The test-section inlet was defined as a *pressure inlet* for both cases. The test-section outlet and diffuser outlet were defined as *pressure outlet* for Case 1 and Case 2 respectively.

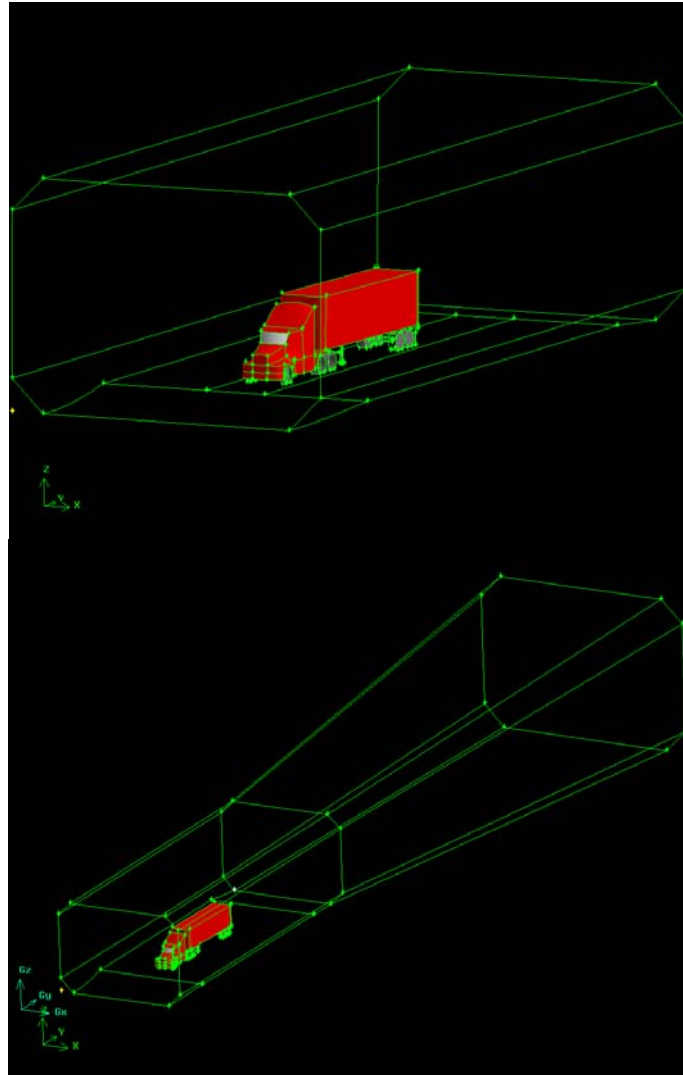


Figure 11. Computational models with and without diffuser

By default, GAMBIT treats all the boundaries surfaces of the tractor-trailer as walls when exporting the mesh. If necessary, the boundary type for a topological entity can be changed once the grid file is read by the solver (FLUENT). The continuum was selected to be a fluid. The mesh was then exported to be read by the solver.

CFD Analysis Results

At the coarse grid level, three Case 1 simulations were completed for varying inlet speeds of 60, 70 and 80 mph, which were specified via total and static pressure at the inlet. A coarse grid diffuser case (Case 2) was solved for a pressure-specified inlet speed of 80 mph. To complete the grid sensitivity study, a fine and ultra-fine grid were solved for Case 1 at a pressure-specified inlet speed of 80 mph to arrive at an optimal grid. Due to computational resource limitations and time constraints, this study could not be conducted on Case 2. All CFD and experimental studies are zero yaw angle cases.

The general trend of the flow remains the same in all cases, Hence, flow visualization and contour plots are shown only for the coarse grid Case 2 that includes the diffuser with a pressure specified inlet speed of 80 mph. Figure 12 shows the general flow characteristics around the vehicle, and Figure 13 shows the general flow associated with the vehicle wake. Figure 14 shows wind velocity detail in the vicinity of the rear of the vehicle.

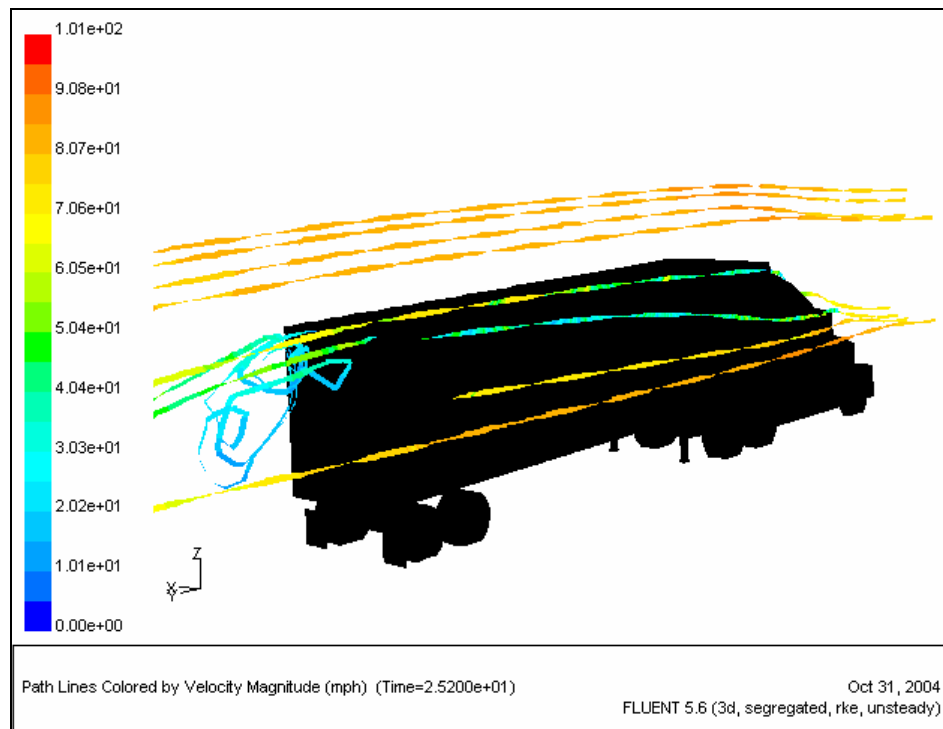


Figure 12. General characteristics of flow around a tractor-trailer shown by stream tubes.

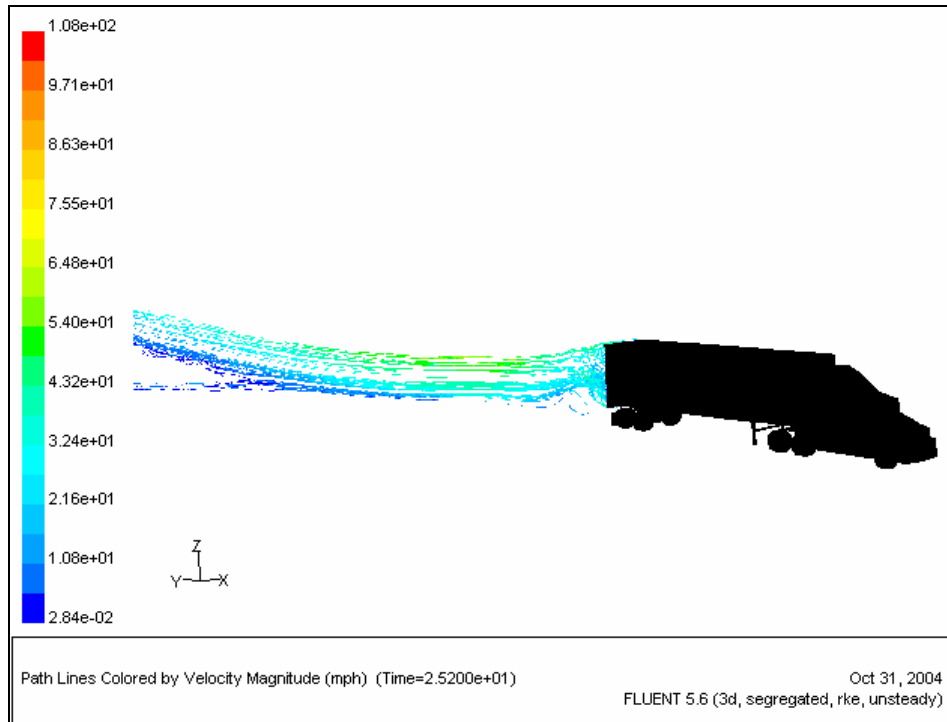


Figure 13. Path lines of downstream trailer wake

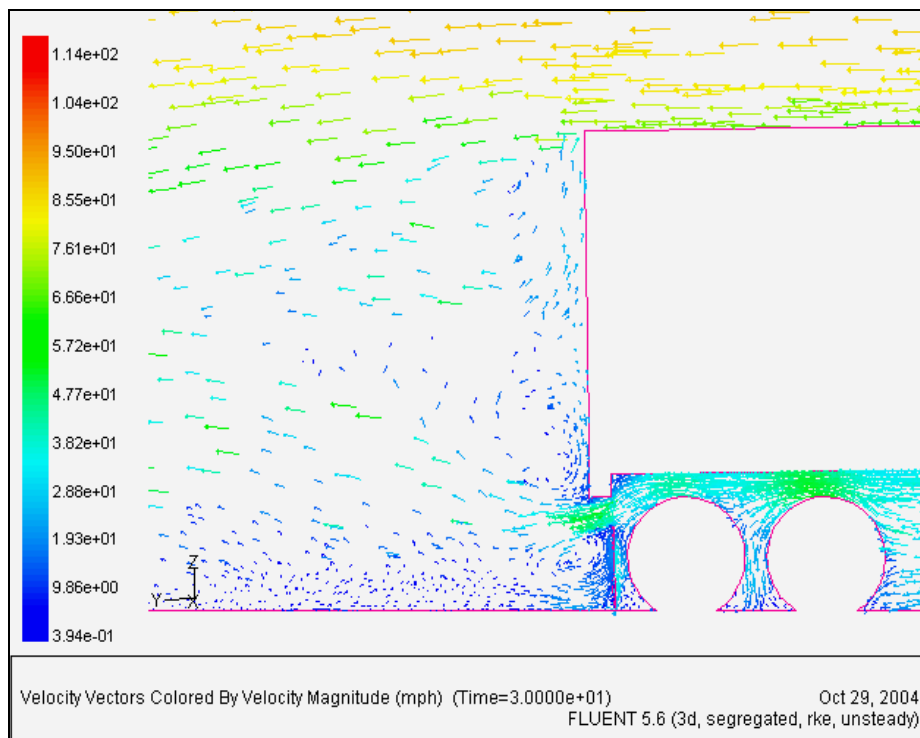


Figure 14. Velocity vectors on a longitudinal plane on right side of vehicle

For the sake of the present study, the characteristics of greatest interest are those pertaining to the floor (i.e., the pavement surface) and the space immediately above it. Near the ground, Figure 14 shows low velocities in the plane. Twin vortices form immediately behind the trailer, resulting in the predominant air movement along the ground immediately behind the vehicle being perpendicular to the plan shown in the figure.

Figure 15 shows the static pressure along the tunnel floor. There are three areas where concentrations of negative pressure can be observed: in the vicinity of the first and second axles (nearest the bottom of the figure) and immediately behind the vehicle.

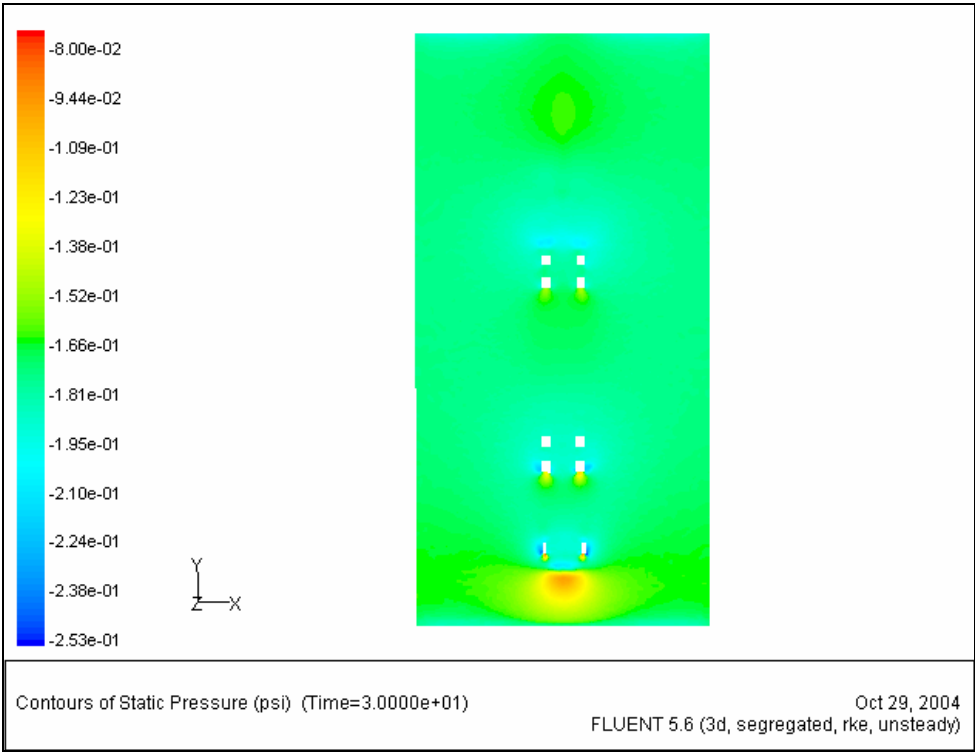


Figure 15. Static pressure distribution on the tunnel floor

Figure 16 shows the total pressure along a plane coincident with the right side of the vehicle. The greatest negative pressures adjacent to the ground plane occur behind the vehicle. This confirms the observations of the performance of the SHRP Rumble Mat, namely that it lifted off the pavement in the wake of tractor trailers (as opposed to underneath the vehicle).

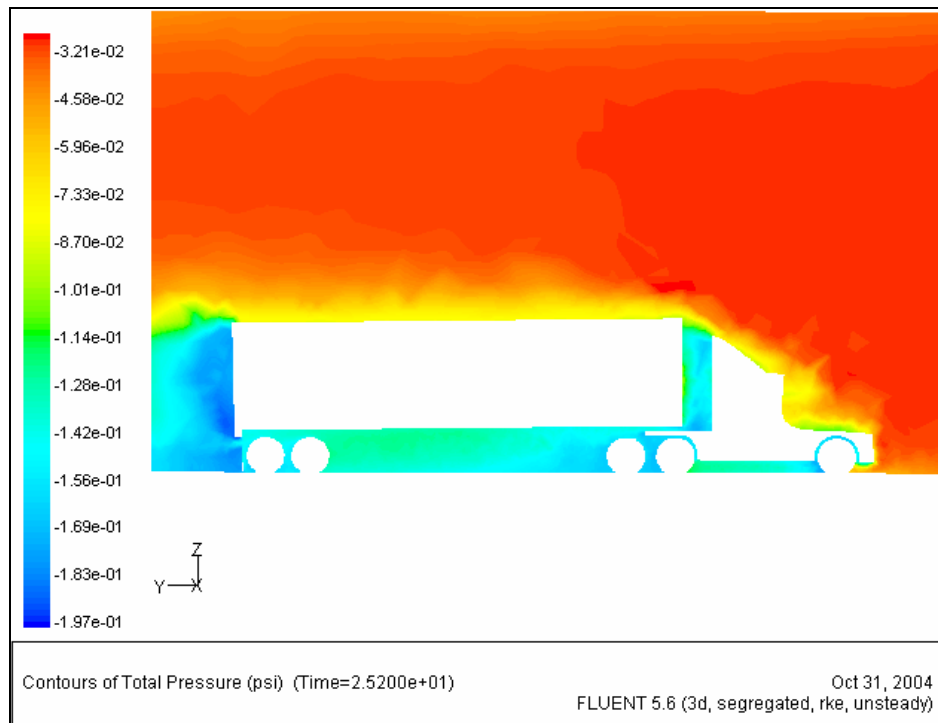


Figure 16. Total pressure along a longitudinal plane on right side of model

Figure 17 is a comparison of centerline floor pressures under the trailer measured experimentally and as predicted computationally for Case 1 and Case 2, at a test-section inlet speed of 80 mph. The grid resolution is coarse in both cases. It can be seen that centerline pressures between 2 and 20 inches on the X-axis for both Case 1 and Case 2, are in good agreement with the experimental data in terms of magnitude as well as trend. The predicted values for Case 2 in this region are more closely matched by the experimental data and fall within the 5 percent error range.

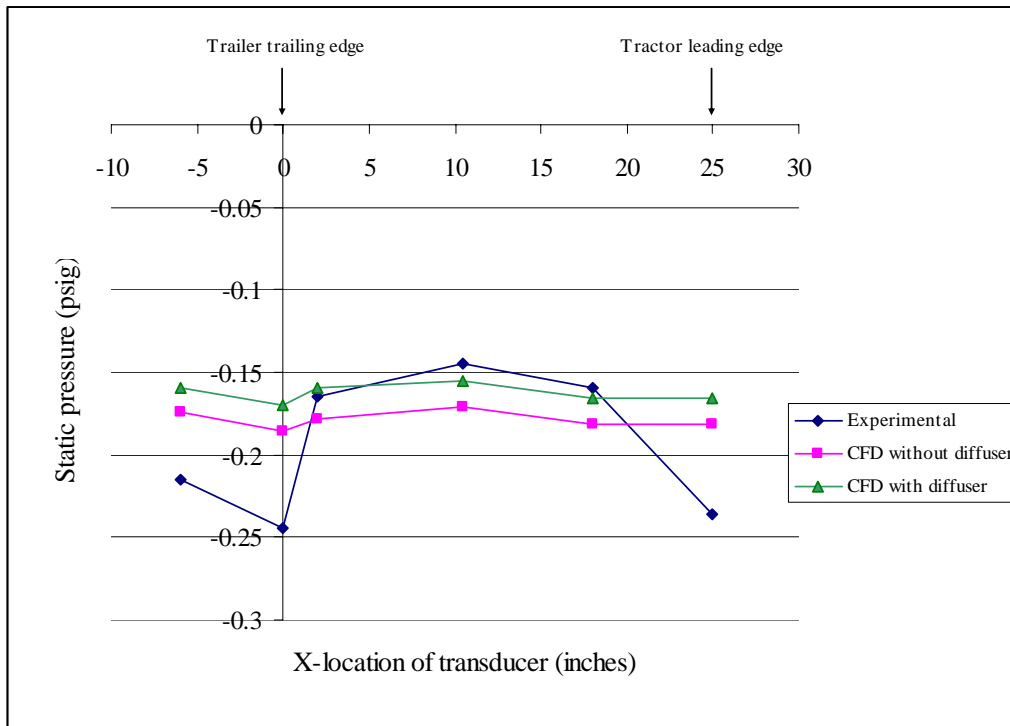


Figure 17. Comparison of experimental and CFD centerline floor pressures under model at an inlet speed of 80 mph and zero yaw

The discrepancy in floor pressure at the trailing edge is probably due to the decreased venturi effect seen by the computational model at the trailing edge of the under-carriage as a result of geometry simplification. Compared to the computational model, because of the smaller cross-sectional area experienced by the flow as it exits the under-carriage in the experimental model, the velocity of the flow is higher and hence pressure is lower. It is also suspected that the mesh resolution is not fine enough to resolve the small vortex core and a diffused response is predicted by the coarse grid.

The reason for the discrepancy in floor pressure at the location just aft of the tractor front bumper is not as apparent. A uniform profile is assumed at the inlet whereas in reality the flow upstream

would adjust to the presence of the model and thus, at the inlet the profile would be non-uniform. Also, in the CFD model, the inlet is a little more than one vehicle length ahead of the tractor and that may not be enough for the flow to fully develop. The effect of geometry simplification at the rear of the trailer would also propagate upstream.

A source of error in experimentation could be that the pressure transducer range is 5 psi and the pressures being measured lie within the lower 10 percent of that range. Although a steady independent power supply was used to excite the transducers, even a small voltage drift would be sufficient to cause a significant error. Hence, the experimental data must be verified to eliminate possible error in data acquisition.

CFD Results for Influence of Bypassing Trucks

Flow characteristics of the bypassing container trucks are studied at four different positions and three different speeds. To generate flow characteristics of the bypassing trucks, a right side wall of the wind-tunnel is moved toward the truck. Four different positions are 10 times (free air case), 2 times, 1 time and 0.5 time truck width (a left side wall of the wind-tunnel is kept at 10 times truck width). Three investigated truck speeds are 70, 100 and 120 mph. A grid is prepared with Gambit and generated mesh is shown in Figure 18 and 19.

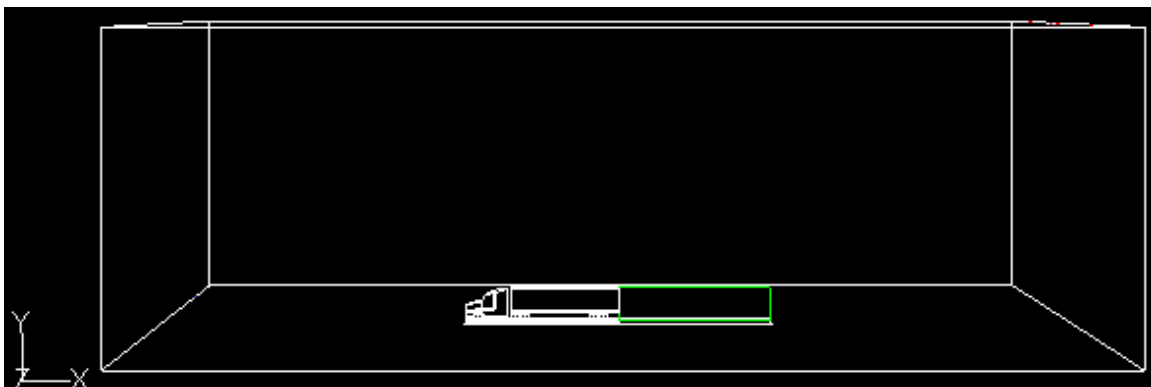


Figure 18 Outline of the Truck Grid for Free Air Case

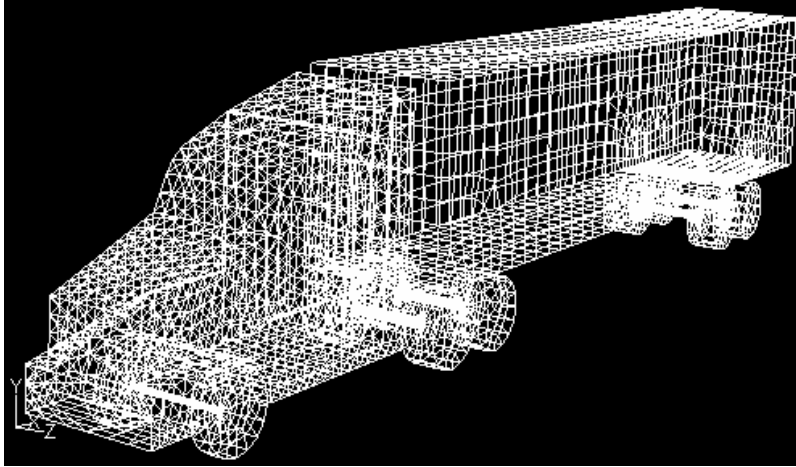


Figure 19 Generated Truck Mesh

Mesh files are imported to Fluent and iterated with velocity inlet and pressure outlet boundary conditions. Calculated flow characteristics of the truck at 70 mph in the free air case and residual are shown in Figure 20 and 21.

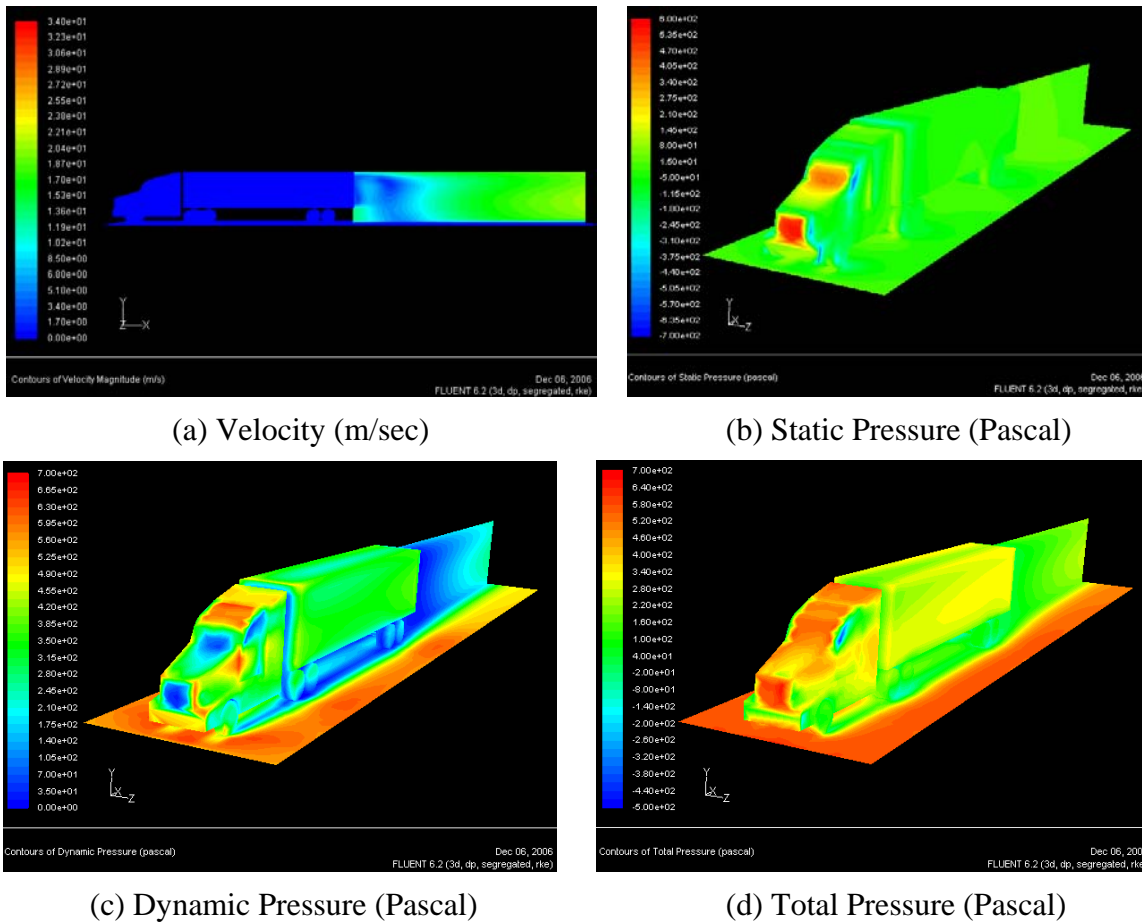


Figure 20 Flow Characteristics of the Truck (Free Air & Speed: 70 mph)

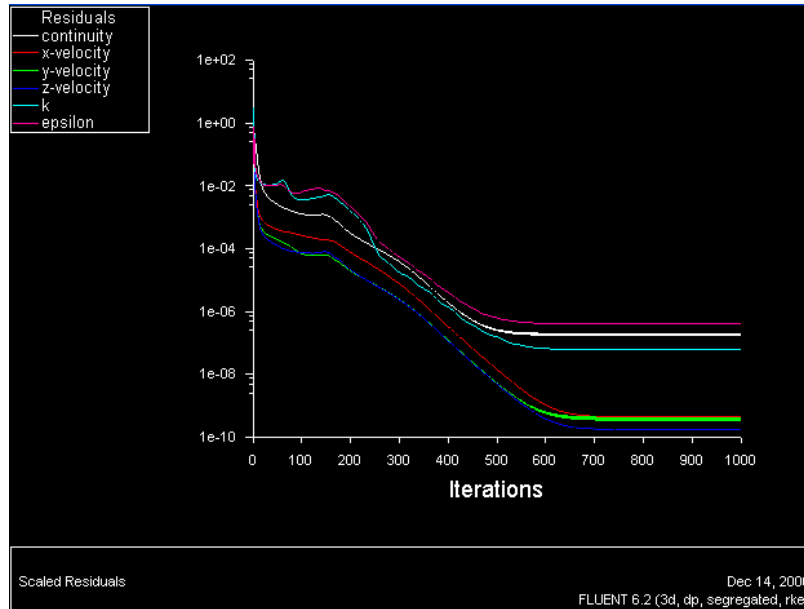


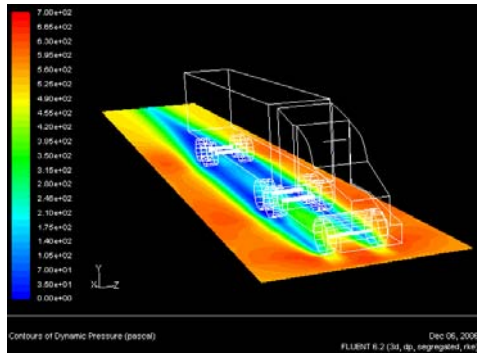
Figure 21 Residuals of the Truck in Free Air Case (70 mph)

Computed flow characteristics of the bypassing trucks at 4 different locations are shown in Figure 22. Only dynamic pressure fields of the bottom of the truck and rear bottom fields are shown, but flow trends are all similar to this. As two trucks bypass to each other closer, low pressure regions along a center line of the truck move toward to each other. For more detailed study the bottom surface is divided to Bottom Right and Bottom Left and Center, but only forces on Bottom Right and Left are compared. These regions are shown in Figure 23.

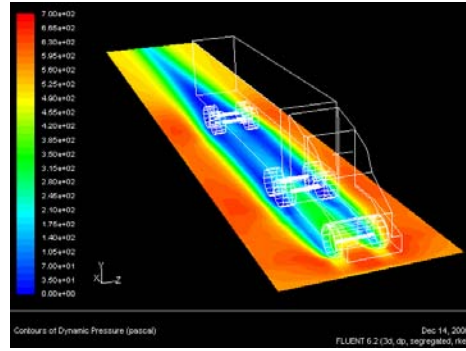
Pressure, Viscous and Total forces are computed for each surface and compared:

$$Force\ Increment(\%) = \frac{Bottom\ Right - Bottom\ Left}{Bottom\ Right} \times 100$$

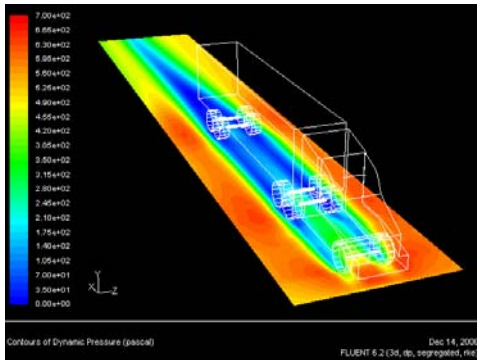
The results are tabulated and plotted in Table 2 and Figure 24. Two flow patterns between the bypassing trucks are detected. For free air to 1 time truck width Total Force increases, which means the bypassing trucks are pushed away from each other more strongly as the distance is shortened. However, for $\frac{1}{2}$ time truck width Total force is suddenly changed to a negative value and the percentage is much larger, which means the bypassing trucks are pushed into each other instead of pushing away. When two trucks bypass each other too closely, there is not enough space and time that the flow is fully developed. Thus, the low pressure regions around the trucks, especially behind the containers, have a major impact and generate the suction force.



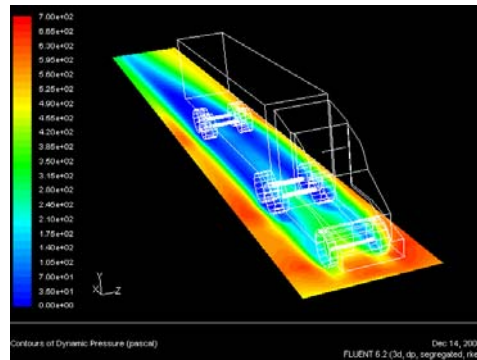
(a) Free Air



(b) 2 Times Truck Width

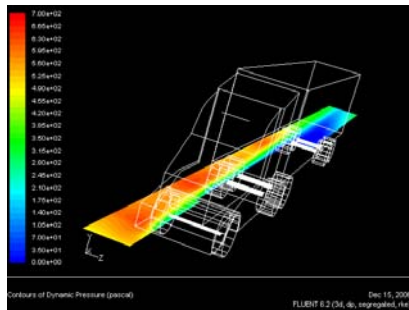


(c) 1 Time Truck Width

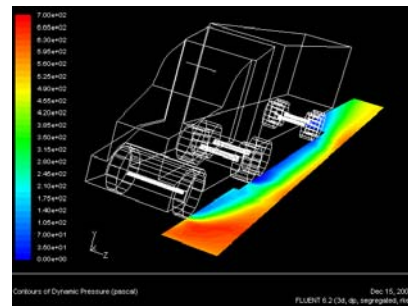


(d) 1/2 Times Truck Width

Figure 22 Dynamic Pressure Distributions (70 mph)



(a) Bottom Right



(b) Bottom Left

Figure 23 Pressure Distributions of the Bottom Surface of the Truck

Table 2 Force Increment of the outside bottom surface of the truck at 70 mph

Distance	Pressure Force (%)	Viscous Force (%)	Total Force (%)
Free Air	0.49	3.54	0.74
2	1.66	1.79	1.66
1	5.28	-5.71	4.76
1/2	-8.42	-12.96	-8.71

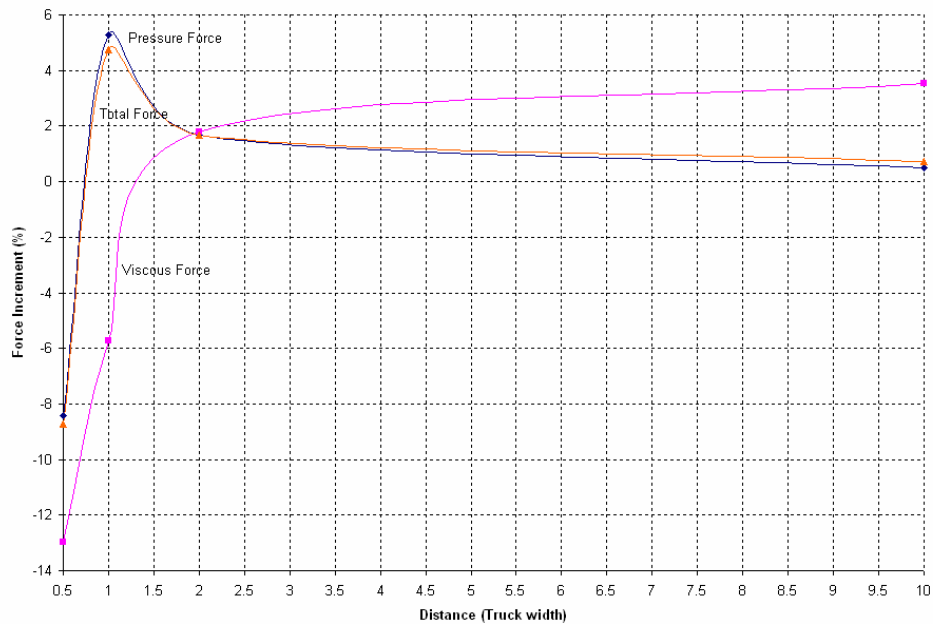


Figure 24 Force Increment of the outside bottom surface of the truck at 70 mph

The suction force between the bypassing trucks is further studied at the three different speeds, 70, 100 and 120 mph. The results are presented in Table 3 and Figure 25.

Increments of the Forces stay about the same, but stronger flow fields are generated as the speed of the trucks is increasing. Flow fields studied include:

- D.F, Difference of the Force (N, kg.m/sec²) = Bottom Right – Bottom Left

- D.F (N, kg.m/sec²) divided by g, g = 9.8 m/sec²

- D.F (kg) divided by the Bottom Area (Right + Left, 114.61 m²)

- D.F (kg/m²)

Calculated D.F (kg/m²) is applied to one side of the truck container (Length x Height, 12m x 2.85 m). The results are tabulated in Table 4. When two trucks are bypassing at the speed of 120 mph, 8.67 kg, 18.99 lbs, of the suction force is acting on the bypassing side of the truck containers. This suction force might be critical because of generating unbalanced flow fields around the bypassing trucks at relatively high passing speed, 120 mph. Also, the unbalanced flow field might have significant effects for vehicles following behind the trucks depending on situations. Further study of the flow effect might be needed.

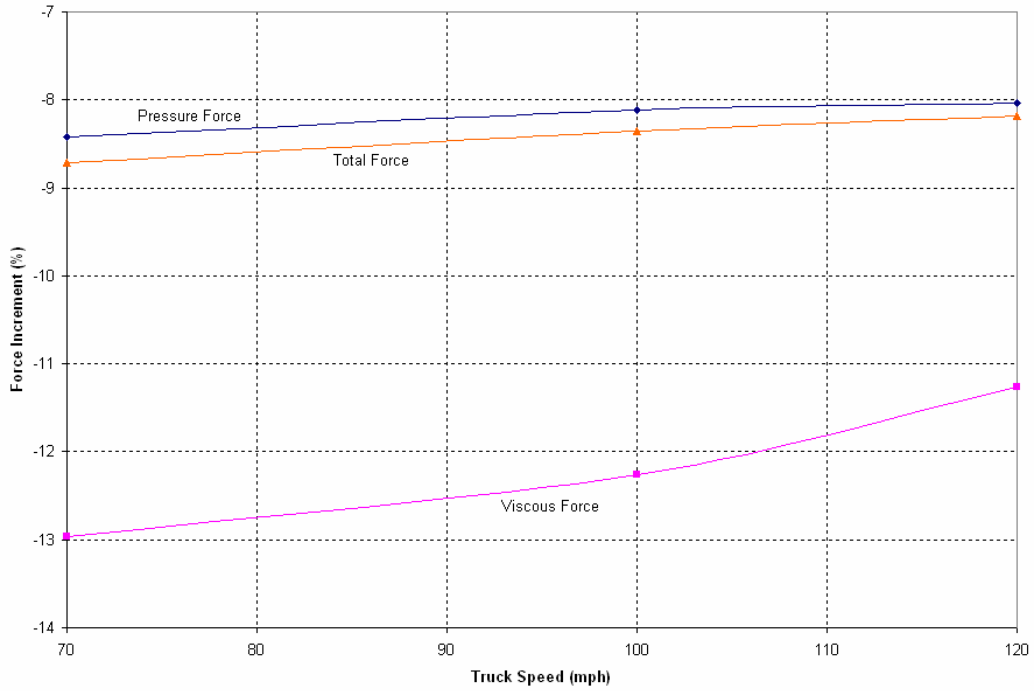
Table 3 Force Increment of the outside bottom surface of the truck at the 1/2 distance

Speed (mph)	Pressure Force (%)	Viscous Force (%)	Total Force (%)
70	-8.42	-12.96	-8.71
100	-8.12	-12.26	-8.35
120	-8.04	-11.26	-8.18

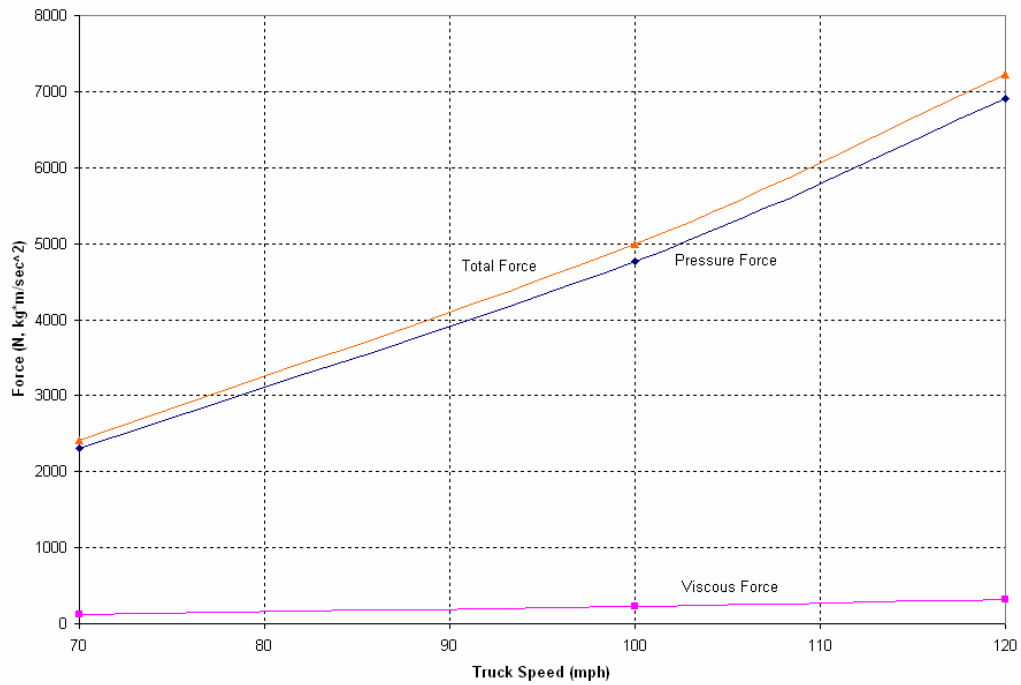
Table 4 Generated Suction Force at the 1/2 distance

Speed (mph)	Bottom Right (N)	Bottom Left (N)	D.F (N)	D.F (kg)	D.F (kg/m ²)	Force acting on the bypassing side of the container (kg)
70	1160	1260	-100	-10.20	-0.089	-3.04 (6.66 lbs)
100	2397	2596	-190	-20.31	-0.177	-6.05 (13.25 lbs)
120	3473	3758	-285	-29.08	-0.254	-8.67 (18.99 lbs)

* Negative sign represent Suction Force



(a) Force Increment of the outside bottom surface



(b) Increment of the Force (N, Bottom Right + Left)

Figure 25 Force of the outside bottom surface of the truck at the 1/2 truck width

Vehicle Modeling Analysis

Another issue encountered with devices intended to serve as portable rumble strips has been longitudinal creep, the tendency of the device to move down the highway in response to the impact force between the strip and vehicle tires. Direct measurement of the forces acting in the tire-strip interaction would be very difficult and beyond the scope of this work. However, as with the aerodynamic modeling, computer models can provide insight where empirical measurement is infeasible.

Two companion computer simulation packages, CarSim and TruckSim, were used to examine passenger cars and heavy trucks, respectively, with respect to the motion and forces involved in the tire-strip interaction. Three vehicles were selected to use in simulation runs, a typical passenger car, a large SUV, and a tractor-trailer. Figure 26 shows the maximum horizontal loads observed between the tires and the strip for both passenger vehicles at various speeds. The maximum vertical loads—2,600 lbs for the hatchback and 5,300 lbs for the SUV—were nearly constant for all speeds examined.

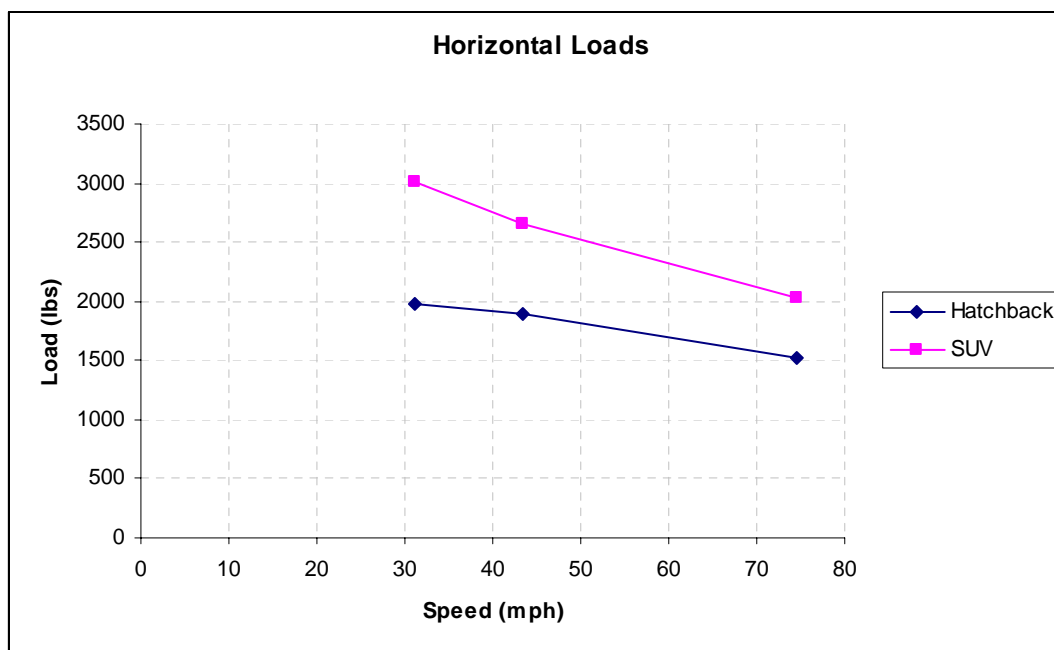


Figure 26. Horizontal load for passenger cars.

Figure 27 shows the maximum horizontal loads between the tires and the strip at various speeds for each axle of the tractor trailer cab. The maximum vertical loads associated with the tire-strip contact were nearly constant with speed, and were 9,892 lbs for the front axle, 26,977 lbs for the most forward of the rear tandem pair, and 25,177 lbs for the rearmost axle. Note that empirical validation of the simulation data is beyond the scope of this project, and thus the values obtained from the simulation packages must be considered estimates only.

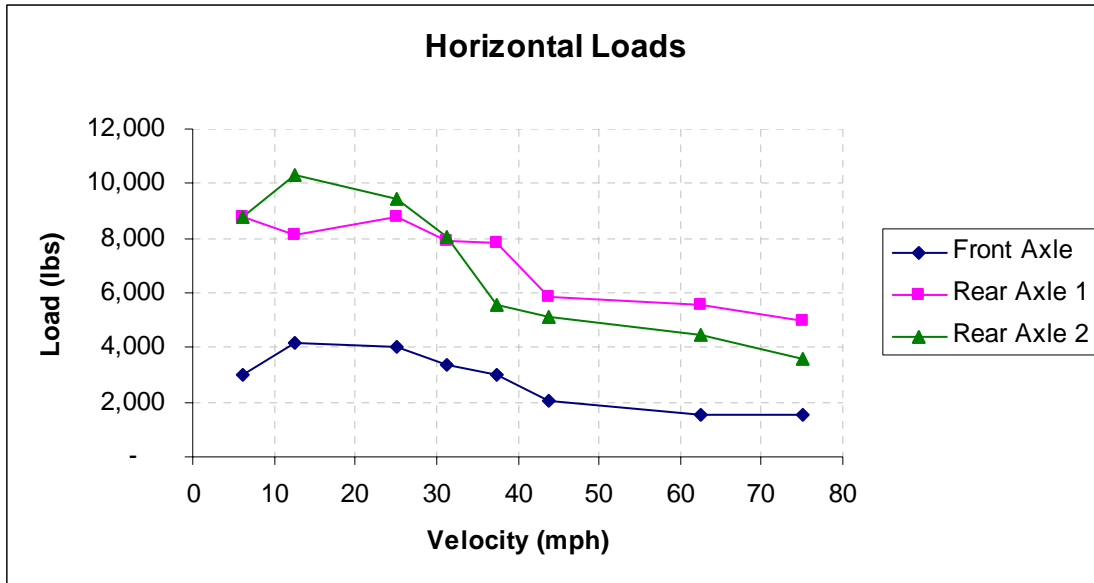


Figure 27. Horizontal loads on cab axles of a tractor trailer.

Speed-Force Relationship

For both the passenger car and for the truck, a phenomenon was observed in the simulation data that seemed counter-intuitive. At highway speeds, the peak horizontal force *decreased* as speed *increased*. Previous studies considering sound and vibration have cited a parallel phenomenon in which the sound and vibration from rumble strips as perceived by the driver is less at higher speeds. Other studies have observed the exact opposite. To examine this phenomenon further, the data from a previous study was reprocessed. In the previous study, the focus was on the difference between the peaks and the ambient noise (or vibration, as the case may be). In the reprocessing, the absolute magnitudes of the peaks were considered along with the duration of the peaks and the area under the peaks (i.e., sound level times duration), as a surrogate for energy imparted to the vehicle through the impact with the strips. For both the sound data and the vibration data, the peak values generally increased with increases in speed. When the area under the peaks was taken into consideration, however, the opposite pattern emerged. As speed increased, the total energy of the event (as represented by the sound level times time) decreased. No hard conclusions can be drawn from these observations, but they do provide some external evidence that the results obtained from CarSim and TruckSim with respect to the relationship between speed and forces is valid. A more complete discussion of this data is provided in Appendix A.

Sliding Forces

The forces acting to push the strip horizontally are large, explaining why creep has been observed in past studies, sometimes even when adhesives were used. The vertical forces

involved are even larger, though, begging the question of how to utilize these vertical forces to help keep the strip from moving during the traversal. In addition to that peak magnitudes of these forces, two other aspects of the system must be considered: the coefficient of friction between the strip and the tire, and the relationship between the instantaneous vertical force and the instantaneous horizontal force throughout the traversal. If the coefficient of friction of the strip on the pavement is high enough, perhaps the vertical force can keep the strip from sliding under the horizontal loading.

Estimating Frictional Resistance to Sliding

Regardless of the material comprising the strip itself, the lower surface could be lined with a different material with a higher coefficient of friction. Given that, the assumption was made that some material with characteristics similar to tire rubber would be appropriate, since the demands are very similar (i.e., provide good traction and be durable). Typical values used by transportation professionals for the coefficient of friction of automobile and truck tires are between 0.40 (20 mph) and 0.28 (70 mph). These values represent wet pavement, because highways must be designed to accommodate a wide variety of circumstances, including wet weather. The device under development, however, is unlikely to be in use under adverse weather conditions, and it could be stipulated that additional means be used to secure the device if it must be used on wet pavement. Thus, a coefficient representing dry pavement could be used. Values for the coefficient of friction of rubber vary widely based on composition. Some values are shown in Table 5.

Table 5. Values for the Coefficient of Friction for Rubber

Contacting material and condition	Coefficient
wet pavement (20 mph) (green book)	0.40
wet pavement (70 mph) (green book)	0.28
concrete (Center for Advanced Frictional Studies, NSF)	1.0-4.0
steel (Center for Advanced Frictional Studies, NSF)	1.6

A conservative value appears to be 1.0, and this value was selected for use in design analyses. Given that value, the vertical loads from the vehicle would generate sufficient friction between the pavement and the strip to prevent slippage, based on the *maximum* loads reported by TruckSim and CarSim.

Temporal Relationship of Forces

The second aspect of the problem is the temporal relationship between the vertical and horizontal loads. When the tire initially impacts the strip, the horizontal load are at a maximum, decreasing as the tire mounts the strip, while the vertical load increases to a maximum occurring some time after the initial impact.

A close examination of the data output by CarSim and TruckSim showed that horizontal force of the tire on the strip did peak before the vertical force reached its maximum value. But it also showed that the maximum ratio of vertical to horizontal force remained below 1.0, providing

evidence that a rubber liner may be sufficient to prevent sliding. The value was high enough, however, that the concern remained, especially in less than ideal conditions.

Preliminary Design

The design process comprised a combination of empirical observation and mathematical analysis. The initial focus was the resistance to lifting, which seemed to be the primary shortcoming of other devices tried in this context. A design was developed based on the lift analysis and other anticipated issues, such as the potential for the device to slide. Empirical observations revealed other issues that needed to be addressed, such as the device tipping under braking loads or bouncing after impact with the tire. The testing also confirmed that sliding was not a critical problem, even without the use of flanges (a potential remedy to sliding, discussed later). Based on the testing, three mathematical analyses—lift analysis, tipping analysis, and stress analysis—were used to identify design specifications that would satisfy the respective criteria. The final design was tested empirically.

A total of three design concepts have been developed, each based on characteristics of and addressing problems identified in the previous conceptual design. Resistance to lift was the primary motivating factor driving the initial design. This is the design that was used in all empirical tests as well as in the vehicle simulations (rumble strips were not modeled in the aerodynamic or CFD analyses). The initial design was modified to address the problem of tipping, as observed in the video taken during testing. The final design concept was then developed to address concerns pertaining to bounce. The following sections present a chronological account of empirical and analytical observations and resulting design decisions.

The design described in the original work plan (shown in Figure 28) was quickly abandoned when the wind tunnel data showed that the weight of such a device would have to be exorbitant in order for it to resist the lifting forces in a truck wake. The design concept shifted to focus on an individual strip. If multiple strips were desired, several could be deployed together, but for design and analysis purposes, they would be treated independently.

A side view and a top view of a draft design are shown in Figure 1 and Figure 2, respectively. This will serve only as a starting point for applying the results of the various analyses.

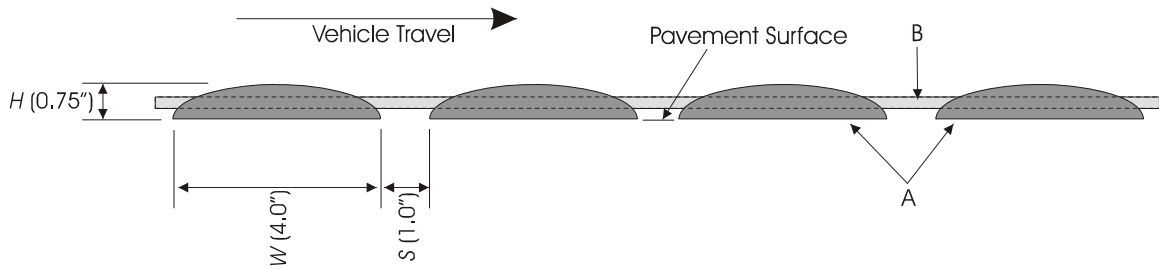


Figure 1. Side View

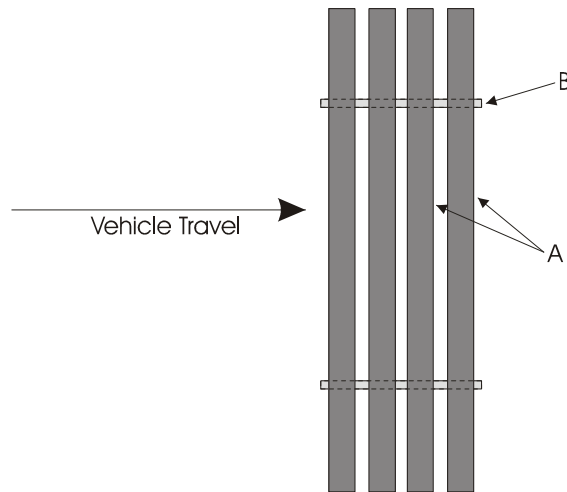


Figure 2. Top View

Dimensions:

- Height: $0.25'' < H < 0.75''$
- Width: $1.0'' < W < 4.0''$
- Spacing: $1.0'' < S < 20.0''$

Part A (strips) comprises strips with a semi-ellipse cross section. Each strip must be either 4-ft long (one unit for each wheel path, or 10-ft long (one unit for both wheel paths). Strips may be made of rubber.

Part B (joiners) comprises a joining rod or cable, approximately $\frac{1}{4}''$ in diameter.

Figure 28. Conceptual design described in the original work plan.

Profile

The semi-elliptical shape of the initial conceptual design would eventually prove to be viable conceptually, but extremely inconvenient in terms of fabrication, especially for the prototypes. The most effective shape with respect to maximizing the weight per unit area (i.e., maximizing the lift resistance) would be a rectangular profile, which makes the entire area of the main bar the maximum height, whatever that turned out to be. However, concern was expressed that the presence of a sharp corner on the upper leading edge of the strip might be enough to damage a car tire under certain conditions (e.g., prolonged high speeds in high heat). A rounded profile seemed to provide a balance between weight per unit area and a tire-friendly leading edge.

A cursory examination of the geometry of a tire impacting a semicircular strip—shown in Figure 29—revealed that a significant portion of the strip at the leading and trailing edges of the profile did not come into contact with the tire during traversal.

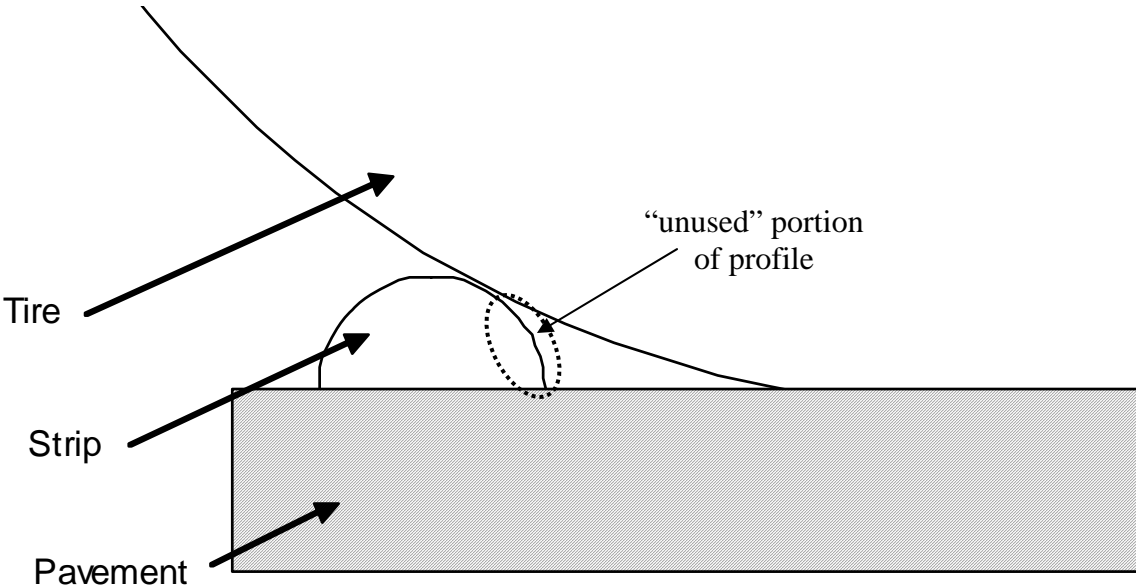


Figure 29. Sketch of initial tire-strip impact.

To take advantage of this characteristic of the tire-strip interaction, the edges of the profile were trimmed, thereby increasing the weight per unit area of the strip, since the portion being trimmed is that with the least thickness. Figure 30 shows a cross-section of a trimmed bar design. The dashed line represents the surface of the strip without being trimmed. The amount of trim was expressed in terms of inches measured from the outside surface of the trimmed bar to the outside surface of a semicircular cross-section with the same height.

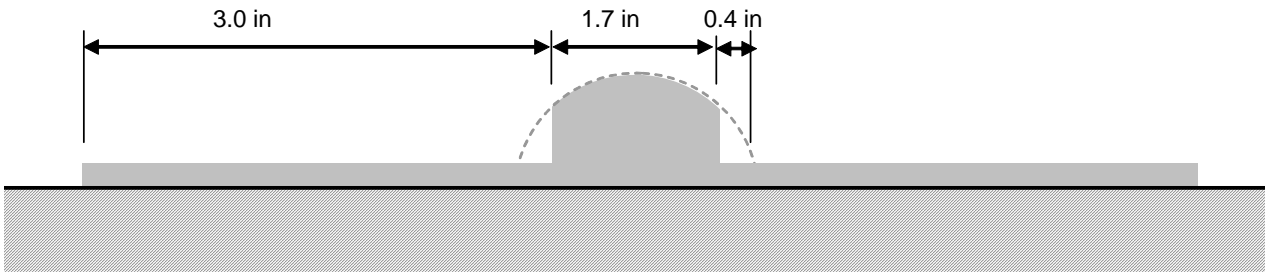


Figure 30. Illustration of a trimmed bar design.

Flange Design

Because the simulation data suggested that sliding may be a problem in any but ideal conditions, flanges were added to the design. The flanges were intended to allow the weight of the tire itself to hold the device in place during the initial impact with the strip. Several flange concepts were examined. The primary difficulty was the conflicting advantages of flexible flanges versus rigid flanges.

Flexible Flanges

The effective lifting force on the device is determined by the average weight to unit area. Flanges made of a flexible material would allow them to simply curl upward, reducing the effective area of the device when negative air pressures were trying to lift it off the pavement. However, there is also an area of significant negative pressure in advance of the front axle of a truck. A flexible flange would lift upward and the front axle would push it over top of the strip, defeating the purpose of the flange.

Rigid Flanges

A flange made of a rigid material would not be pushed over the strip by the front axle, but because it is rigid, it adds to the area of the strip. While it also adds a little weight to the strip, the net effect is a significant reduction in the overall weight to unit area. The reduction would vary with the dimensions and composition of the strip, but would be likely to be at least a factor of 2. Such a reduction could not be accommodated with available materials.

A solid rigid flange was infeasible, but it was recognized that the majority of the flange was not strictly necessary for the purpose of preventing sliding. The need was for some portion of the flange to be pinned underneath the tire during the initial impact with the main bar of the strip, which is when the ratio of horizontal forces to vertical forces was expected to be the highest. So, if the leading edge of the flange were the right distance from the main bar, only that leading edge would be required to hold the device in place. So a truss flange was developed with two cross members, one set at a distance from the main bar appropriate for truck tires and the other at a

distance appropriate for passenger car tires. The truss design would contribute to the overall device area only a fraction of the area associated with the solid flange, but its effectiveness in preventing sliding should be equal.

Figure 31 shows the initial conceptual design of the strips using a rigid truss flange. Simultaneously to the development of the flange design, the overall approach shifted to a segmented design for several reasons, including easier storage and deployment, and the potential for the joints to be flexible, thus helping accommodate uneven pavement due to rutting.

The design shown in the figure was refined, adding an additional cross member to the flange to help guarantee that both truck tires and passenger car tires would hold the flange stationary during initial impact with the main bar. An initial design for the coupling of the individual pieces was also developed. The design would allow tool-less installation and disassembly and secure operation. It would provide one degree of freedom so that the joint placed in the wheel path could adapt to whatever amount of rutting might be present. The flexible joint would also help to accommodate some bouncing without displacing the entire strip. Specifications for the refined design were developed, and renderings of the CAD model are shown in Figure 32.

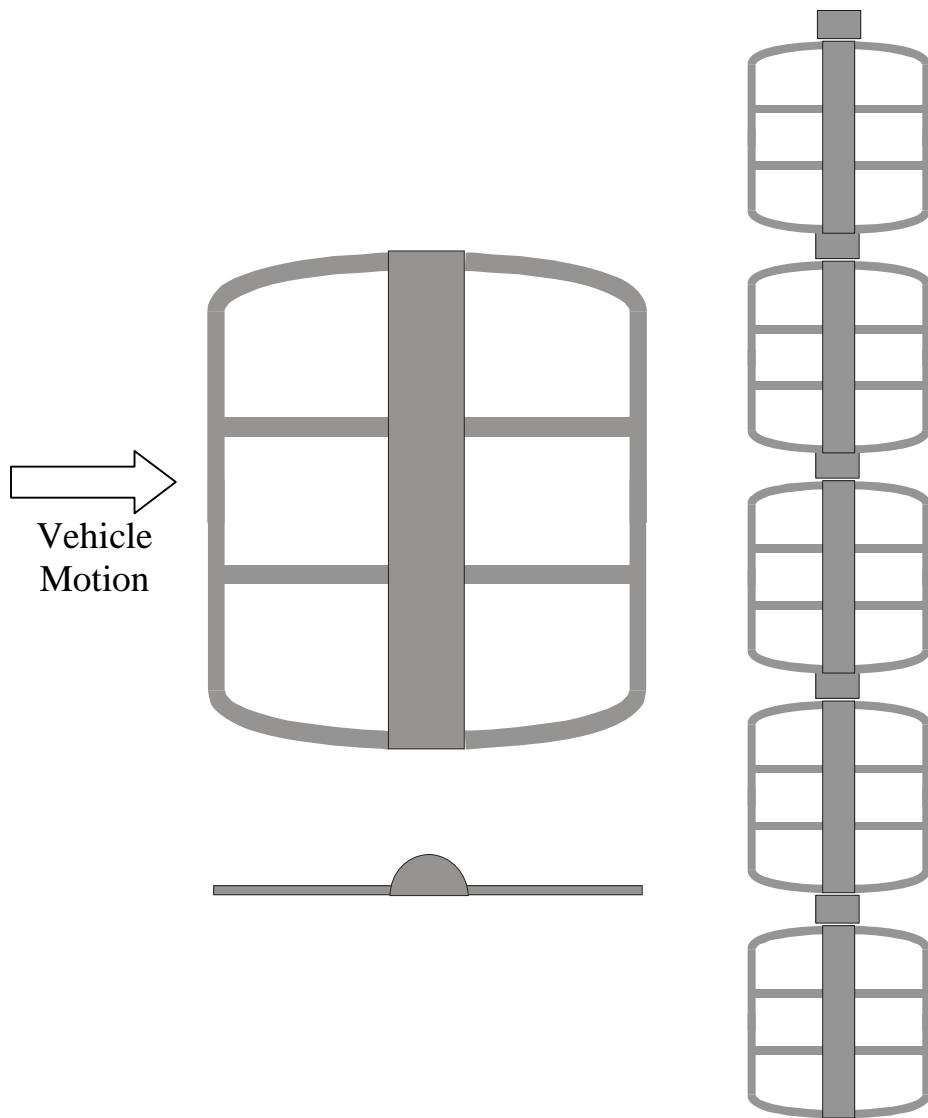


Figure 31. Conceptual design using segmented strip and rigid truss flanges.

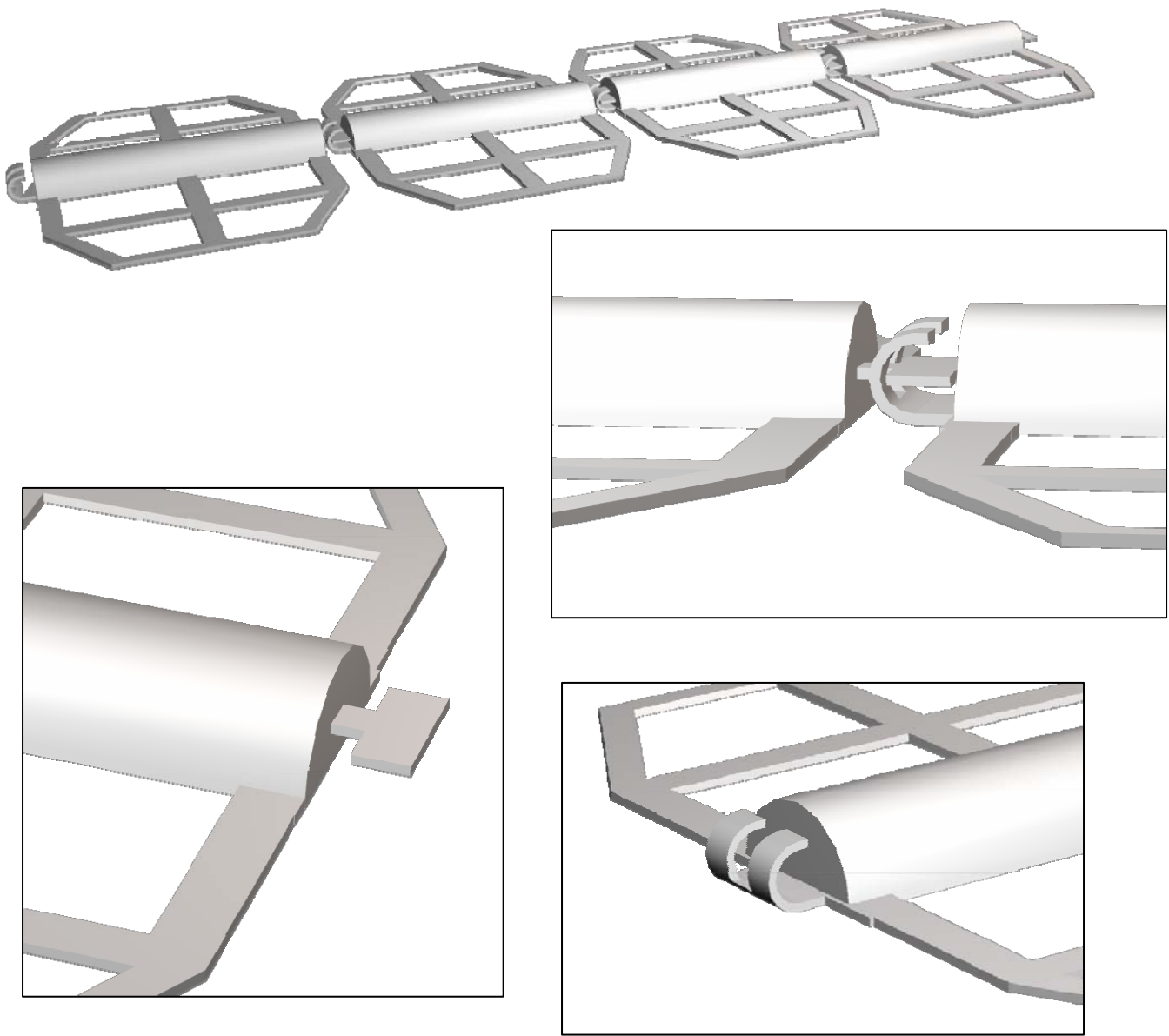


Figure 32. Initial fully specified design.

Using data collected during the first field test, it was determined that a single cross bar on the flange could be located so as to be effective for both passenger cars and for heavy trucks. The tapered corners were removed to ensure that a tire could not hit right on the gap and not be properly resting on the flange during impact with the bar. The resulting design is shown in Figure 33.

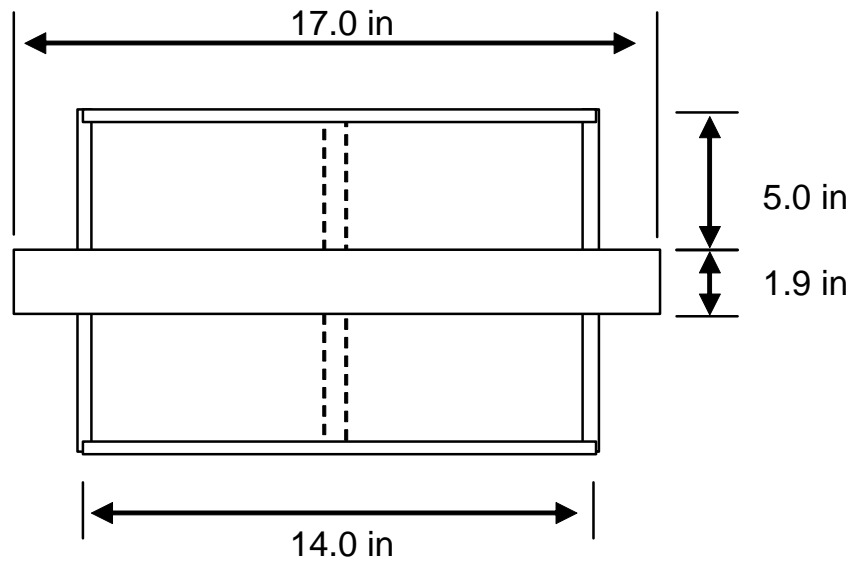


Figure 33. Flanged design with single cross member.

Composition

Identifying the most appropriate material composition for the strip began by setting several restricting parameters. It is worth noting that the number of parameters affecting the design that are unknown (and undeterminable under the scope of this work) is substantial. Consequently, many of the parameters must be initially set based on subjective assessment of the related issues. The numbers can be expected to need adjustment when the results of the field testing are considered, but some starting value was needed.

First, a nominal height of 1 inch was chosen. Heights of 0.75 inches are acceptable (i.e., do not generate so much noise and vibration that a driver might be alarmed and respond erratically). (Meyer, 2003) The upper limit for an acceptable height is unknown, but it is likely greater than 0.75.

The flanges were set to be ¼-inch thick. The competing goals associated with the flange thickness were minimizing the thickness to minimize the horizontal forces involved in the initial contact with the flange (i.e., make sure the strip doesn't slide when the tire impacts the flange) and maximizing the thickness so that the flange would add as much weight as possible and (more importantly) to increase resistance to bending, such as during installation and transport. If a flange were to become bent, it would present a safety concern significant enough that the affected unit would have to be taken out of service immediately. The thickness chosen was a subjective balance between these two issues.

The third parameter to be established was the design value for the negative pressure responsible for the lifting force on the strip. The wind tunnel data was extrapolated to a wind speed of 100 mph (representing a truck traveling 70 mph into a 30 mph headwind), and the corresponding pressure taken from the graph shown in Figure 34. A value of 0.36 psi was used as the preferred design value. A poll of the agencies involved in the SWZDI suggested that a combined wind speed of 90 mph (0.31 psi) would likely be acceptable for this device. Thus the design value of 0.36 psi should be considered as being conservative.

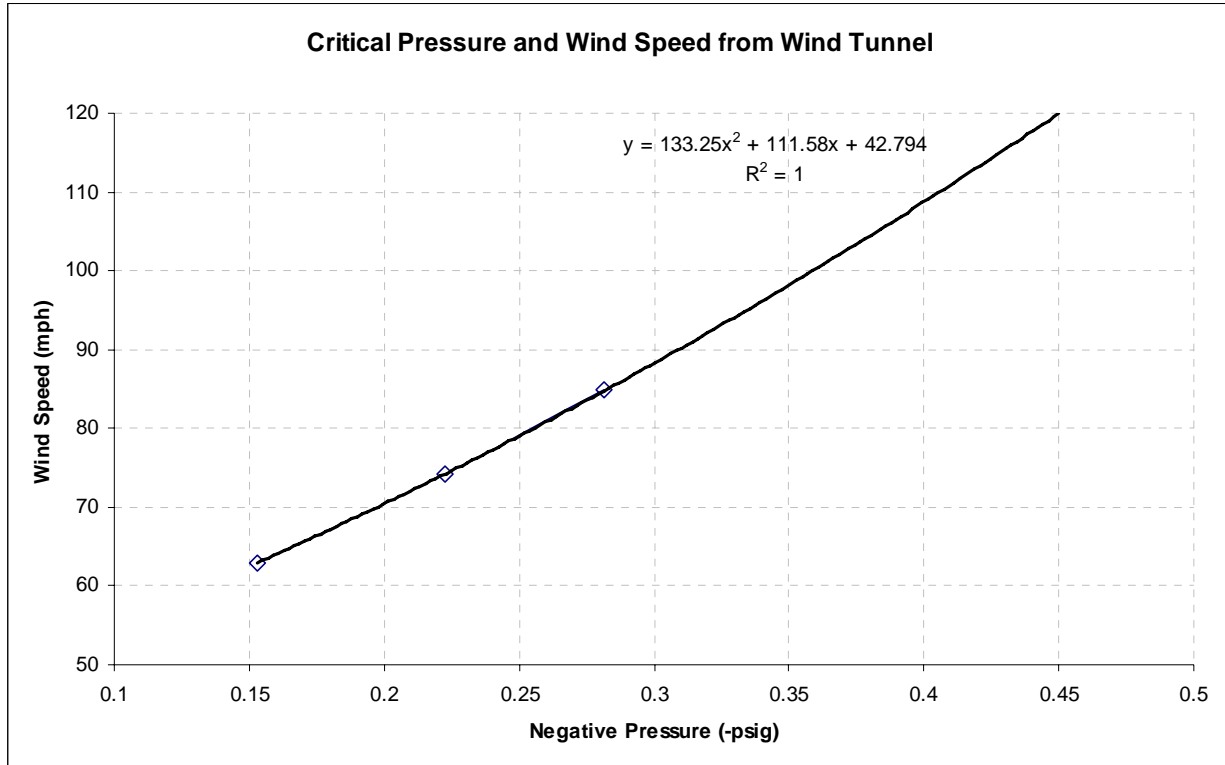


Figure 34. Plot of critical pressures from wind tunnel data.

The addition of flanges—even truss flanges—reduced the average weight per unit area of the device substantially. Given the restrictions, if the device were fabricated entirely from steel, it would still have a weight per unit area less than the needed 0.36 psi. A denser material (e.g., lead) would have to be employed to provide the necessary lift resistance. The device must also be durable, however, and lead is far too soft a material to withstand the magnitude of stresses that would be associated with the forces indicated by TruckSim. So the steel bar would have to be hollowed out and filled with lead. The lead would provide the needed weight and the steel would provide the structural strength.

Preliminary Prototypes

Field Test 1

The initial field test (3/25/2005) was conducted at the Lawrence Municipal Airport using a taxiway that had been closed to all aircraft. The primary goal of this test was to determine the height of the strip that would be used in further study. The two competing requirements that pertain to the strip height were 1) the strip should be perceptible by drivers of heavy vehicles (e.g., tractor trailers), and 2) the strip's effect on passenger cars should not be so severe as to prompt erratic maneuvers. The strip must also not be so large as to cause physical damage (e.g., tire failure), but it was thought probable that the driver perception would be more restrictive than the physical considerations. If both requirements cannot be satisfied, preference must be given to Requirement 2 because of the greater safety implications. The initial test was to identify the largest height of strip that would be acceptable with respect to Requirement 2. In subsequent tests, the perceptibility for drivers of heavy vehicles would be examined.

Sixteen 2-ft long strips were fabricated from wood, with heights between 0.75" and 1.50". Each strip was fabricated with a semi-dodecagon (i.e., 12-sided) cross-section intended to emulate a semi-circular cross-section. A sample is shown in Figure 35. Figure 36 shows a sample of each size of the prototype rumble strips. From left to right, the strips shown have radii of 1.50", 1.25", 1.00", and 0.75", respectively.



Figure 35. Cross-section of a 1.50"-radius prototype.



Figure 36. Section view of four sizes of prototype rumble strips, 1.50'' to 0.75'' (L to R).

Two of any given size—one in each wheel path—allowed a subjective evaluation of driver perception for each size of strip. Beginning with the smallest size, the strips were traversed in a typical passenger car (1992 Honda Accord), first at slow speeds, and then at higher speeds up to about 30 mph. Subjective evaluation was done by each of the 5 researchers present and conclusions reached by consensus. Several important observations were made.

The strips with heights of 0.75'' and 1.00'' were obviously not egregious in their effect.

The strips with a height of 1.25'' were also deemed acceptable, although closer consideration and additional passes were necessary to reach consensus.

The strips with height of 1.50'' were questionable for all observers with respect to the acceptability of the strips effects. The consensus was that they should not be ruled out, but everyone was much more comfortable selecting 1.25'' for the radius of the working design.

The strips bounced significantly, especially at speeds of 30 mph or more.

Field Test 2

The second test occurred the following week (3/28/2005), at the same location as the first test. The purposes of this test were as follows.

1. Examine the relationship between various parameters and speed for both a passenger car and for a truck.
2. Collect data that could help quantify the forces active in the interaction between the tire and the strip.
3. Determine if the strip slides during impact.

4. Compare the performance of the strips with and without flanges.
5. Observe the perceptibility of the strips for a truck driver.

Numerous parameters were monitored during the tests. Inside the vehicle were two researchers. One was responsible for driving and providing subjective assessment of the perceptibility of the strips. The other researcher operated a sound meter connected to a laptop computer. The peak sound level for each pass was recorded as read from the sound meter. The signal from the meter's *line out* port was sent to the laptop computer's microphone jack so that the entirety of each pass could be recorded for later spectral analysis. Special software was used to ensure the computer's recording system (including the sound meter and its integrated microphone) was properly calibrated.

The speed of the vehicle was monitored by the driver using the vehicle's speedometer and also measured by a researcher outside the vehicle using a Kustom Signals ProLaser III LIDAR speed gun.

Another researcher was posted on the closed taxiway in case any aircraft inadvertently made their way onto it.

One of the test strips was outfitted with two accelerometers, one tracking vertical movement and the other tracking horizontal movement in the direction of the test vehicle's travel. No significant transverse movement was expected, and none was observed. The data from the accelerometers was recorded on a computer stationed nearby.

The strips were also monitored by a high-speed video camera so that the tire and the strip could be tracked visually during traversal. At 30 mph, the duration of the contact between a vehicle's tire and the rumble strip is only a little over two hundredths of a second. Standard video captures 30 frames per second (fps), or about one frame every 3 hundredths of a second, meaning it would provide at most one image during traversal. The video system used operated at 1000 fps, or about one frame every thousandth of a second. This provided about 25 images during traversal at 30 mph, varying inversely proportional with the speed of the test vehicle. One researcher was dedicated to operating the video and accelerometer systems. Two additional researchers assisted with these systems as necessary and made sure the strips were properly positioned at the outset of each run.

The wooden strips were outfitted with flanges made from a piece of flexible rubber (cut from a floor mat). In an earlier section it was pointed out that flexible flanges present several problems. Those issues are not applicable in this circumstance because the test was not intended to examine the issue of lift. The rubber flange was glued to a strip of sheet metal. The metal strip was centered on the bottom of the wooden strip (metal toward the wood). Holes were drilled through the rubber and metal into the wood, and the flange assembly was attached with screws. This technique (i.e., using the metal strips), permitted the flanges to be removed and reattached as needed, either to test a different size of strip, test a different width of flange, or replace a failed flange. Figure 37 shows one of the rumble strip assemblies in place for testing.

In order to collect useful data with the accelerometers and video system the strips had to be free to move. However, if movement were more dramatic than expected, a 24-in long strip turned

end up under a passing vehicle could cause significant damage to the vehicle and pose a safety risk for the driver. To ensure that such a scenario could not occur, a strap of nylon webbing was positioned over each end of each strip. The webbing was secured at each end by a 2" concrete nail driven into the pavement. The nails were driven through rubber pads to facilitate easier removal with a crowbar after the testing was completed. As shown in Figure 38, the straps were placed so that the rumble strips were free to move, but the range of their motion would be limited to approximately an inch in any direction.



Figure 37. Wooden prototype rumble strip in place for testing.



Figure 38. Nylon restraining strap.

Stepping through the video afforded several observations. First, the tire does deform significantly, but does not envelope the strip (i.e., during part of the traversal, the tire is not touching the pavement at all). Figure 39 shows several frames from one run, demonstrating that the tire rests entirely on the strip for a significant portion of the traversal.

Second, the strip did not slide, even when no flanges were present. The rubber was trimmed to within an inch of the strip, leaving the rubber lining the bottom of the strip. The truck traversed the strip several times, and the video clearly shows that no sliding occurred.

The video also revealed that the strip bounced significantly shortly *after* impact. Bounce may be from three sources: compression and expansion of the material, flexure of the bar, and lateral tipping of the bar (i.e., a see-saw action resulting when the bottom of the strip does not sit flush on the pavement). It is expected that the latter two causes are of greater concern than the first. Because of the complexity of modeling these actions mathematically, they were considered conceptually, addressed in subsequent design modifications, and tested empirically.


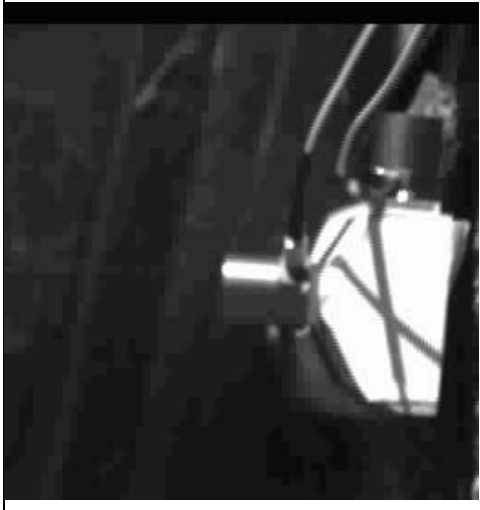
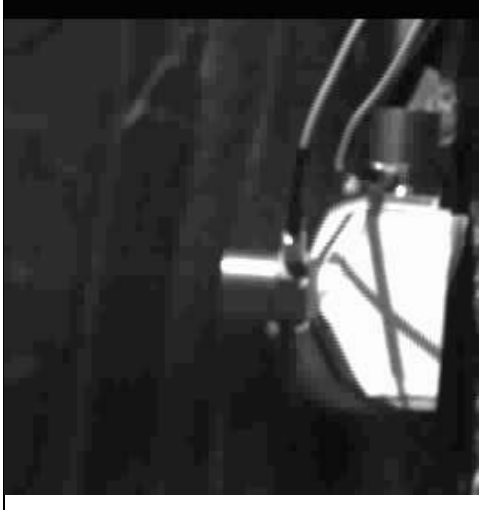
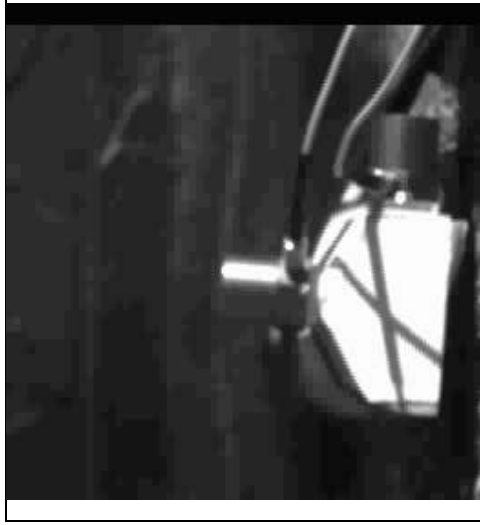
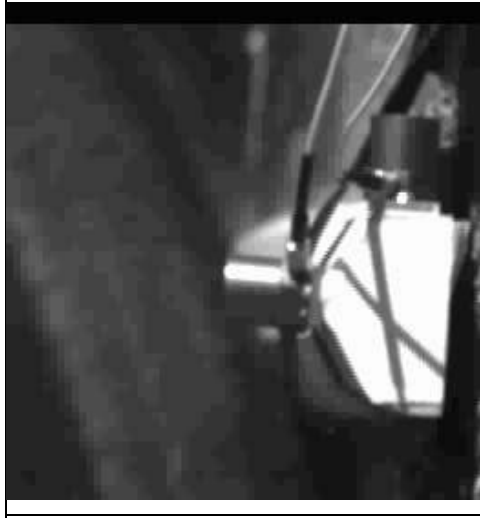

	<p>First Contact, frame 182 Distance to inside of dark ring: 10.75 units (2.7")</p>		<p>Begin lift, frame 192 Distance to inside of dark ring: 7 units (1.75")</p>		<p>Vertical, frame 194 Distance to inside of dark ring: 7 units (1.75")</p>
	<p>Touch Pavement, frame 197 Distance to inside of dark ring: 7 units (1.75")</p>		<p>Last contact, frame 207 Distance to outside of dark ring: 8 units (2.0")—comparable to frame 2</p>		<p></p>

Figure 39. Key frames from video of truck tire on strip.

The video also enabled the identification of the initial and departure contact angles. Figure 40 shows the angles associated with the frames in Figure 39. The chronological order of the angles is from right to left, following the action in the video. The initial contact with the strip was at an angle of 24 degrees from vertical, measured perpendicular to the features (i.e., rings) of the tire, intended to represent the line from the center of the tire to the center of the strip.

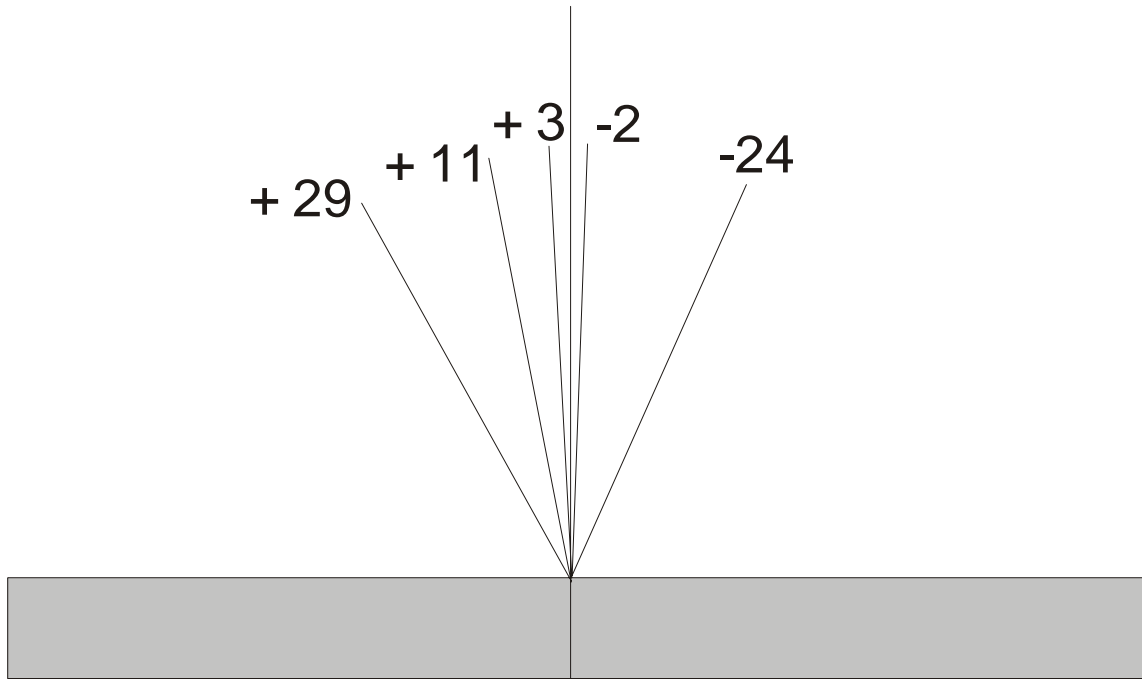


Figure 40. Angle of contact (in degrees) at time of each image.

Establishing Design Values

For subsequent analyses and design decisions, several values had to be identified. Values were intended to be conservative wherever possible. Assumed values include the following.

- Density of steel = 0.283 lb/in³
- Density of lead = 0.409 lb/in³
- Design deceleration rate = 0.5G
- Yield strength of steel (tension) = 36 ksi
- Yield strength of steel (shear) = 21 ksi
- Total Height of Strip = 1.25 in
- Design vehicle = tractor trailer
 - Max axle weight = 20,000 lb
 - Incident angle = 70 deg
- Desired Speed = 100 mph combined vehicle speed + headwind¹

¹ Derived from an informal poll of traffic engineers from states associated with the SWZDI.

Field Test 3

The third test (4/4/2005) was conducted at the Lawrence Municipal Airport. The wooden prototypes were used, and the test vehicle was a full-size sedan. The purpose of the test was to obtain a more complete set of runs at various speeds and to examine the effect of braking on the response of the strip. Test procedures followed were identical to those of the previous test. The same equipment was used and the same measurements taken.

In the passenger car, the sound inside the vehicle was clearly perceptible at all speeds. Figure 41 shows a spectrogram of the sound inside the passenger car as it traveled over the rumble strip. The sound from the front and rear tires hitting the strip can be clearly identified and distinguished. Most of the rumble strip-related noise occurred in the frequencies below 1 kHz. Other studies have cited 400 Hz and even 100 Hz as the upper end of the sound generated by rumble strips. Perhaps the difference is that previous measurements have been taken on strips with significantly lower profiles. After passing the rumble strip, the ambient sound levels tapered off as the vehicle slowed at the end of the run.

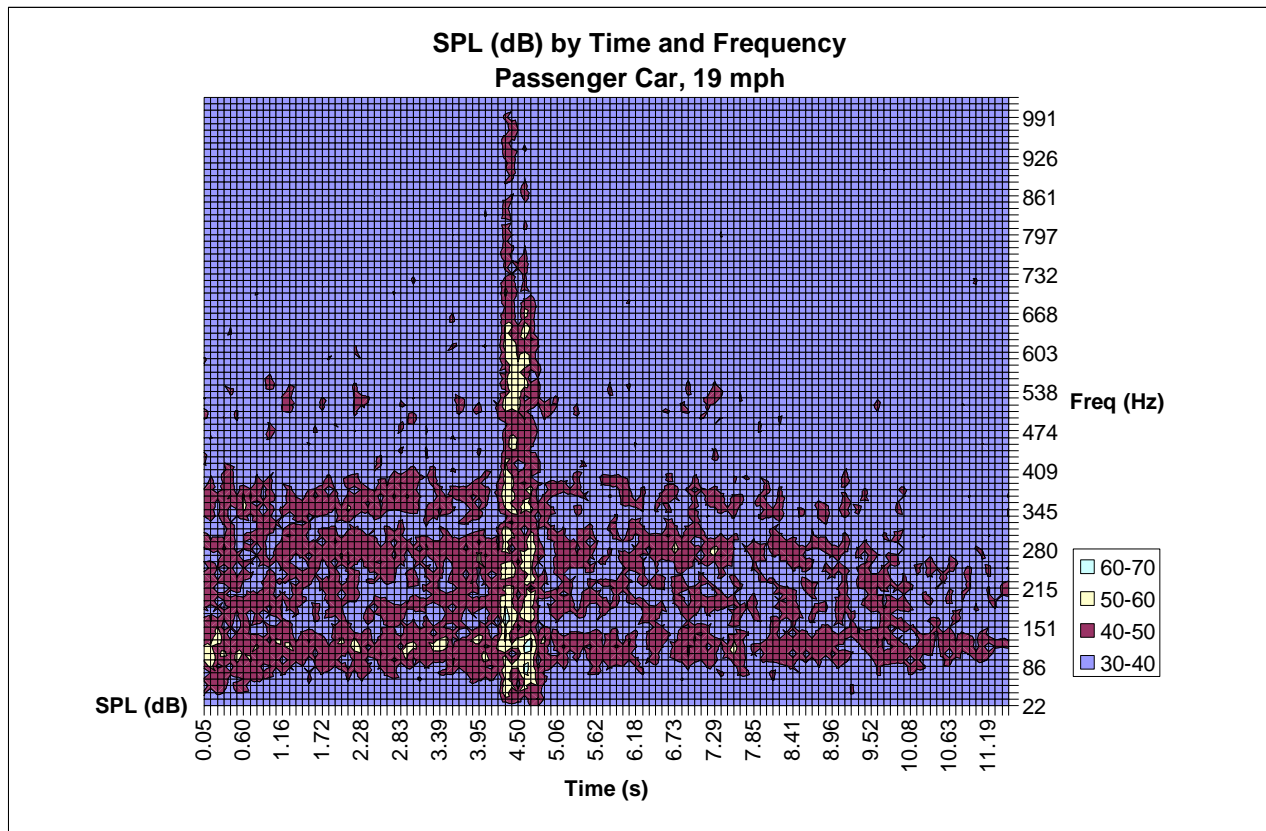


Figure 41. Spectrogram for passenger car at 19 mph.

Figure 42 shows the spectrogram for the passenger car at 39 mph. The recording does not show very much prior to the rumble strip, but an increase in the baseline noise is evident relative to the data taken at 19 mph. It can be easily seen in the 400 Hz to 600Hz values. As with the lower speed, the noise from the rumble strip occupies primarily the frequencies below 1 kHz. The data shows graphically and numerically what was sonically evident to the observers in the vehicle: the rumble strips are clearly distinguishable from the ambient noise.

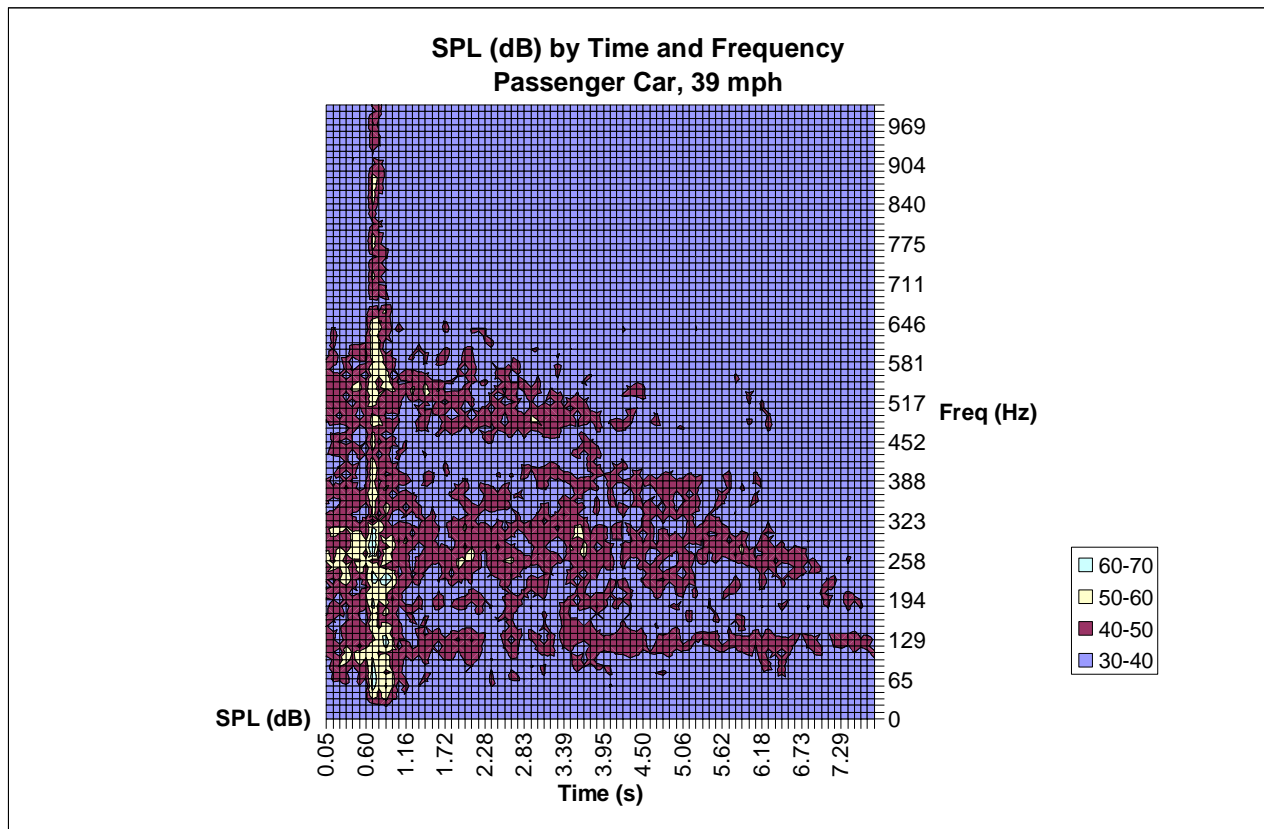


Figure 42. Spectrogram for passenger car at 39 mph.

The perceptibility of the rumble strip for drivers of large trucks has been a major consideration of this study from the outset. The truck used in Test 2 was a dump truck provided by KDOT. Figure 43 shows the spectrogram for one of the runs with the truck at 20 mph. The rumble strip noise can be seen, and the two axles are somewhat distinguishable, but not nearly so well defined as with the passenger car, even though the time separation between the axles of the truck is 60% greater than that of the car. Nonetheless, the strips were perceptible inside the dump truck.

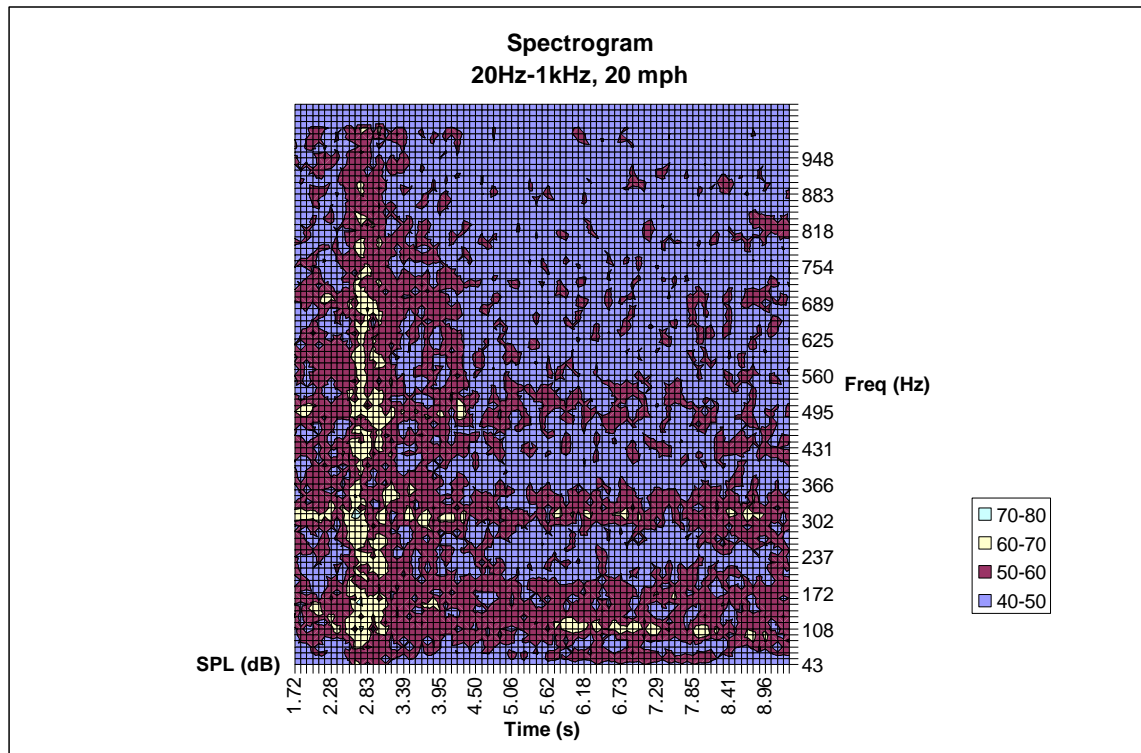


Figure 43. Spectrogram for dump truck at 20 mph.

At 37 mph, the sound from the lead axle's contact with the strip persists past the contact with the rear axle, making the two indistinguishable from each other. Together, they can be clearly seen in the spectrogram shown in Figure 44. The sound is discernible from the ambient noise inside the truck cab, but it is not very conspicuous. That is to say, if someone were listening for the sound, they would easily be able to hear it, but if they were unaware of the strips in advance, they would be unlikely to identify the noise as an intended warning device.

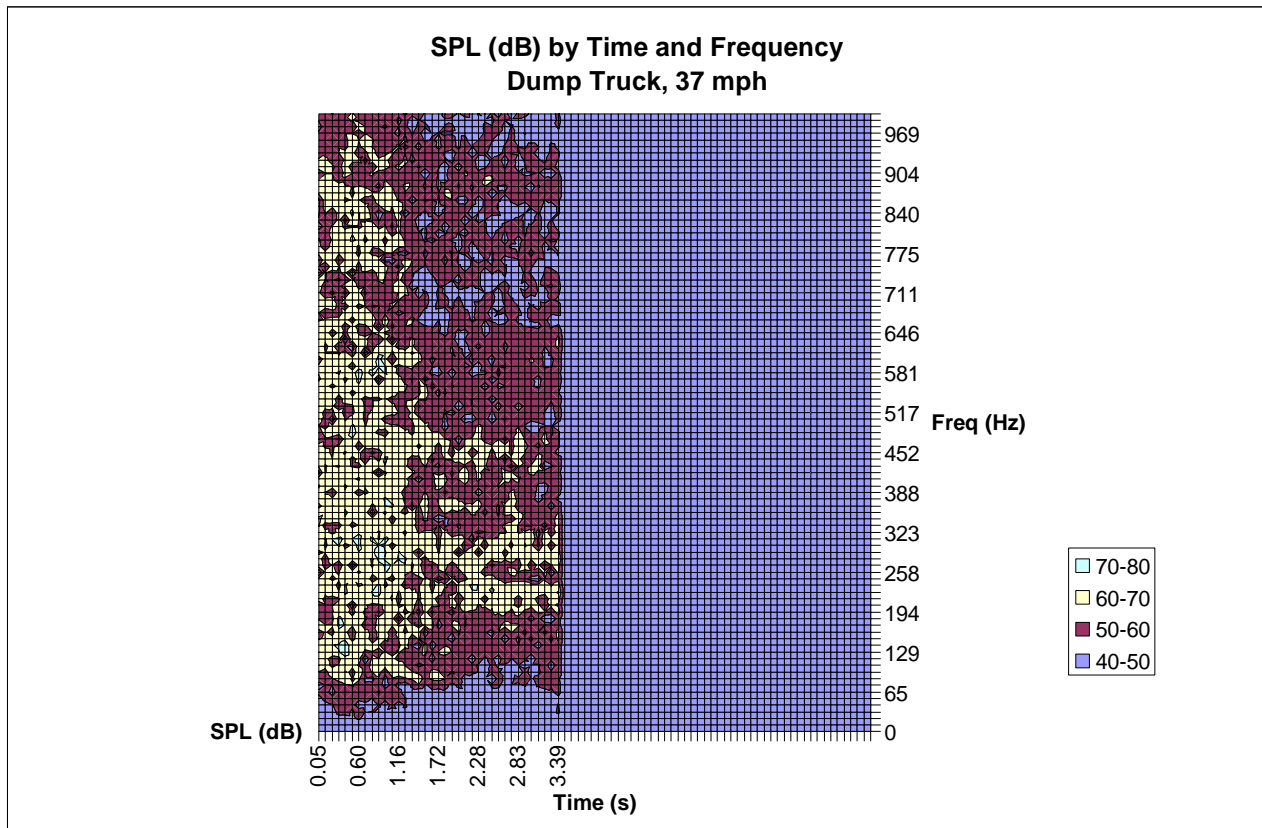


Figure 44. Spectrogram for Dump Truck at 37 mph.

The same phenomena can be observed by looking at the raw wave forms, shown in Figure 45 and Figure 46. The noise generated by the strips is clearly identifiable, although for the truck the two strips cannot be distinguished from one another. In Figure 45, the car data has been amplified to show a level of detail similar to that of the truck data. Figure 46 shows the raw (i.e., unamplified) wave forms, illustrating the difference in both the strip noise and the ambient noise preceding and following the strip.

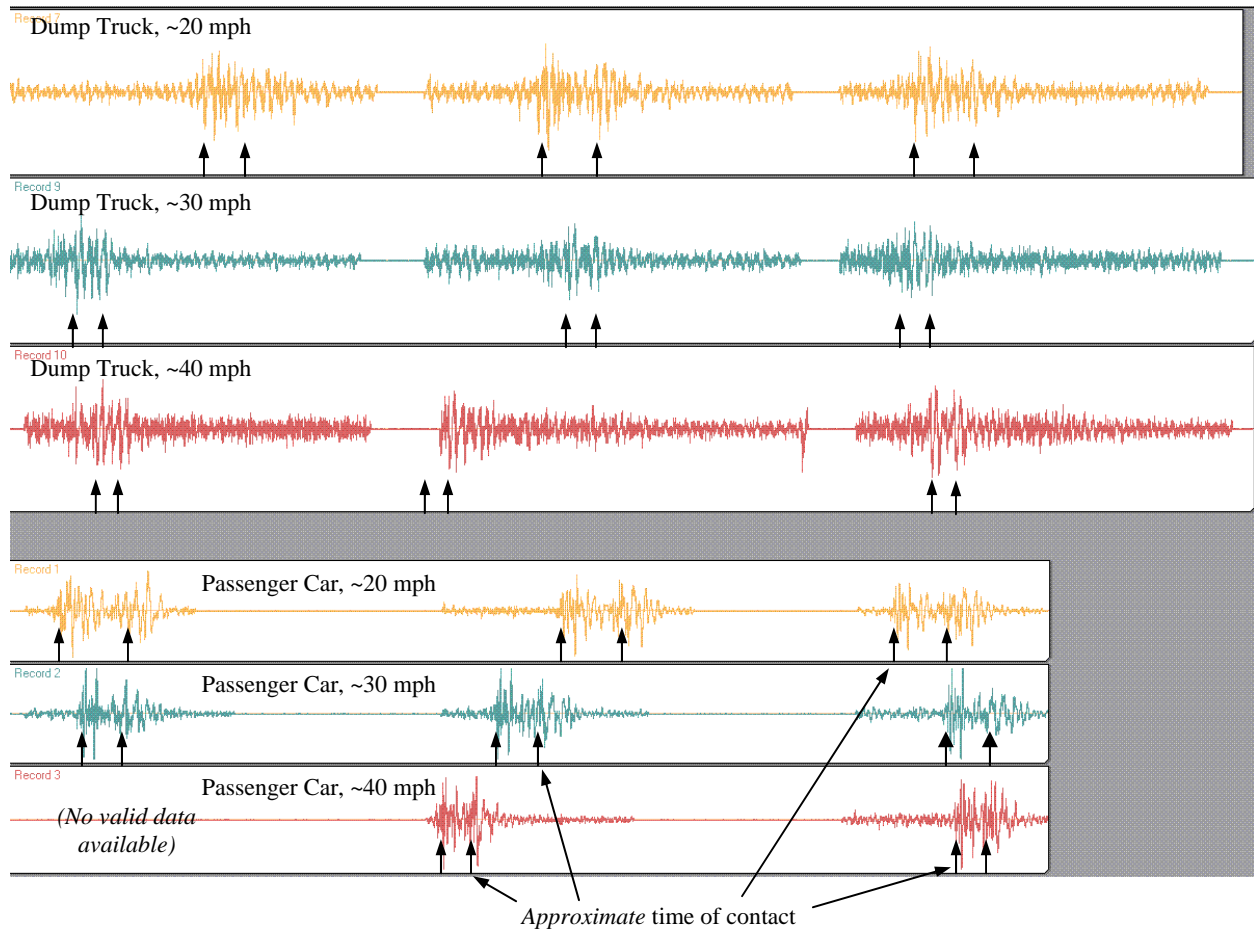


Figure 45. Wave forms for passenger car and dump truck at 20, 30, and 40 mph.

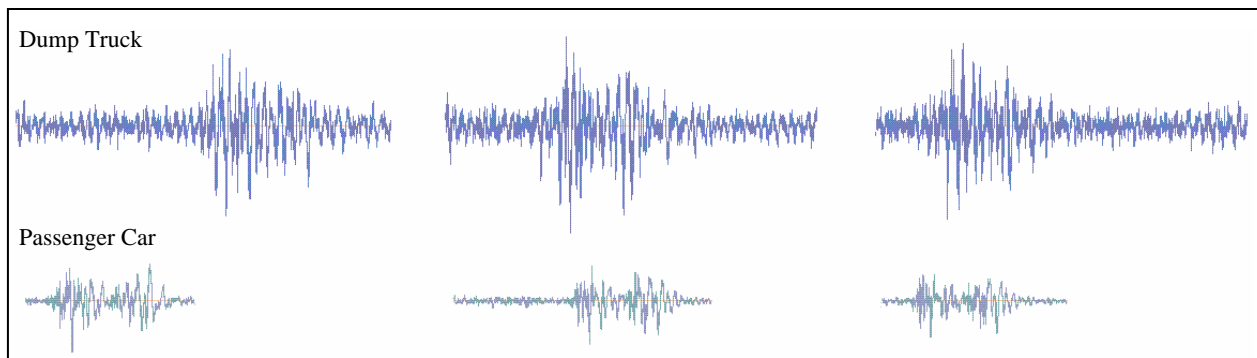


Figure 46. Wave forms for truck (top) and car (bottom) at 20 mph.

Revised Design

The video from Test 2 revealed that the strip did not slide, even without the flanges, so they were not necessary for the sake of their originally intended purpose. However, under moderate braking in a passenger car, the strip tipped, rotating about its long axis (i.e., the top of the strip moved in the direction of vehicle travel). The tipping was restricted by the restraining straps, demonstrating the displacement would have otherwise been significant (i.e., the strip would have flipped, possibly leaving the pavement). Given that this strip was made of wood, the specifics of the strip's reaction are of limited interest because an actual model, which would be made of steel, would respond differently. However, because any tipping of the strip would be unacceptable, further analysis was merited.

The design was revised to include shorter flanges intended specifically to help prevent tipping. The field tests showed that a flange could extend up to about 2 inches from the strip and not come into contact with the tire. The significance is that the thickness of the flange can be greater if the tire is not going to be contacting it. The conceptual design including the short flanges is shown in Figure 47. The ring-style flanges were later replaced by wedge-shaped flanges in order to provide the necessary strength.

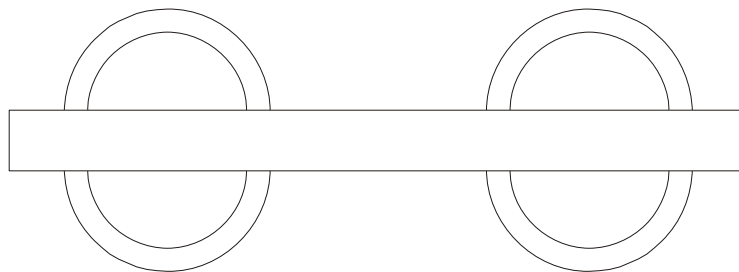


Figure 47. Conceptual design—top view.

The flanged design was still unable to fully satisfy all of the design criteria (e.g., tolerable combined vehicle+headwind speeds were less than 100 mph). To improve the lift resistance without reducing the tipping resistance, the weight per unit area of the strip had to be increased while the breadth of the strip was maintained. This was accomplished by modifying the semi-circular cross-section. Essentially the cross-section was split down the middle and a rectangular section inserted between the halves. The breadth of the box in the center, or *centerbox*, could be adjusted as needed. This allowed the width of the main bar to be increased sufficiently to prevent tipping without the use of flanges, which reduced the average weight per unit area of the design. Two caveats remained. First, the strip would be much heavier and would have no flanges to serve as handles for lifting and carrying the device during installation and removal. Second, it was unknown how the added breadth would affect the sound and vibration. It was suspected that the effect would be negligible, but the suspicions would need verification before the strip could be recommended for production.

The introduction of the centerbox provides some control over the weight per unit area of the overall device. By increasing the width of the centerbox, flanges could be added back into the design primarily for use as handles. They would also provide an additional safety factor with respect to tipping. Figure 48 shows renderings of a model of this design. The connector design was also refined. Renderings of those portions of the overall model are shown in Figure 49.



Figure 48. Renderings of CAD model with centerbox and flanges.

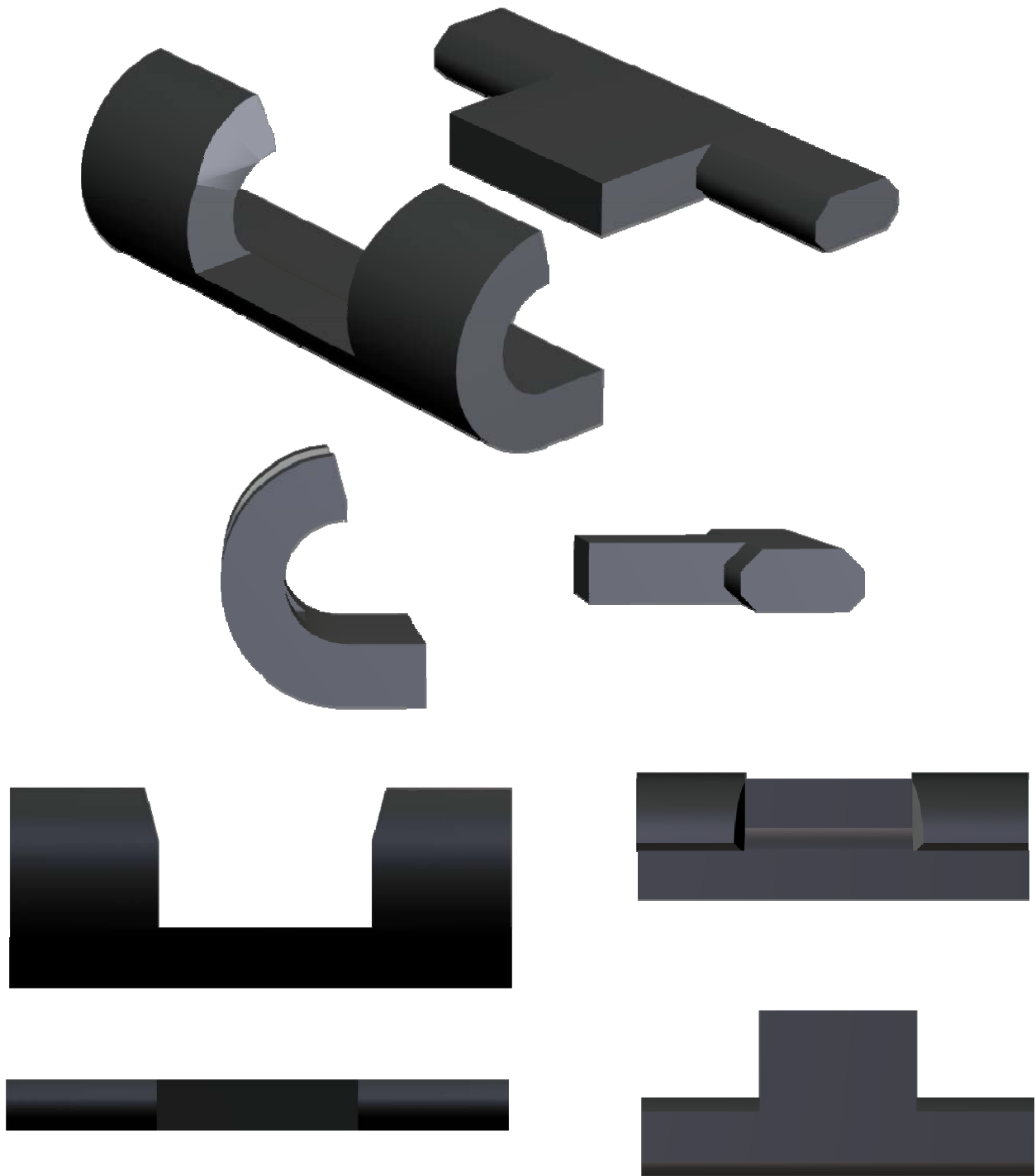


Figure 49. Renderings of the connector models.

Given that the 1.25-in strip height is considerably more than typical rumble strip heights (0.5 to 0.75 inches is typical for Kansas), the decision to make the strip broader is cause to re-evaluate the height, as well. Much of the displacement represented by the strip is absorbed by the tire, shocks, and suspension of the vehicle. When the duration of the displacement is greater, the time response of the vehicle's components transfers more of the displacement to the chassis (and on to the driver). The relationship between strip height, width, and driver perception is largely unknown. However, the relationship between height, width, and lift resistance is fairly easily described, so the issue can be examined from the perspective of lift-associated criteria.

Figure 50 shows curves representing two values for the tolerable combined wind speed (vehicle speed plus headwind). As the height of the strip decreases, the needed breadth of the strip must increase to compensate in terms of overall weight per unit area. For a tolerable combined wind speed of 100 mph, heights below about 1 inch require very broad strips. If the design wind speed were reduced to 90 mph, the analogous thickness would be a little over 0.8 inches. In addition, as the breadth increases, so does the overall weight of the strip. A 1.25-in x 4-in cross-section results in a total weight for a 4-ft long segment of just over 90 lbs, while a 4-ft segment of a 1.0-in x 10.3-in cross-section would weigh over 200 lbs, more than double the weight of the thicker strip. A recommended deployment of 2 strips, each comprising two 4-ft segments with a 2-ft gap between them would weigh over 800 lbs. A segmented design would make it possible for the installation to be done by two workers, but such weight would at least reduce if not eliminate any advantages the strips might otherwise offer in terms of easy installation, removal, and transport.

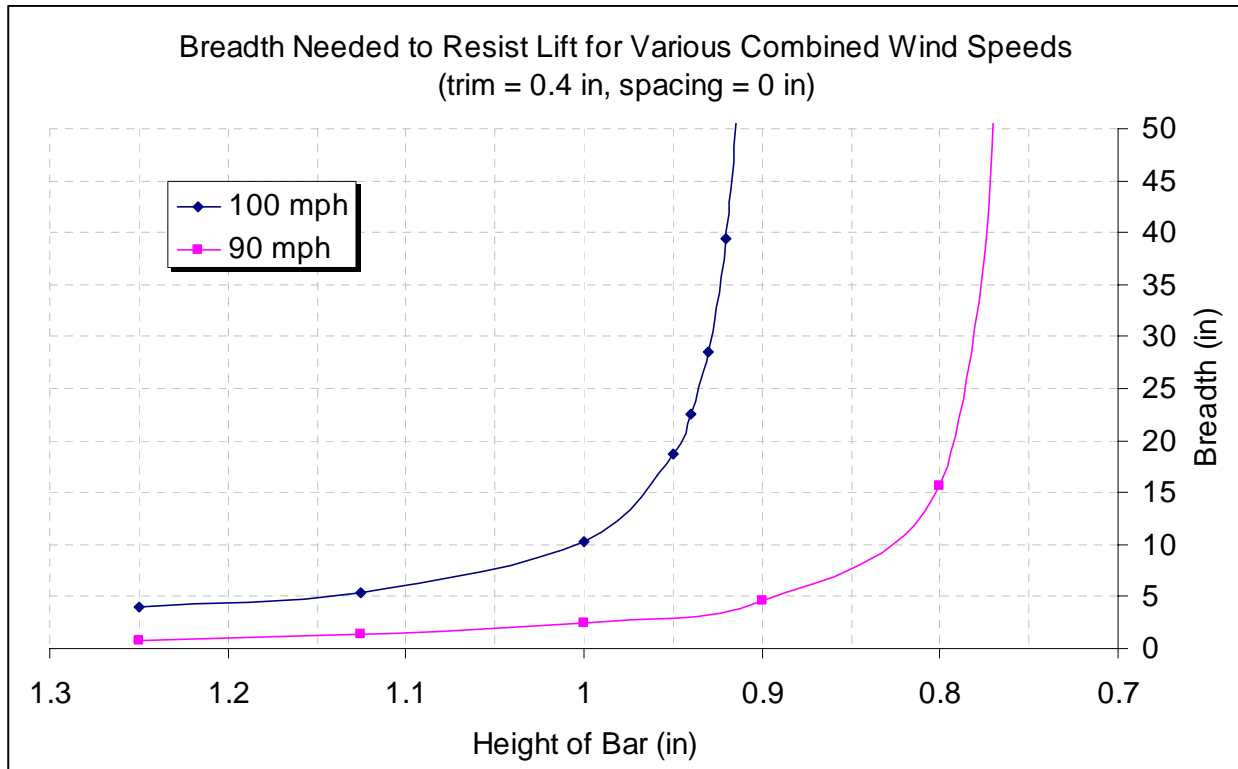


Figure 50. Relationship between the bar height and the breadth needed to resist lift.

It is also possible that a strip 20% thinner but 2.5 times broader may actually have a *more* severe effect in terms of driver perception, rather than less severe.

Given these considerations, the height of the strip could be reduced, but not by more than about ¼ inch, and the tradeoffs in terms of weight and of effect severity cast doubt on the wisdom of such a change. The 1.25-in height remained the design team’s preference.

Final Prototypes

The tests using wooden prototypes supported the premise that a portable rumble strip (i.e., a rumble strip deployed without any physical attachment to the pavement) could be designed that would neither slide under the lateral loads during impact with a vehicle nor lift from the pavement in the wake of a truck. Following the third test, the primary concern still unresolved was that of bounce. Displacement due to bounce could prove negligible if it were small and the strip returned to its original position (i.e., did not creep down the highway or rotate about the vertical axis from bounce). However, even small displacements could be very significant when considered cumulatively (i.e., for 1000 vehicles, for example). The segmented design was developed, in part, to reduce the effects of bounce, reducing the degree to which they are transferred from one piece to the next. When it was developed, the length of each piece was a balance of three considerations.

1. The weight of each piece should not be so large that they are difficult to handle.
2. The length should not be so great that one piece might span a wheel rut, creating a situation in which the piece may behave as a spring rod.
3. The length should be long enough to ensure that the lift resistance is conservative. (The connectors have a small weight per unit area, so the longer each piece is, the fewer connectors that are necessary, and the higher the overall weight per unit area.)

With the knowledge gained from the earlier testing done, the design was revisited to consider what could be done to minimize bounce. The segmented design was introduced in part to reduce bounce. By segmenting the strip further (i.e., making the pieces smaller), the bounce would be further damped. The effect of the connections on lift resistance was the primary reason the piece length was not shortened previously, but with the addition of the centerbox in the cross-section, the breadth of the piece could be extended to compensate for whatever lift resistance might be lost in the spaces between the pieces. If the pieces were not autonomous (i.e., if they can be semi-permanently connected), the distance between the pieces can be reduced, further minimizing the effect on lift resistance.

With this line of thinking, the design was modified to incorporate smaller pieces strung together with two cables and separated by rubber spacers. Figure 51 illustrates the modified design concept. Two cables were used to help control torsional displacement both during handling and during use. Rubber spacers were used to maintain a set separation distance between pieces. Each piece had a square footprint, guaranteeing that its resistance to tipping would not decrease when the contact angle was other than perpendicular, for whatever reason (i.e., the vehicle path was not perpendicular to the strip). 8 to 12 pieces would be strung together to form a 2-ft strip. The ends would be outfitted with appropriate connectors so that two strips can be joined to create longer strips. Five 2-ft units could be attached for one continuous strip across the lane, or two 4-ft sections could be set in the wheel paths, leaving room in the center or on the edge of the lane for motorcycles and bicycles. A 2-ft section would weigh between 40 and 70 lb, depending on the spacing and piece size.

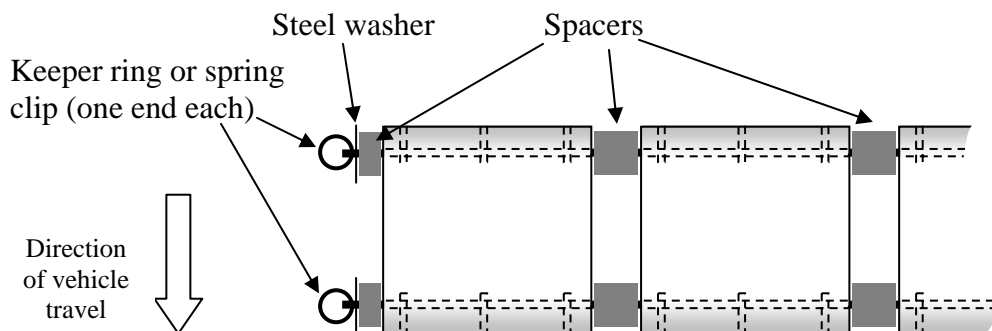


Figure 51. Proposed Assembly

For ease of fabrication, the rounded portions of the cross section were approximated with straight edges, much as was done with the wooden rumble strips. Figure 52 shows a typical cross-section.

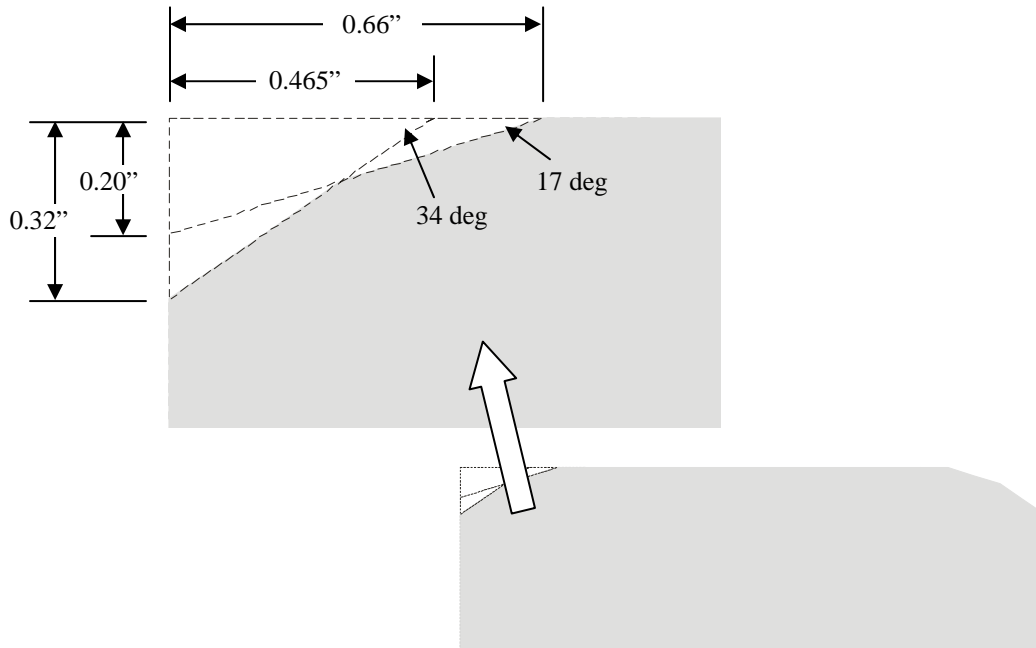


Figure 52. Corner treatment specifications.

In preparation for the final tests, two prototypes were fabricated, one with a breadth of 4 inches and the other with a breadth of 6 inches. The prototype design allowed spacers to be added and removed in order to examine the effect of spacing on performance. While this design should help to minimize bounce, it cannot be eliminated entirely. The severity of the bounce that occurs was a primary focus of the final test.

The spacing between the pieces affects the performance in two ways. First, the spacing can decrease the lift resistance of the overall device. If the spacings are sufficiently wide, they would not be counted in the footprint of the device with respect to the area over which the total weight is averaged. However, small spacings may behave as part of the unit with respect to aerodynamics. Air flow can become bound in small spaces such that the negative pressures responsible for lift act on both the steel pieces and on the spaces filled with bound air. The spacing threshold beyond which this phenomenon occurs depends on several parameters, including the wind speed and direction. Since these parameters are highly variable, it was conservatively assumed that the spaces between pieces must be included in the overall area of the device. Figure 53 shows the maximum spacing given the footprint of each individual piece, assuming a strip thickness of 1.25-in and a combined wind speed design value of 100 mph.

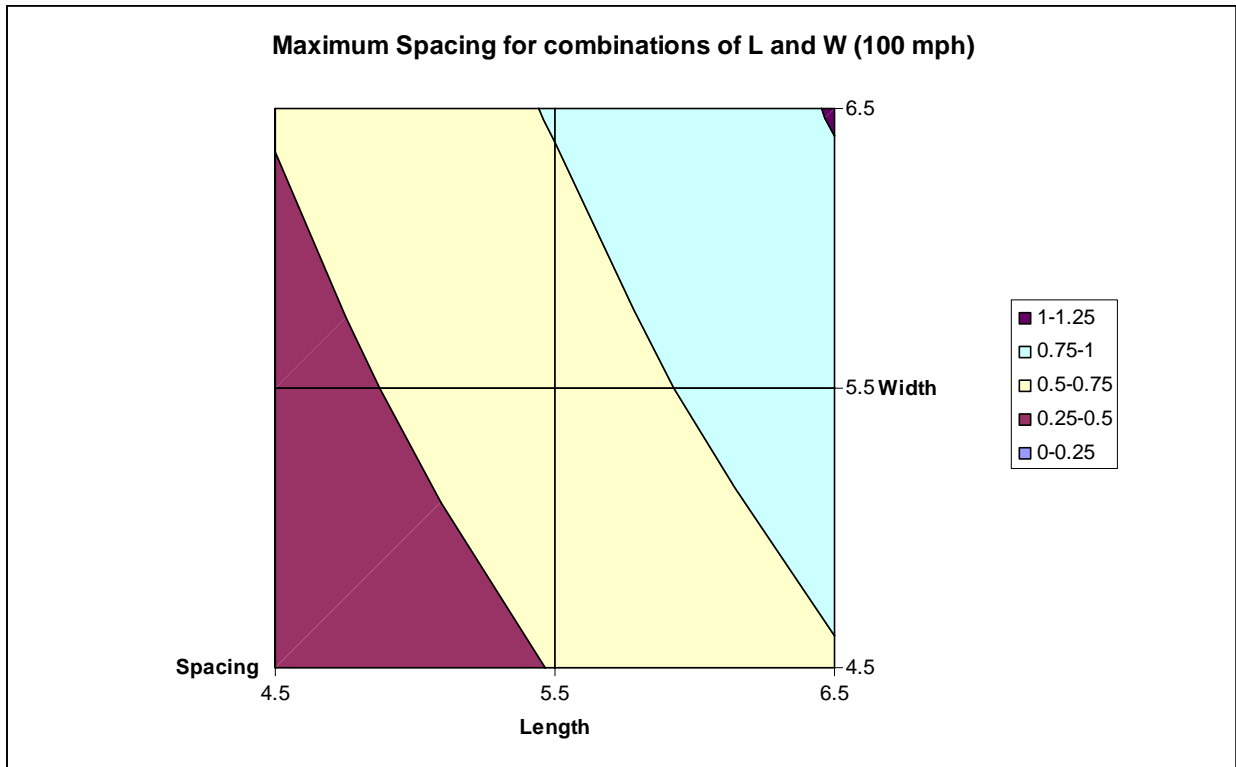


Figure 53. Maximum Spacings for Exterior Dimensions

The second effect of the spacing pertains to the damping properties of the device. When bounce occurs, how much displacement is transferred to adjacent pieces depends on the spacing, as well as other parameters including the stiffness and size of the spacers and the tension on the cable. Another factor that may play a significant role is whether or not each piece is rigidly connected to the cables or free to slide along the cable.

Final Design

Following the completion of earlier tests, discussions among the design team led to a reduction in the width of the strip elements to a uniform two inches. The primary reason for the change was to reduce fabrication costs by minimizing the cutting required. Rounded upper corners were maintained (approximated by a double bevel). The number of cable connectors was reduced to two for the test prototypes (although three may still be advisable for the production design as an added safety measure). Rubber spacers were used between the elements. Spacings averaged approximately 0.25 in. Two prototype strips were fabricated, one with 4-in elements (i.e., in the direction of traversal) and the other with 6-in elements. Each strip comprised 12 elements, each two inches wide. The total length of each strip was 26 inches. The elements were strung together with a steel cable, which ran through one side of the strip and back through the other. The loose ends were fastened to each other at one end using a cable clamp. Polyurethane

grommets were used as spacers to allow the cable on the ends to be used as a makeshift handle, as shown in Figure 54. A rubber hose used for pneumatic traffic counters was sliced to produce the rubber spacers that were placed between the strip elements. Each spacer was approximately ¼ in thick, and a single thickness was used between each two elements. The cable holes were placed in the same location for both the 4-in and the 6-in strips relative to the outside edge.



Figure 54. End treatment of 4” strip (actual size).

Field Test 4

The prototype strips were tested at the Lawrence Municipal Airport on November 12, 2005 using a passenger car at speeds between 20 mph and 40 mph. The purpose of this test was to verify that the strips do not flip under loading nor bounce so egregiously as to present a safety concern. Because this was a preliminary test, the high speed video equipment was not employed. Standard video was used to document the test. The net response of the strips to loading was recorded, but the details of the response could not be captured as the event duration was of similar magnitude to the frame rate.

The strips were traversed at 20 mph, 30 mph, and 40 mph. At 40 mph, several passes were made without resetting the strips to see if how response differed when some elements were already displaced prior to traversal. The strip was traversed while applying the brakes, and a final pass was made in which the strips were hit near the end, rather than in the center as with all prior passes.

The leftmost image in Figure 55 shows the state of the 4-in strip as it was when reset between passes. The movement at all three speeds was opposite the motion of the vehicle. The movement appears to be very similar at 30 mph and 40 mph, both of which show noticeably more movement than the 20 mph case.

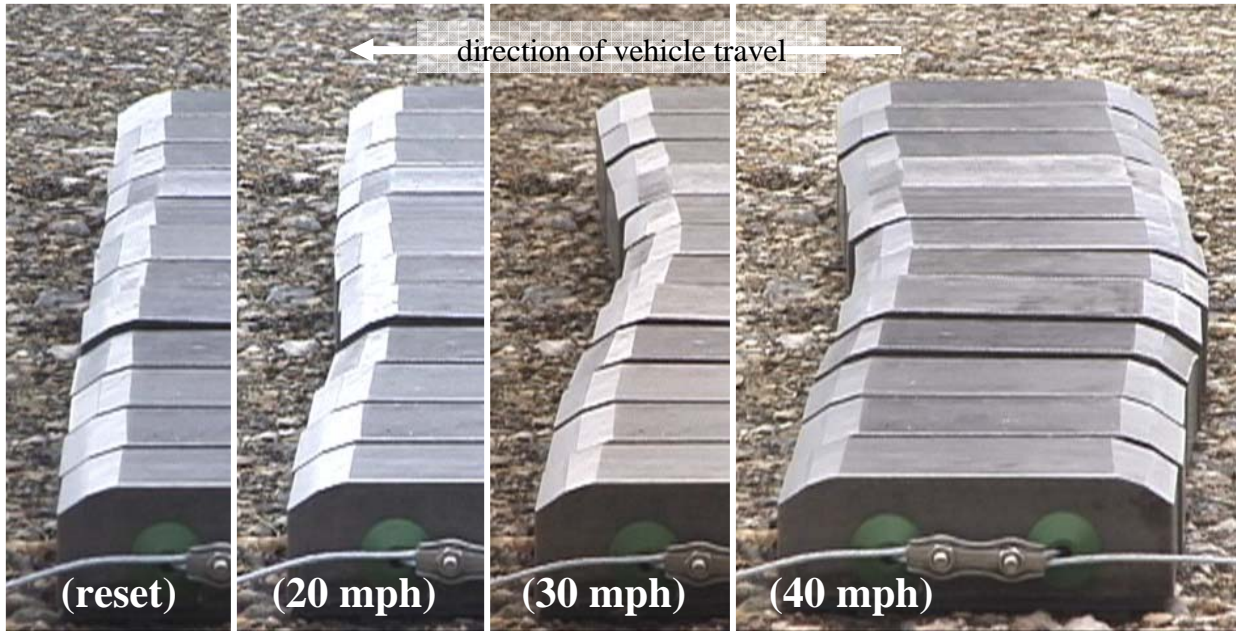


Figure 55. Strip state as reset and following one pass at 20 mph, 30 mph, and 40 mph.

At 40 mph, several passes were made without resetting the strip in between passes. Figure 56 shows the state of the strip as reset on the left, and as observed following four successive passes, in order of observation from left to right. Motion continued to be opposite the motion of the vehicle.

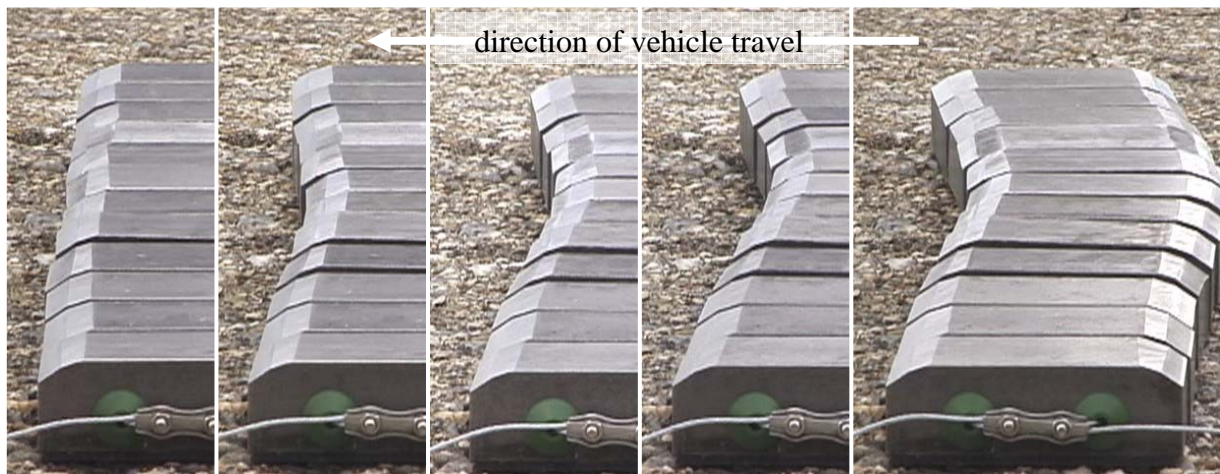


Figure 56. Movement on four successive passes (i.e., without resetting).

The relative positions of the strip as depicted in the images in Figure 56 are superimposed in Figure 57. The leftmost line in Figure 57 represents the strip alignment prior to traversal. The line deviates from vertical in the figure, reflecting the angle of view of the camera. The maximum translation of any element during the first two passes was approximately half an inch. During the third and fourth passes, the maximum movement was approximately a quarter of an inch. It is important to note that the near end of the strip did not move throughout the four passes.

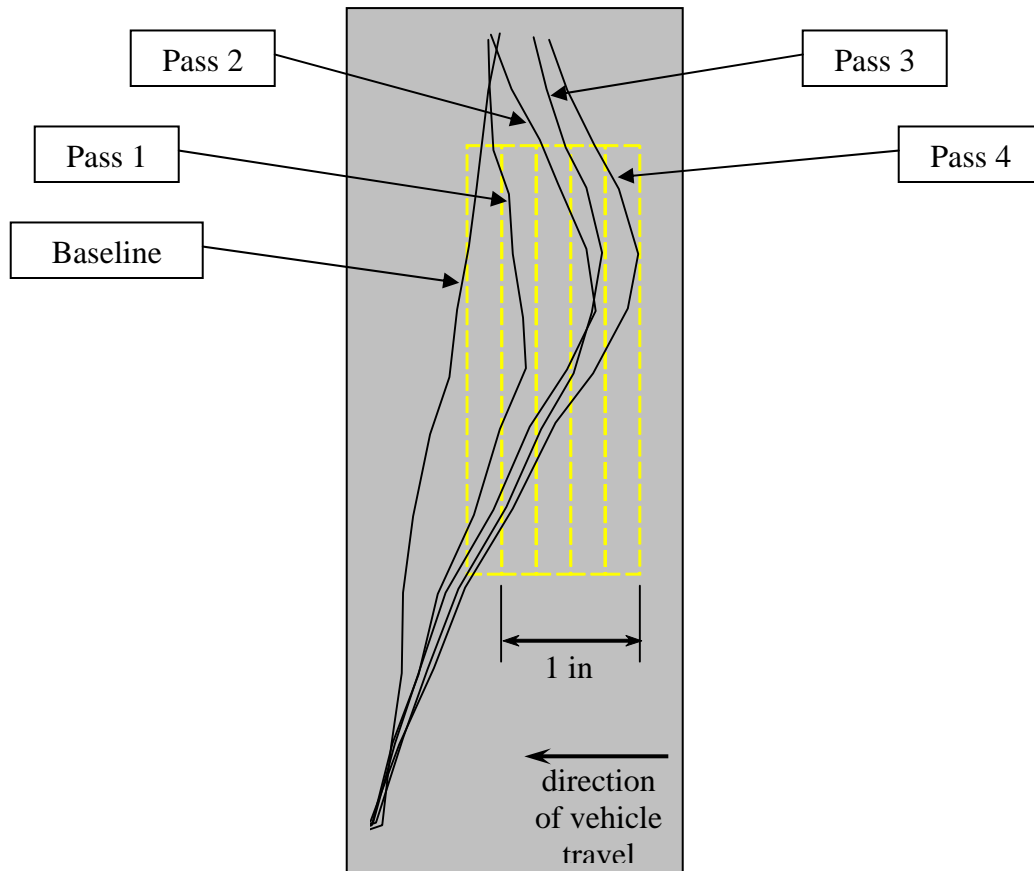


Figure 57. Movement of 4-in strip during successive traversals

The reverse movement of the strip is evidence that the movement is due to bounce. The loading from the tire is down and forward, causing the elastic response to be up and backwards. The bounce response seemed to be most severe during braking. The bounce of the strip can be seen in Figure 58. The strip just prior to traversal is shown on the left, and the strip during the response is shown on the right. The upper half of the image on the right appears particularly dark because the vehicle tire was in the frame during a portion of the exposure. Note that the four elements nearest the camera do not move at all. The response is localized to the elements contacted by the vehicle tires.



Figure 58. Bounce of 4-in strip during traversal while braking

While significant vertical displacement was observed during braking, the horizontal displacement was relatively small. There were no indications of potential for tipping or any other behavior that could be deemed a safety concern. Therefore, the results of this test support the potential of the design to be an effective device for use as temporary rumble strips and suggest that safety risks are very small with respect to further testing. Based on these results, plans for a final test were developed which would include a tractor trailer at highway speeds, considered to be the design case.

Field Test 5

The final test in this project involved two prototypes of the final design traversed by a loaded tractor trailer at highway speeds. The strip elements were reassembled into two strips, each with 24 elements and a length of 52 in. As before, one strip was comprised of 4-in elements and the other strip of 6-in elements. The added width of the strips was necessary to accommodate the tractor trailer, whose wheel separation varied and whose dual tires were nearly the width of the strips used in the previous test. The 4-in strip weighed 65 lbs and the 6-in strip weighed 95 lbs. The vehicles used included a typical SUV for the initial test run and a loaded grain truck for the remainder of the runs. The truck traversed the strips at various speeds, with and without applying the brakes while over the strips. As in the previous test, several runs were made

without resetting the strips to observe the effects of multiple passes. The truck was a typical 18-wheeler in terms of axle spacing and dual tires. The truck was loaded, providing a near worst case loading of the strips. The truck height was slightly less than that represented by the scale model in the wind tunnel and computer modeling, but the difference would not significantly affect the negative pressures generated at the pavement surface.

The prototype strips comprised 2-inch wide steel elements with rubber spacers that were approximately 1/4-inch thick on average. The elements were strung together with steel cable passing through two drilled holes located about an inch from each end of each element. The length of the bars was 4 inches in one strip and 6 inches in the other. In each strip, 24 bars were strung together to provide a strip length of approximately 4.5 ft. The strips were centered on the wheel paths, resulting in approximately 2 feet between the strips.

To record the response of the strips to the loading, a high speed video camera was employed. The camera was set to record 1000 frames per second with an exposure of 1/2000 sec. Still images were taken of the strips between runs and net movements per run were measured and recorded by hand.

A complete suite of test cases was not possible due to time constraints, but the subset of test cases implemented was able to effectively examine the most significant parameters addressed in the full suite. Table 6 shows the test cases implemented. The strip indicated in the “Strip” column is the strip nearest the video camera. Net movements per run were recorded for both strips after every run.

Table 6. Test Cases Executed

Run ID	Vehicle	Strip	Speed	Other	Notes
10	Car	4"	40 mph		No video due to failed memory card
34	Truck	4"	30 mph		08; no movement until last dual axle; first of last two axles caused strip elements to bounce upward (about 60 deg from horiz), and second axle made contact in mid-air, pushing it back to the pavement. Strip then bounced backward (about 30 deg from horiz)
35	Truck	4"	45 mph		10; responded to each axle similarly, some increase roughly proportional to axle weight
36	Truck	4"	60 mph		12; all translation occurred after axle 3
37	Truck	4"	60 mph	do not reset strip	16; all translation occurred after axle 3
38	Truck	4"	60 mph	do not reset strip	18; all translation occurred after axle 3
39	Truck	4"	60 mph	do not reset strip	20; all translation occurred after axle 3
41	Truck	4"	60 mph	braking	22;
48	Truck	6"	60 mph		24;
53	Truck	6"	60 mph	braking	26;

The first test case was a passenger car, shown in Figure 59. The video of the run was lost due to a faulty memory card, but the net movement of the strips was recorded and is presented in the results section of this report.



Figure 59. Passenger car traversing strip.

In the second and subsequent test cases, a typical tractor trailer was used. The truck, shown in Figure 60, was a loaded grain truck. The computer modeling done earlier showed that the worst case would be that of a loaded truck. The height of the truck was about two feet less than that of a standard box trailer, but the critical obstacle was the bounce of the strips, rather than the negative air pressures. Furthermore, the difference in height would not have a significant impact on the air pressures generated by the truck at the pavement surface. Note that the camera can be seen in the bottom left of Figure 60.



Figure 60. Tractor trailer used for testing.

The third test case executed (run ID 35) showed a conspicuous pattern in which the elements at the end of the strip were reported to have translated $\frac{1}{4}$ in. In most other runs, these elements did not move. Upon suspicion that the movement of the strip was misrecorded, the video was reviewed to see if translation could be confirmed or disproven. Figure 61 shows a partial frame captured from the beginning of that video (bottom) and one captured from the end of the video (top). Lines are superimposed to help relate key features in the two images, and at the top of the upper image a scale is provided showing quarter-inch divisions. It does not appear that the end of the strip translated at all, and certainly not as much as $\frac{1}{4}$ in. It is assumed that either the baseline was misread while measuring or else the strip was reset to $\frac{1}{4}$ in off the baseline. To compensate for the apparent error, a quarter of an inch was subtracted from every measurement related to that strip on that run.

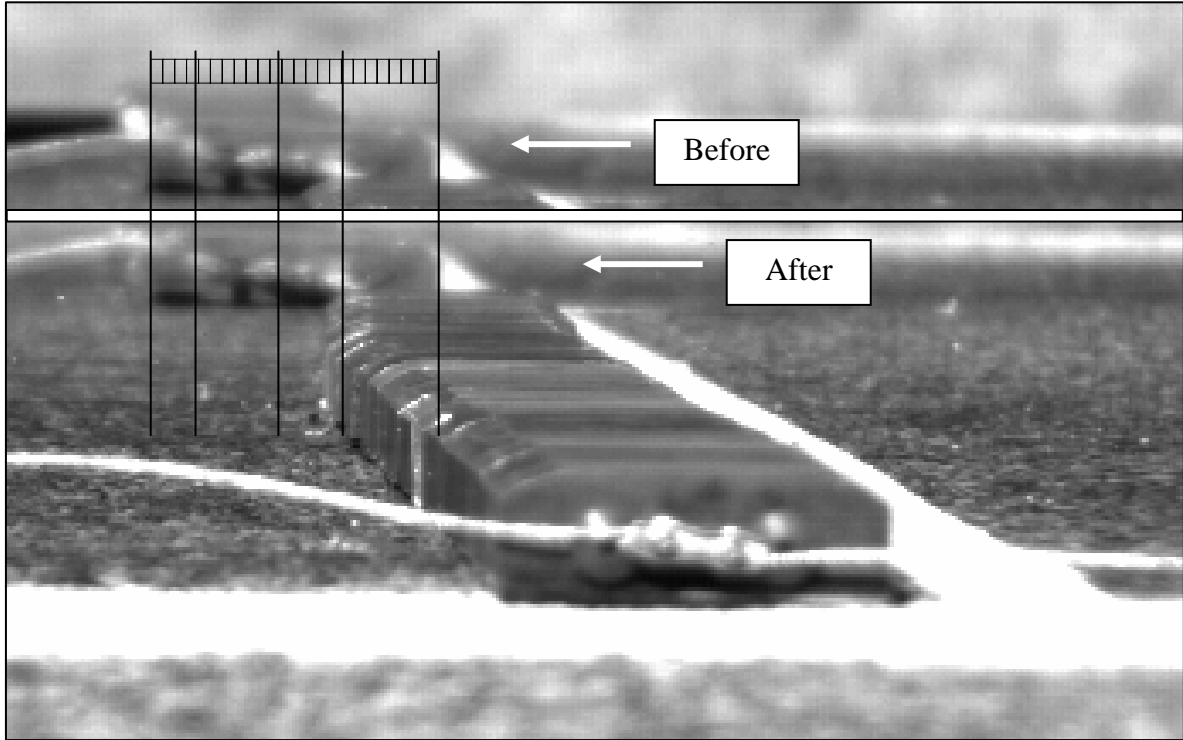


Figure 61. Before and After Images of Test Run 35.

Results

The segmentation of the strip was a successful design decision, effectively containing movement to the area of contact of the tire. Figure 62 shows the movement of the strips for both the passenger car and for the truck. There was no movement toward the right end of the strips (i.e., beyond element 18). The location of the movement in the other strips varied with the location of the tires' contact with the strip. There was more movement in the 6-in strip in the case of the truck, but this was the exception, as is discussed later in this report. It appears that the truck was too far left in this run and the double tires only partially contacted the 4-in strip. That is ample cause for the unexpectedly small amount of movement in the 4-in strip compared to the 6-in strip.

As predicted by the earlier analyses and tests, the design was successful in overcoming the negative pressures in the truck wake. No movement was observed that attributable to negative pressures in the truck's wake. No lateral movement of the strips (i.e., perpendicular to segment centerline) was observed. No evidence of sliding was found.

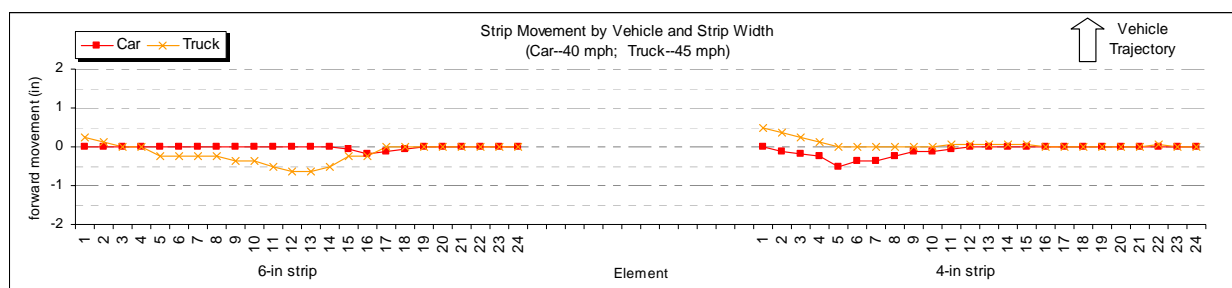


Figure 62. Strip Movement by Vehicle and Strip Width

Effects of Speed

The strips were traversed by the truck at three speeds: 30 mph, 45 mph, and 60 mph. The results showed that the movement of the strips was due to the strips bouncing in response to the load applied by the vehicle tires. The vertical component of the bounce varied with the weight of the loading, based on typical axle loadings (the truck's actual axle loadings are not known). Nearly all the movement in the 6-in strip was counter to the vehicle's trajectory (i.e., it bounced backwards relative to the motion of the truck). For the 4-in strip, the movement was backwards at the lowest speed and forward at the two higher speeds.

As stated previously, the backwards direction of the movement is attributable to the tire loading having a significant horizontal component, pushing the strip forward as well as down. When the tire leaves the strip and the rubber exhibits its elastic response, the strip is propelled upward and back, opposite the loading, as would be expected for a bounce response.

At 30 mph, there was almost no net movement in the 4-in strip following the first three axels. Axle 4 caused strip elements to bounce at about 60 degrees to horizontal. Axle 5 made contact with the strip elements in mid-air, pushed them back to the pavement, and caused them to bounce at about 30 degrees to horizontal, resulting in the backwards movement shown in Figure 63.

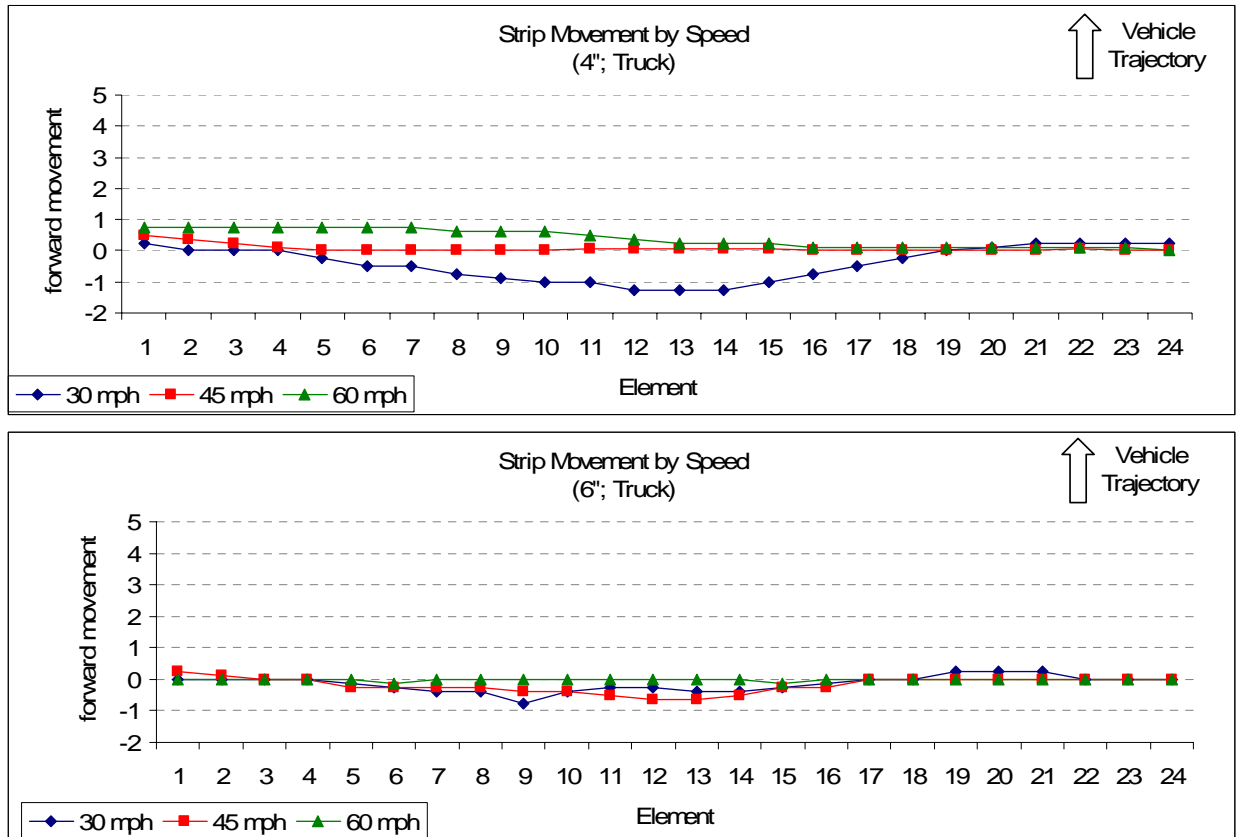


Figure 63. Strip Movement by Speed

As speed increases, the vertical component of the loading remains nearly constant while the horizontal component of the loading decreases. Presumably, at low speeds the horizontal force elicits an elastic response, propelling the elements backward. As the horizontal force decreases, the bounce response becomes more purely vertical, until the wind forces overcome the bounce response, resulting in a net forward movement.

Figure 64 through Figure 66 show the 4-in strip at the apex of each bounce during Run 36 (60 mph). The local nature of the movement (i.e., movement localized to the elements that contacted the tires) can be clearly seen. The outside distance for axles 2 and 3 is about 12 inches less than the outer distance for axles 4 and 5. As a result, axles 2 and 3 cross the strip near the end while axles 4 and 5 cross the strip several elements away from the nearest end. Because of this offset, axles 3 and 5 provide an illustration of the greater movement that occurs when the strip is struck near the ends. The loading on axle 5 similar to that of axle 3, yet the resulting bounce was smaller because of the added resistance of the elements to the immediate left of the tires.

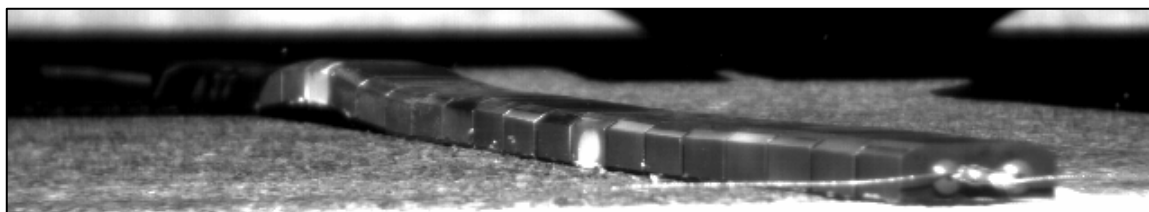


Figure 64. Maximum vertical displacement following axle 1 (RunID=36).

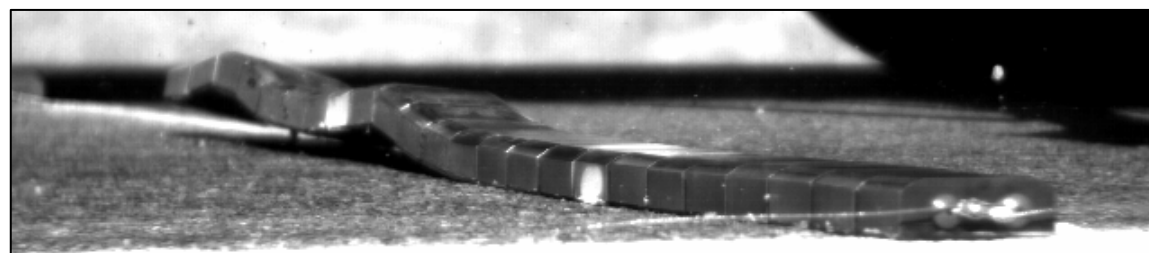


Figure 65. Maximum vertical displacement following axle 3 (RunID=36).

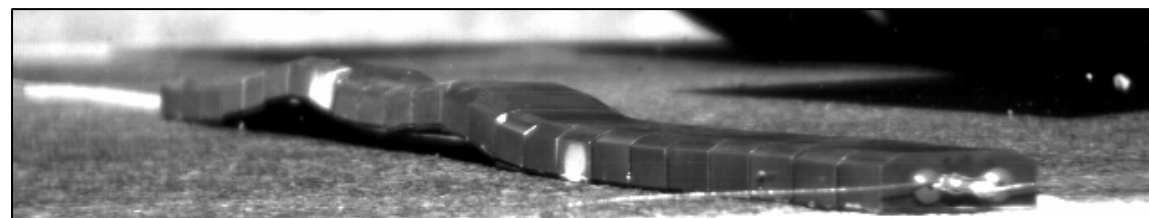


Figure 66. Maximum vertical displacement following axle 5 (RunID=36).

Translation

Several passes were made without resetting the strips. The 4-in strip moved significantly, although the far right end did not move at all. The 6-in strip moved very little, as shown in Figure 67. The largest movement in the 6-in strip was less than an inch, while the 4-in strip moved about 4.5 in. Note that the movement in both cases was near the end of the strip, and the opposite end did not move. Had the strip been continuous across the lane, the movement would have been reduced or eliminated.

Review of the video footage confirms the conclusions above. In the video it can be clearly seen than in each of the 4 runs made without resetting the strips, the only net movement occurred following axle 3, because it crossed near the end of the strip. After axle 1 and after axle 5, the elements at the end of the strips did not move. Elements struck by the tire bounced vertically, but were held from translating horizontally by the adjacent elements.

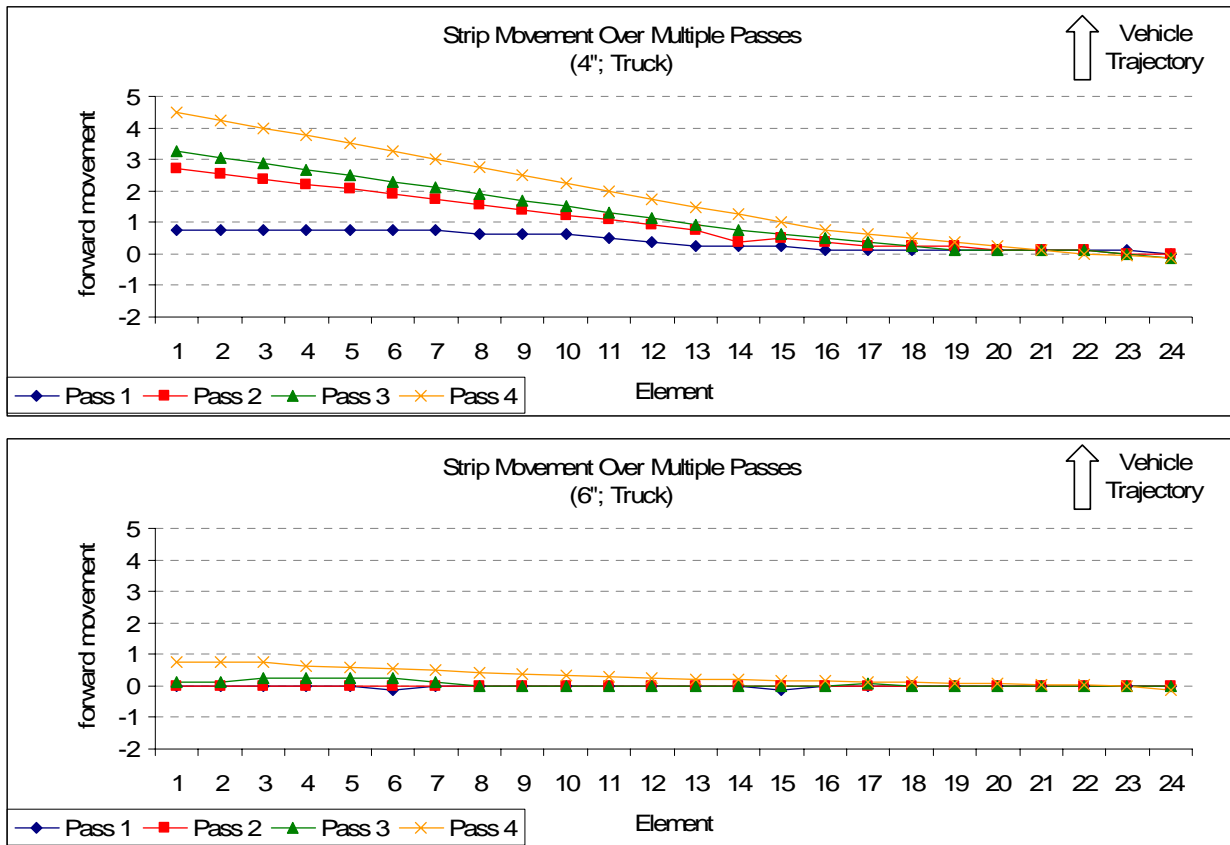


Figure 67. Strip movement over multiple passes

Braking

Braking while traversing the strip is a foreseeable scenario, and two passes were made while braking. The strips were reset prior to each of the runs represented in Figure 68. As expected, movement under braking load was greater than that observed without braking. The right end of the strip still did not move.

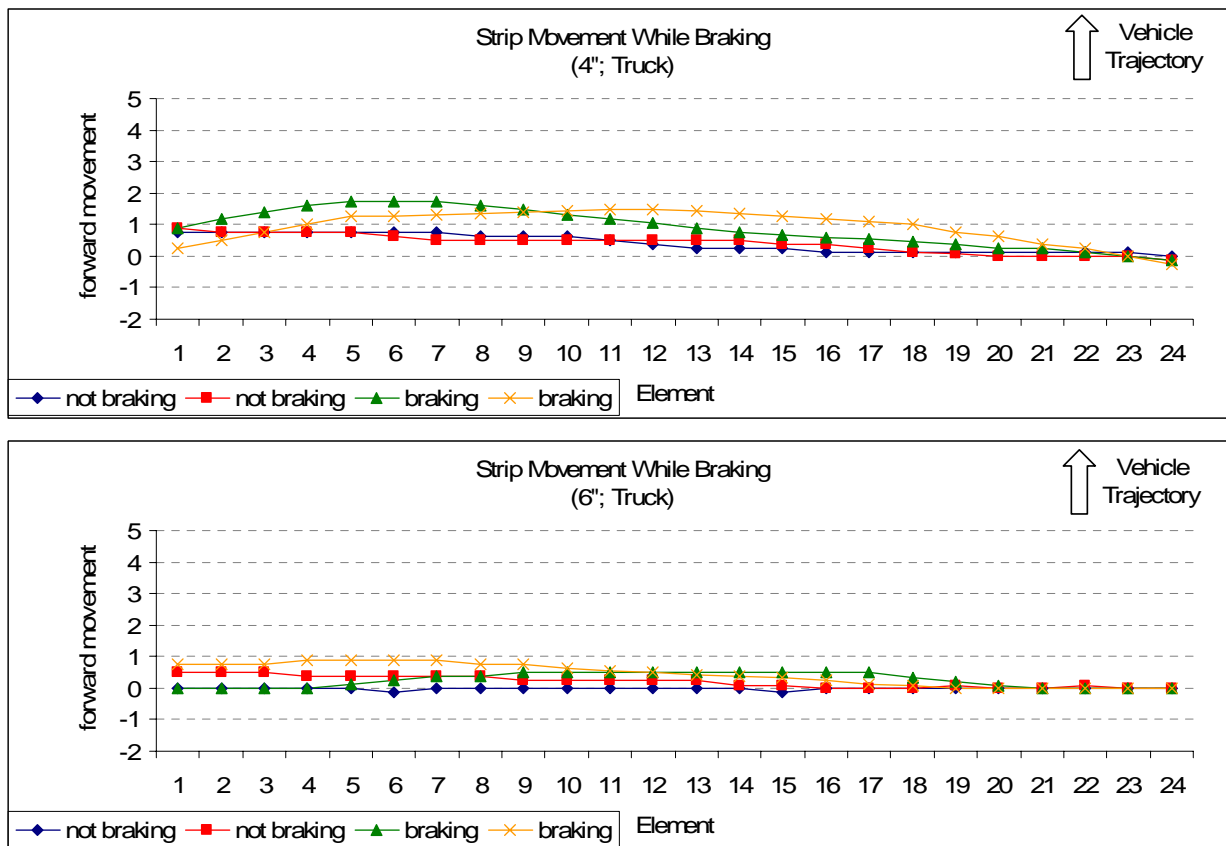


Figure 68. Strip movement while braking

Braking while traversing the strips resulted in approximately twice the amount of bounce and net translation. Table 7 and Table 8 show images of the strips with and without braking for axle 3 and axle 5, respectively. The bounce was significantly more acute, but the elements on the end farthest from the contact area did not move.

Table 7. Effects of braking on 4-in and 6-in strips (axle 3).









	No braking	Braking
4"		
6"		

Table 8. Effects of braking on 4-in and 6-in strips (axle 5).

	No braking	Braking
4"	 A close-up photograph showing a 4-inch wide metal strip on a road surface. A tire is positioned above the strip, and the strip appears relatively flat and undistorted.	 A close-up photograph showing a 4-inch wide metal strip on a road surface. A tire is positioned above the strip, and the strip is significantly curved and distorted due to the braking force.
6"	 A close-up photograph showing a 6-inch wide metal strip on a road surface. A tire is positioned above the strip, and the strip appears relatively flat and undistorted.	 A close-up photograph showing a 6-inch wide metal strip on a road surface. A tire is positioned above the strip, and the strip is significantly curved and distorted due to the braking force.

Conclusions and Final Design

This study supported the premise that a portable rumble strip (i.e., a rumble strip deployed without any physical attachment to the pavement) could be designed that would neither slide under the loading of a tractor trailer at highway speeds nor lift from the pavement under loading of the negative air pressures in the truck wake. Movement was observed due to the strip bouncing following the contact with the truck tires, but the tests suggest that the movement can be contained to the portions of the strip contacted by the tires, and the strip as a whole kept stationary.

The spacing of the pieces cannot be changed dramatically (i.e., it cannot be so large as to pose problems for motorcycles, scooters, etc.), and small changes are unlikely to significantly change the behavior of the strips.

The height of the strips seemed adequate. In a passenger car, the strips were not alarming, and the effects were clearly perceptible to the driver of the truck, who stated that they “would definitely get your attention.”

Bounce Reduction

Movement related to bounce is not problematic so long as there is no net translation and the strip is not in danger of flipping over. The design developed in this study was shown to remain in place (i.e., no net translation of the strip as a whole) even though individual elements experienced noticeable bounce. Under traffic, some net translation might be observed as successive vehicles pass over the strips at various lane positions. With each pass, the elements struck may translate, while the adjacent elements hold the strip as a whole in place. Over time, vehicles may cause all of the individual elements to experience some translation, resulting in a net movement of the strip as a whole.

While the results of this study suggest that this is not likely to be a significant problem, there are several relatively simple modifications that may potentially reduce the amount of bounce experienced under loading, thus reducing whatever net translation might occur and whatever risk of flipping that might exist. The following modifications may be effective at reducing the amount of bounce occurring during traversal.

1. Reduce the amount of slack in the cable connecting the strip elements
2. Reduce the thickness of the underlining
3. Use a different material for the underlining
4. Use a continuous strip (or several shorter strips attached at the ends)

Installation and Removal

The 6-in strip was very unwieldy for one person to handle, and would be impossible for many workers to lift by themselves. The 4-in strip was considerably better, but still would pose difficulties for some. Either strip could be managed by two people, although gripping the strip was somewhat difficult. Using 2-ft lengths as originally proposed is recommended, provided a satisfactory means of attaching the strips can be found.

Effective deployed lengths should be 10 to 12 feet to minimize overall movement.

Areas For Future Development

1. Couplings need to be tested. The coupling design shown in Figure 48 and Figure 49 may be effective for joining small segments (e.g., 2 ft long) together to form a deployed length of 10-12 ft.
2. Underlining material, thickness, and adhesive should be studied.
3. Longer duration field testing is needed to determine if 4-in strips would suffice.

Acknowledgments

In addition to author Gaurav Mathur, whose Master's Thesis served as the bases for portions of this report, Graduate research assistants Sylvia Bianchi, Riaan Myburgh and Seung-Jae Huang were an integral part of the first half of this work, conducting some of the computer analysis and participating in the first two tests.

The authors would like to express their deep appreciation to the The Kansas Department of Transportation for their support in the execution of this study. In addition to being one of the states providing funding, they also assisted in identifying sites for testing and provided traffic control for the field test.

The high-speed video camera and related technical support was provided by Motion Engineering. The tractor trailer used in the study was provided by Carlson Trucking.

References

- Bayraktar, I., (2001) "Simulation of External Truck Aerodynamics Pressure Contours and Velocity Streamlines," http://www.amtec.com/Product_pages/bayraktar.html, pub. AMTEC.
- Benekohal, R.F., Kastel, L.M., and Suhale, M., (1992) "Evaluation and Summary of Studies in Speed Control Methods in Work Zones," Report FHWA-IL-UI-237. Illinois Department of Transportation.
- Carlson, P., and Miles, J. (2003), *Effectiveness Of Rumble Strips On Texas Highways: First Year Report*, Report FHWA/TX-05/0-4472-1, Federal Highway Administration, Washington, D.C.
- FHWA (1998), "Shoulder Rumble Strips: Effectiveness and Current Practice," Federal Highway Administration, Wyoming Division Office.
- Federal Highway Administration, (2000)"Manual on Uniform Traffic Control Devices: Millennium Edition", Part 6, FHWA, Washington, D.C..
- Fontaine, M., Carlson, P., Hawkins, G., Jr., (2000) "Evaluation of Traffic Control Devices for Rural High-Speed Maintenance Work Zones: Second Year Activities and Final Recommendations," Report FHWA/TX-01/1879-2, Texas Transportation Institute.
- Harwood, D., (1993)"Use of Rumble Strips to Enhance Safety: A Synthesis of Highway Practices," NCHRP Synthesis 191, FHWA, Washington, D.C.
- Meyer, E., (2000)"Evaluation of Orange Removable Rumble Strips for Highway Work Zones," Transportation Research Record No. 1715, Transportation Research Board, Washington, D.C.
- Meyer, E., (2003) *Guidelines For The Application Of Removable Rumble Strips*, KDOT Project RE-0286-01 Final Report, Kansas Department of Transportation, Topeka, Kansas.
- Noel, Errol C., Ziad A. Sabra, Conrad L. Dudek; (1989) Work Zone Traffic Management Synthesis: Use of Rumble Strips in Work Zones, Publication No. FHWA-TS-89-037, Federal Highway Administration, Washington, D.C.
- Owens, R. (1967)"Effect of Rumble Strips at Rural Stop Locations on Traffic Operation," Highway Research Record No. 170, Transportation Research Board, Washington, D.C.
- Richards, S. H., Wunderlich, R. C. and Dudek, C. L., (1985)"Field Evaluation of Work Zone Speed Control Techniques," Transportation Research Record No. 1035, Transportation Research Board, Washington, D.C.

Stout, D., J. Graham, B. Bryant-Fields, J. Migletz, J. Fish, and F. Hanscom, (1993)
“Maintenance Work Zone Safety Devices Development and Evaluation,” SHRP-H-371, National
Research Council, Washington, DC.

Zaidel, D., Hakkert, S, Barkan, R., (1986)"Rumble Strips and Paint Stripes at a Rural
Intersection," Transportation Research Record No. 1069, Transportation Research Board,
Washington, D.C.

Appendix A: Discussion of TruckSim Results

According to TruckSim, the horizontal peak force decreases with increasing speed above a threshold. At very low speeds, the opposite is true. The peak force decreases as speed approaches zero. The inverse relationship between speed and peak horizontal force seems counterintuitive. In a previous report on some rumble strips work ([CTRL+click here](#)² then select [Final Report]), on pg 42 of the report (pg 52 of the PDF file) is a listing of some of sound measurements taken on several rumble strips in several vehicles at several speeds. The numbers shown are actually the difference between the peak sound level and the baseline (smooth pavement). While the differences show an inverse relationship with speed, the absolute measurements increased with increasing speed. Another project funded by this study took measurements in which noise increased up to the maximum speed tested (47 mph (76 kph)). Figure 69 shows a plot of the average measured values.

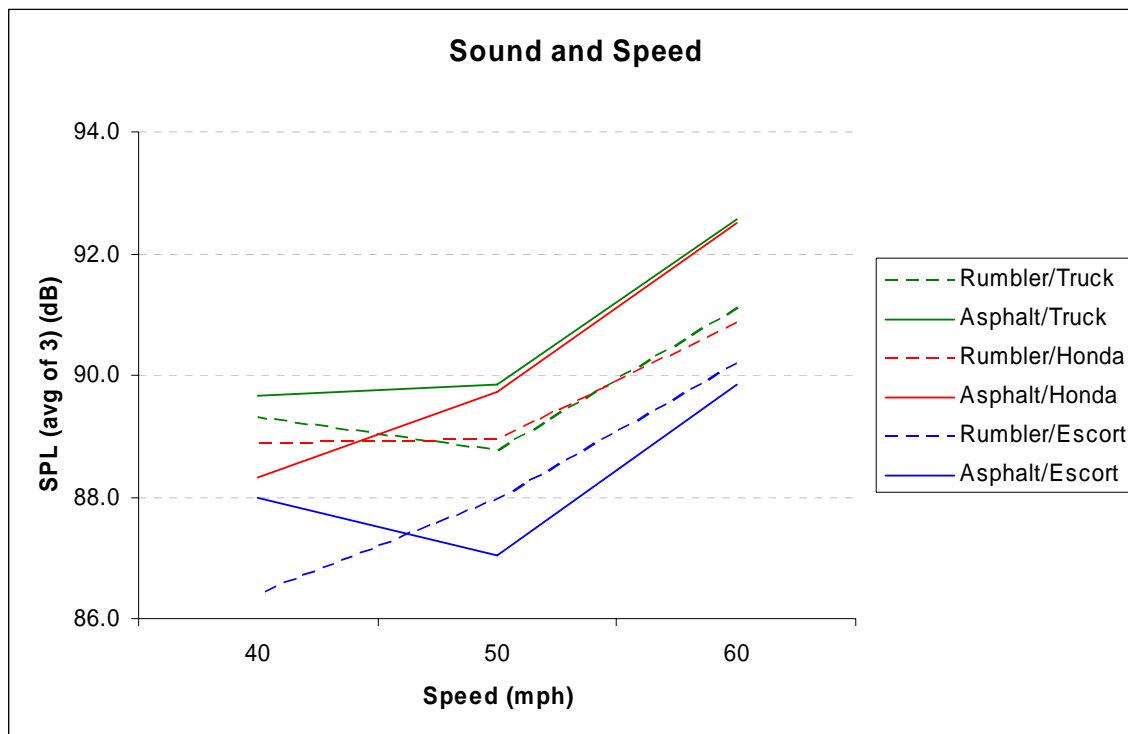


Figure 69. Sound Pressure Levels (SPL) versus speed by vehicle and strip type.

² <http://meyerits.com/RumbleStrips/index.html>

Figure 70 shows the measured data for a number of strip types and experimental configurations collected from another site. These measurements are sound levels inside the vehicle. There is a clear trend of increasing sound levels with increasing speed.³

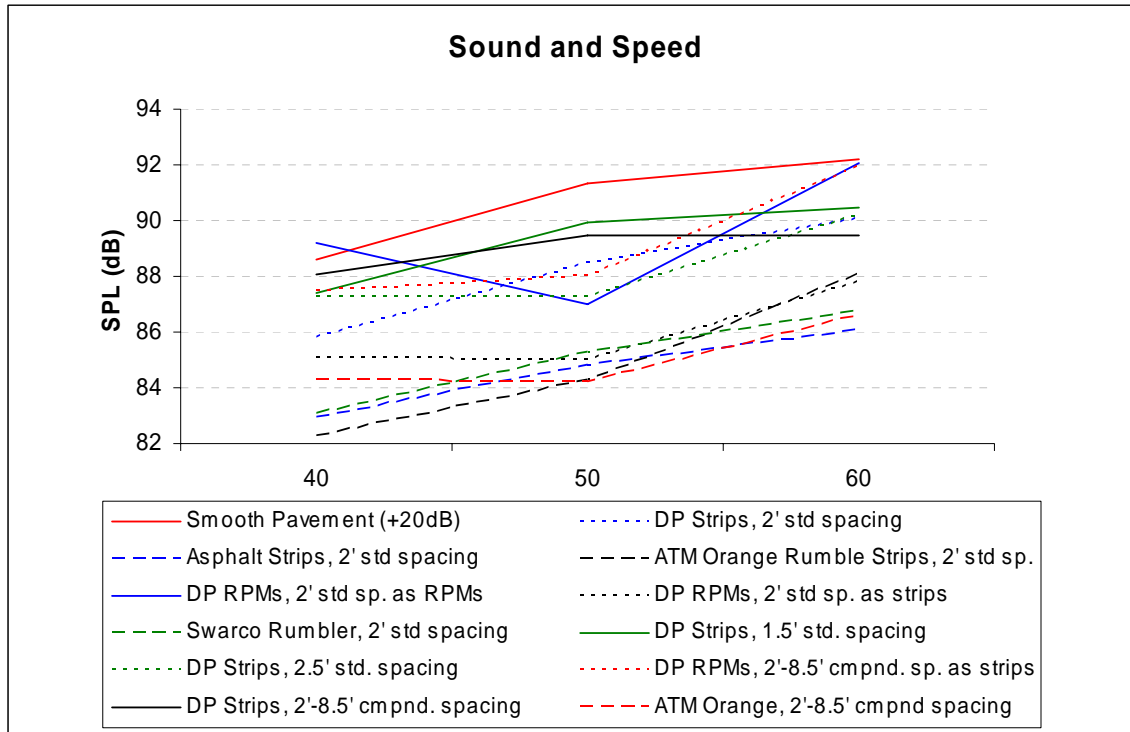


Figure 70. Sound Pressure Levels (SPL) versus speed for various strip types and configurations.

The vibration data is less consistent, probably because the collection methodology was less than optimal. A single-axis accelerometer was affixed to the center of the vehicle roof oriented to measure vertical movement. The vibration of the roof panel may have obscured the vibration of the chassis in the data. Nonetheless, vibration appears to have a positive relationship with speed in the data. Figure 71 shows the change in vibration with speed for a variety of strip types and configurations. Figure 72 shows the changes over 10 mph, 20 mph and 30 mph speed changes. The downward trend of the data points in general may simply be due to diminishing returns (i.e., the higher the starting speed, the less difference an additional 10 mph makes). The 10 mph ranges are somewhat ambiguous, but as the range increases to

³ The departures from the trend could be due to several issues. For example, (1) vehicles may have harmonic response to certain frequencies causing a given speed to yield unusually high sound levels for a given vehicle; (2) while data was to be collected while neither accelerating nor decelerating, small speed adjustments were occasionally necessary while traversing the strips. It is unlikely this had a significant impact on the data, but it is possible; or (3) random variation in the data.

20 mph and then 30 mph, the pattern becomes clearer. When the vibration indices for 30 mph are compared with those at 60 mph, they all show an increase, supporting the trends seen in the sound data.



Figure 71. Vibration and speed for various strip types and configurations.

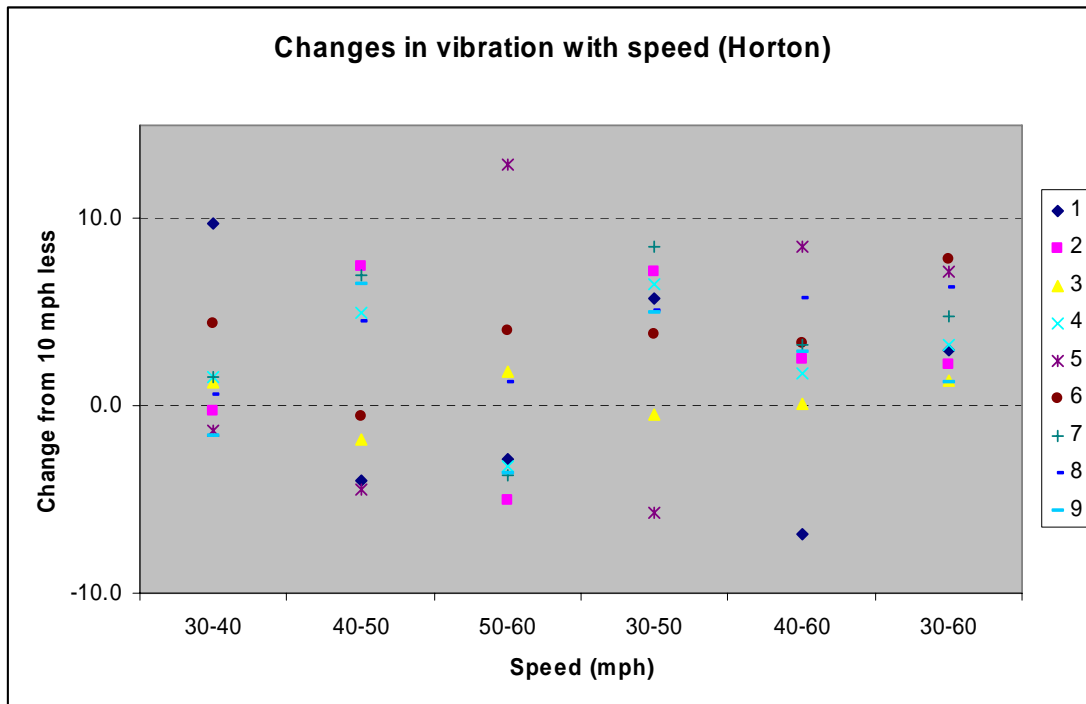


Figure 72. Changes in vibration with speed for various strip types and configurations.

Initially, this data appears to contradict the results of the TruckSim software. This assumes that there is a direct relationship between speed and peak sound and vibration levels associated with the vehicle. However, when the speed increases, the *peak* sound and vibration levels increase, but the *duration* of the interaction between the vehicle and the strip decreases. Perhaps the change in duration is more significant a factor than the peak sound levels, in which case the empirical sound and vibration data may still support the results obtained from TruckSim with respect to force magnitudes.

Figure 73 and Figure 74 show plots of changes in three characteristics of the peaks associated with Figure 72. These data were collected with three different vehicles (two passenger cars and one truck) over an assortment of rumble strip installations with varied strip profiles, numbers of strips, and strip spacings. In both figures, the bottom left plot shows the changes with speed in the area under the curve (dB x time) for the respective peak values. The plots in the bottom right of both figures show the changes in duration associated with each peak value. Figure 73 shows in the upper left the area of the curve over an estimated baseline threshold which represent the typical peaks observed while traveling over smooth pavement. Noise over smooth pavement changes with speed, but a single value was chosen arbitrarily so that the comparison between speeds would have a consistent floor. The upper left plot in Figure 74 shows the peak values, analogous to the vibration data shown in Figure 72. The vibration data in Figure 73 and the sound data in Figure 74 show similar patterns, so we'll focus the discussion on the sound data since the patterns are more distinct and the data collection methodology was more robust.

The peak sound levels shown in the upper left of Figure 74 show that the overwhelming number of samples measured higher peak sound levels at 60 mph than at 40 mph. Between 40 mph and 50 mph, the pattern is not so clear, perhaps because there is a transition occurring in that range or perhaps because the noise in the data (no pun intended) is greater at lower speeds. This trend seems counter to the TruckSim results that show the maximum longitudinal force decreases as speed increases in this range.

However, it is possible that the energy being input into the system (i.e., the vehicle) is decreasing with speed even though the peak sound (and vibration) levels are increasing with speed. Energy must have a time component, so to further investigate this possibility, a sound level threshold was selected at approximately the upper limit of the measurements observed over smooth pavement. From each peak measurement, measurements before and after the peak were examined until 10 consecutive measurements were observed to be below the sound level threshold. These 10 measurements were assumed to be baseline data (i.e., not part of the peak caused by the rumble strip), and the next closest data point to the peak value was identified as the limit of the peak. The values of the measurements between the peak limits were summed and multiplied by the time interval to yield the area under the graph of the peak, which is expressed in units of *sound pressure times time*, or *dB x ms*. The measurement time interval for this data was 3 ms, resulting in an average of about 120 measurements per peak at 60 mph, or just slightly more than a third of a second of data.

When the areas under the peaks were compared at various speeds, the relationship between the area under the curve and speed varied positively with the duration of the peak and inversely with the peak level and speed. It should be noted that these measurements were for groups of 6 to 10 strips spaced between 1.5 and 4 ft apart. This may support the results obtained from TruckSim, although I don't think we can positively conclude so just yet. Even if it does, the question of "why" still stands, but perhaps the TruckSim data is ok after all.

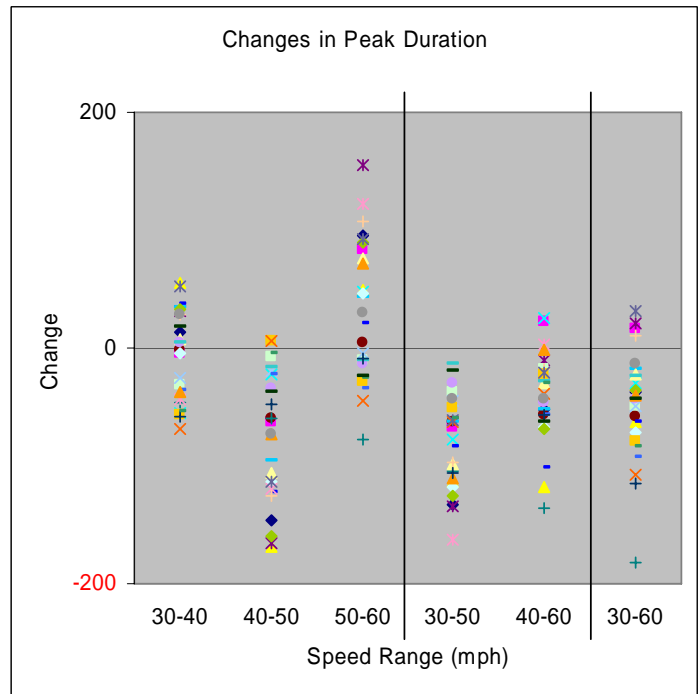
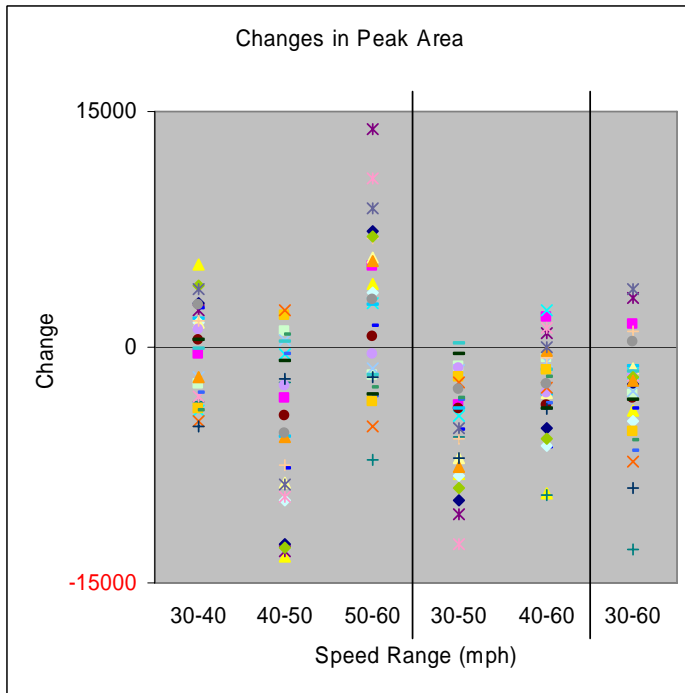
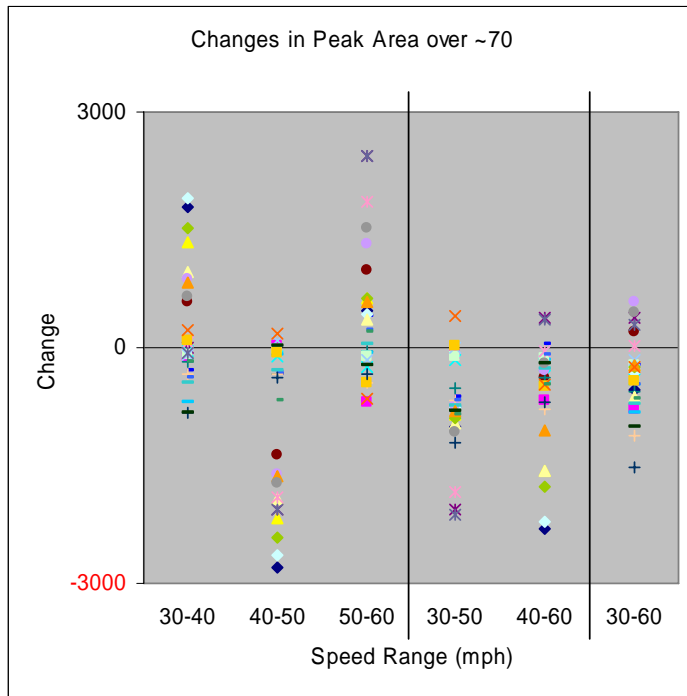


Figure 73. Changes in vibration parameters with speed for assorted strips and vehicles.

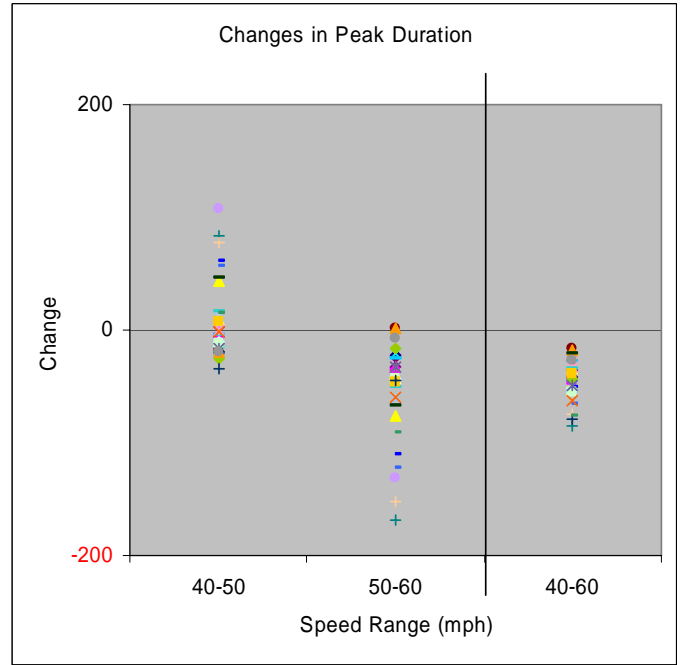
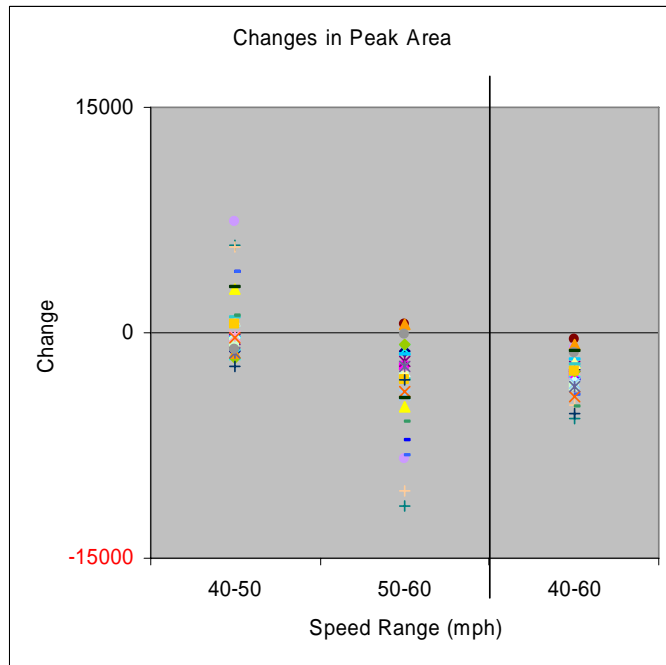
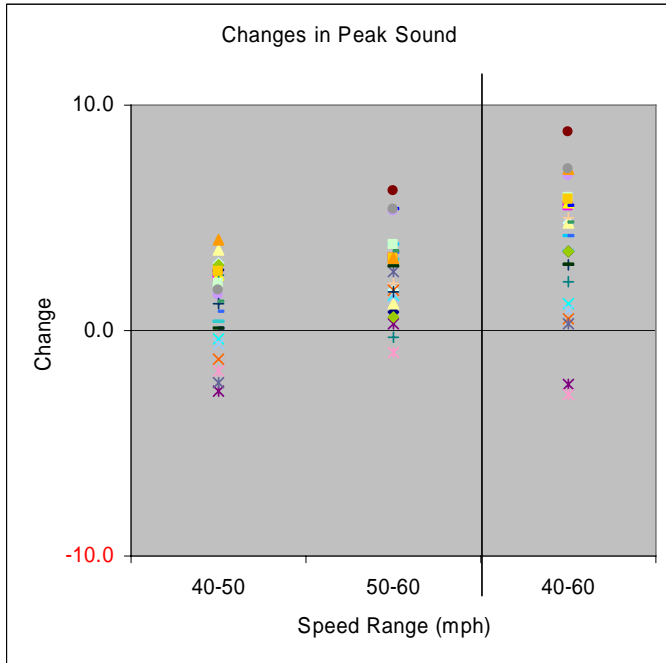


Figure 74. Changes in sound parameters with speed for assorted strips and vehicles.